university of groningen

faculty of science and engineering

MASTER RESEARCH PROJECT

Producing Colour Profiles With Correct Errors Using FDS Data

Jasper Jacob POSTEMA

s3164063

Supervised by:

R. PELETIER

Second examiner:

R. V.D. WEYGAERT

June 28, 2022

Abstract

In this thesis the data generation process of the Fornax deep survey (FDS) is analyzed to create surface brightness and colour profiles for 10 dwarf galaxies inside the cluster. The FDS divided the Fornax cluster in 28 fields and created observations in the u', g', r' and i' passbands. The final images produced by the FDS are created by means of mosaicing of initial observations. Despite this process a residual background is still present in the final images. A method to determine the residual background values together with sensible error is developed in this thesis. This method creates a single background value for an entire image, in contrast to the work of Shivangee Rathi [1], where a 2D polynomial background is fitted to the residual background and applied to the images. After subtracting the residual background from the corresponding images, surface brightness and colour profiles are created. Almost all of the surface brightness profiles roughly follow a power law while most of the colour profiles are flat. A depth of 30 magnitudes/square arcsec was reached for the surface brightness profiles with the best signal to noise. This is comparable to recent research done where similar profiles were created for non-dwarf galaxies [2, 3, 4] and a lot better than recent research into dwarf galaxies [5]. Another advantage of the data produced in this thesis is that the errors have been derived in a sensible way which is often not the case for similar data in other research.

Contents

1 Introduction

The Fornax cluster is the second nearest cluster to us after the Virgo cluster and is situated around the galaxy NGC 1399 [6]. The cluster is part of the Fornax–Eridanus structure of which it is the most massive with a mass of 0.40-3.32 $\times 10^{14} M_\odot$ compared to the total mass of the Fornax–Eridanus structure: 1.30-3.93 $\times 10^{14} M_\odot$ [7]. The Fornax cluster consists of 590 galaxies up to an r'-band magnitude of 21 mag [8]. The Fornax deep survey (FDS) is an optical survey in 4 bands which was performed between 2013 and 2017 with the intend to more accurately analyze the contents of the Fornax cluster and the subcluster Fornax A which is located near the main Fornax cluster than ever before [8]. The most recent previous survey covering the entire Fornax cluster was the Fornax Cluster Catalog (FCC) in 1989 [9]. After this, in 2007, the ACS Fornax Cluster Survey targeted 43 galaxies in the cluster with a spatial resolution better than the FDS [10]. However, the FDS targets the entire cluster with an unprecedented depth, using the Hubble Space Telescope (HST), and not just a collection of galaxies. Other surveys have also been performed in different regions of the cluster and more are in development as well. This indicates that the Fornax cluster was, and still is, an important site of research. Researching the objects present in the Fornax cluster can help gain insight into the evolutionary effects that galaxies and galaxy clusters undergo. Specific galaxy type populations can also be extensively researched using data from the cluster. In this thesis specifically Dwarf galaxies will be the topic of interest, of which the Fornax cluster contains plenty.
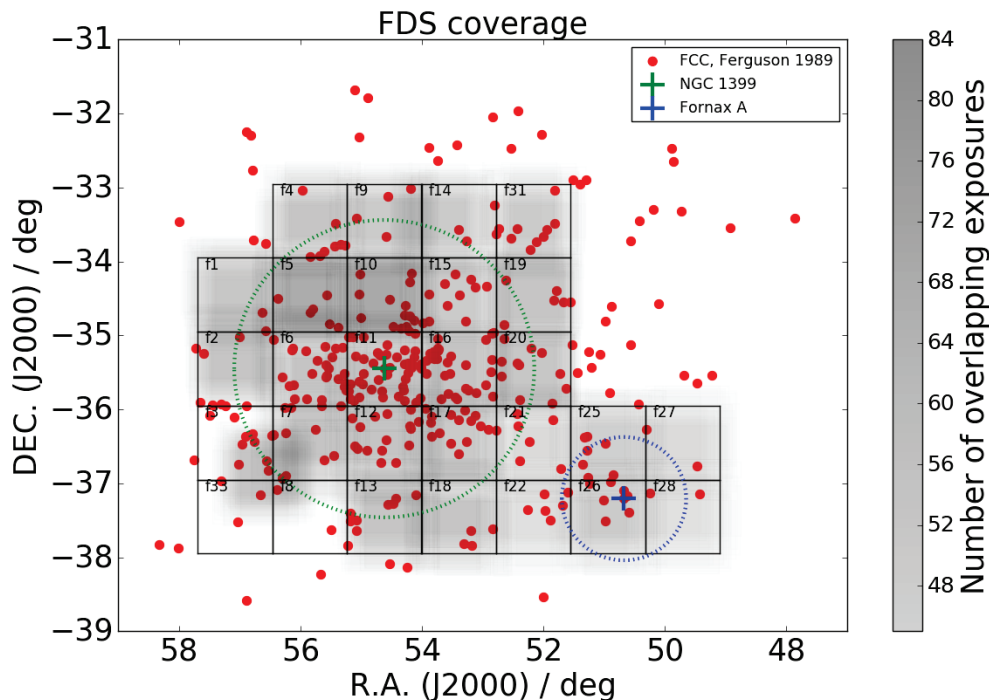

Figure 1: FDS fields and exposure density. The galaxies in the FCC catalog are also shown together with the galaxy NGC 1399 which acts as the center of the main Fornax cluster and the smaller subcluster Fornax A.

The FDS was performed using the OmegaCAM instrument [11] of the survey part of the VLT Surface Telescope (VST) [12]. The resolution of the OmegaCAM is 0.21 arcsec per pixel, the field of few is 1 degree by 1 degree and the camera can use the u', g', r' and i' SLOAN filters. The central wavelengths of these filters are 355.1, 468.6, 616.6 and 748.0 nm. All of the exposures were performed under good photometric conditions, with the darkest sky hours reserved for the u' and g' band observations and each exposure lasted

3 minutes. The Fornax cluster was divided into 28 fields with a size of 1 by 1 degree as can be seen in figure 1. Each field was exposed 75, 55, 55 and 35 times in the u', g', r' and i' filters respectively. The observing strategy is tailored such that the same objects do not appear in the same pixel during a later exposure. This was done by moving to a different neighbouring field after each exposure. After a few exposures another exposure in the original field will be made again, but this time there is an offset of about 10 arcminutes with respect to the original position. The advantage of moving to a different field after each exposure is that the sky background image of an observation run can be made by median averaging the related exposures. This is because the contribution of the bright objects will be cut out due to the median and what is left over is only sky background contribution. When the sky background value is subtracted from each exposure, they will still have a certain residual background left that could not be subtracted. The advantage of not pointing at the same coordinate in each field every time is that by stacking the images of a certain part of the sky on top of each other the systematic effects caused by faulty pixels can be reduced. When the sky background of the original exposures is subtracted, the subtracted images belonging to a certain field and passband can be median stacked on top of eachother to create a final, deeper, image. This stacking is done by giving each exposure a weight depending on the residual background level that is left over, more background means a lower weight. This method of producing the final image with a set of slightly offset original exposures is called mosaicing. The standard deviation of the residual background values in each field can be calculated and is defined as σ. The depth at which the signal-to-noise per pixel is 1σ corresponds to a surface brightness of 26.6, 26.7, 26.1, and 25.5 mag/arcsec^{-2} in the u', g', r' and i' filters respectively [8].

In this part of my thesis I will create a script to analyze data from the FDS [13]. The main challenge of analyzing the data is understanding the systematic effects caused by the way that the images are created. Each image consists of a mosaic of original exposures made using the VST. Each original exposure has a slightly different background level because the images are not all taken at the same time and in the same conditions. We can assume that the background in a certain original exposure has a negligible error compared to the backgrounds of the various frames though, which means that it is constant in the entire space of the exposure with negligible contributions from photon noise. When several original exposures are stacked on top of each other in a certain part of the sky the result is a patch with a unique background level, depending on which original exposures were stacked. A final image consists of many of these patches created from different sets of original exposures, and therefore with different background levels, which means that it is not trivial to get rid of the background signal. The goal of this part of the thesis is to generate deep surface brightness profiles for a subset of the dwarf galaxies in the FDS in a reproducable way. This way the steps taken in this thesis could be repeated for any dwarf galaxy in the FDS without much issue. The aim is to understand what the error in the residual background is at a position in a galaxy. This can help to answer questions about the validity of certain models as the properties of the dwarf galaxies can be compared to their predicted properties. The environment dependence on the evolution of dwarf galaxies can also be more deeply investigated using the data generated in this research. This part of the thesis will serve as an extension of the PhD research of Shivangee Rathi [1]. In her research she developed an algorithm that can find dwarf galaxies in the FDS and create mask images for objects that are not dwarf galaxies. Using this information she was able to create surface brightness profiles in every band of each dwarf galaxy automatically. A place where her research could be significantly improved though is in the generation of these surface brightness profiles and especially their errors. The quality of the images taken by the FDS are good enough to allow for surface brightness profiles that go to a fainter surface brightness, i.e. the profiles could be deeper than the ones produced by Rathi. This problem is caused by the fact that Rathi's background subtraction is not done rigorously enough. The way that their background was determined was by fitting a smooth 2D polynomial to the background. The problem with this is that due to the mosaicing the background is not smoothly distributed over the image, so fitting this smooth background subtraction will be difficult and applying it will introduce errors. With a better background subtraction method the full potential of the FDS could be reached and more impactful results can be obtained. In this thesis an algorithm that creates deeper surface brightness profiles starting from the images and masks created by Rathi will be developed. This will be done

in the g', r', i' and u' passbands. With these surface brightness profiles in different passbands much better colour profiles can be determined that go a lot deeper than previously possible.

2 Method

The first step to creating results from the considered images is to determine the true surface brightness in every pixel. Every image consists of a mosaic of original images taken taken during the creation of the FDS. Each of these original images has a different, small, background pattern. A flat background can still be subtracted in the entire image but this background will have a certain error associated with it. This error ultimately determined the error of the surface brightness values in the images. Furthermore when the results are obtained, they need to be transform into physical units.

After each image in every band has been background corrected and an error has been determined for the sky background, the surface brightness, and its error, of the dwarf galaxies can be determined at different distances from the center. In order to achieve this, the script uses various properties of the analysed dwarf galaxies like their effective radius, Sersic index and axis ratio. This information is taken from a catalog produced by Venhola et al. [8].

When the surface brightness is determined in every band, colours can be determined by subtracting surface brightness values in different bands. All of the possible colour profiles that can be created in this way are also generated by the script.

2.1 Background correction determination and subtraction

Before any background correction or determination can be done, the masks need to be applied to the corresponding images. For each field a mask was developed by Rathi [1]. These masks denote the positions taken up by bright objects that are not part of the dwarf galaxies. Most commonly these are stars or distant galaxies. An example of one of these masks is shown in figure 2 and the result of masking each of the images analysed in this thesis is shown in appendix 5.
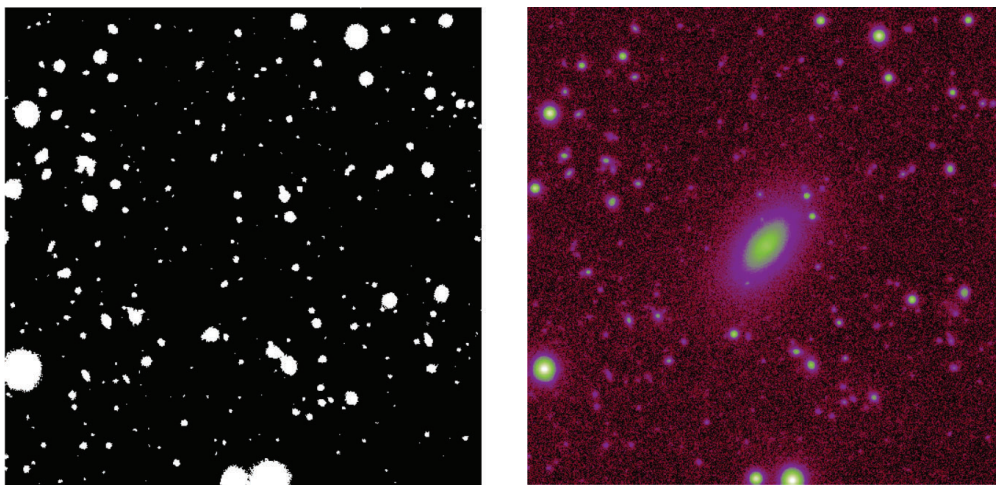

Figure 2: Mask (left) and r' band image (right) of dwarf galaxy FDS10_DWARF189.

By using these masks the script can get rid of the noise generated by those bright objects. This is done by putting the counts of the pixels in the location of the bright objects to 0. The masked images can be seen in appendix 5. The next step is background determination and subtraction. To determine the background, the script needs to make assumptions about the characteristics of the background in each image. The background around a galaxy consists of a large number of patches, tens or hundreds, as a result of the mosaicing, which all have a slightly different background value. The mosaicing and the resulting different patches are shown schematically in figure 3. It is impossible to know retroactively how the patches
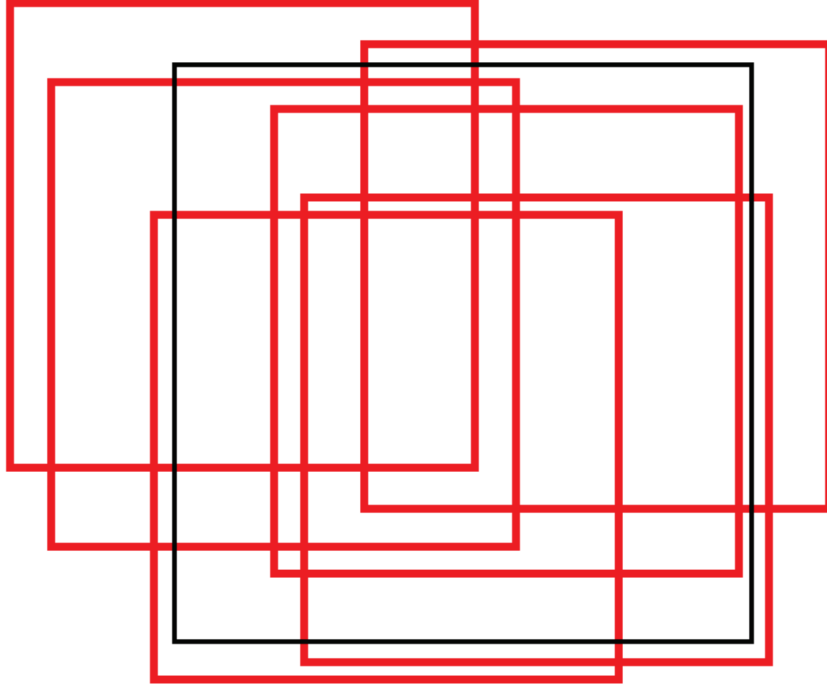
Figure 3: Schematic representation of the mosaicing that is used to generate the final images. Each red square is an original observation, all of which were done at slightly different times in slightly different positions. The black square is the final image. The different patches bound by red lines are all probed by a different combination of original observations and therefore have a different background values.

are oriented in the final image. Though by looking at a small tile in the final image, that does not include any stellar objects, a measure for the background in the tile can be found by taking the median value of the pixels in that tile. If this is done for a sufficient number of tiles, a distribution of background values can be obtained that resembles the distribution of background values of the patches quite well. It is assumed that the background value distribution of all of the patches together follow a Gaussian distribution. The median value of this Gaussian distribution can be taken as the true flat background of the final image with its error being the standard deviation of the Gaussian distribution. It is important that the tiles that are used to estimate the background value distributions only contain empty space, but this is not always easy. The script determines the flat background value in an image as follows.

First, the image is subdivided in square tiles with a certain side length, D. Next, the median value of the pixels in these tiles are calculated. The median is chosen over the average because this would reduce the impact of small non-background on the actual distribution. With this the persisting problem is still the influence of the dwarf galaxy itself on the background noise distribution. Because of this, the last thing that is done is that the tiles that are too close to the center of the galaxy are excluded from being part of the background distribution. What "too close" is varies per dwarf galaxy. In the script it is represented by an ellipse with a semi-major axis that is equal to a the effective radius of the galaxy times 2 which is obtained from a catalog [8]. The catalog also includes the location of the galaxies, their axis ratio and Sersic index. These are all needed to create the ellipse. The factor can vary per image. If a tile falls for more than 50%

inside the ellipse it is rejected.

Initially, the sky background value of the entire image was chosen as the median of the distribution of background values obtained from the squares and its error was the standard deviation of the distribution. This worked well as a measure for the background, but the error was often misrepresented. In the final version of the script, each distribution of background values is fitted to a Gaussian function. The approximation of the background value is the mean of the Gaussian curve and the corresponding error is the fitted standard deviation. This has resulted in more accurate errors.

There is one exception to this method of determining the background. One of the dwarf galaxies, FDS11_DWARF458 , had a badly defined background in the r' and i' bands. The way that the surface brightness distributions are produced for this galaxy is described in appendix 5.

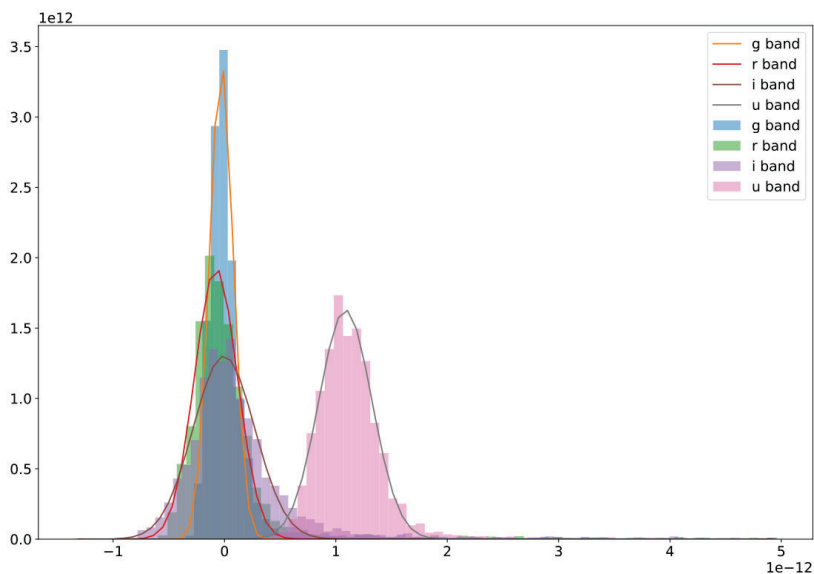An example of a distribution of background counts is shown in figure 4.

Figure 4: Distributions of the background counts fitted to Gaussian distributions for each passband of dwarf galaxy FDS14_DWARF144.

2.2 Surface brightness and colour profile

Now that the background subtracted image can be obtained, the surface brightness profile of the dwarf galaxies can be found in each band. The surface brightness profiles are visualized in terms of AB magnitudes. The AB magnitude, m_{AB}, is defined in equation 1, where I is the intensity per pixel of the object from the FDS images.

$$m_{AB} = -2.5 \log(I) \tag{1}$$

The surface brightness profiles depict the relationship between magnitude and distance from the center of the dwarf galaxy. The flux at every radius is obtained by adding all of the counts of the pixels in a ring centered around that radius. The flux is then divided by the amount of pixels in the ring to obtain the intensity. If there are masked pixels present in the ring, the total amount of pixels is taken to be the total amount of unmasked pixels. Close to the center of the dwarf galaxy, the rings do not have to be very thick

in order to get a reasonable measure of the magnitude. The further away from the center of the galaxy, the wider the rings need to be in order to get a good measure of the magnitude. The rate of change of the thickness of the rings as a function of the distance from the center of the dwarf galaxy can be different per galaxy.

From the 4 brightness profiles per dwarf galaxy, 5 colour profiles are created by subtracting surface brightness profiles from each other. These are: g'-r', g'-i', u'-g', u'-r' and u'-i'. These colours are both plotted as a function of major axis radius and g' band magnitude. For both the surface brightness and colour profile the points are only displayed when the error is smaller than a set value. For the surface brightness profiles this is 1 magnitude in the case of the g' and r' passbands, 0.6 magnitude in the case of the u' passband and 0.1 magnitude in the case of the i' passband. These values were chosen to reflect the fact that the i' passband and in lesser extend the u' passband images are less reliable than the g' and r' passband images for the purpose of this thesis. For the colour profiles the surface brightness values are cut off when the error surpasses 0.25 magnitudes. This makes sure that the produced colour profiles have the highest amount of accuracy possible. For some of the galaxies the background seemed to be less flat than what was previously assumed, namely completely flat. This is the case in the dwarfs FDS7_DWARF326, FDS11_DWARF279, FDS11_DWARF458 and FDS20_DWARF334. For those galaxies, the errors are multiplied by a factor of 2 in order to reflect this additional uncertainty.

3   Results

In this section, the results of the analysis done by the script as explained in section 2 will be explained. Some interesting and noteworthy results will be highlighted and shown while the rest are displayed in appendix 5. Not all of the dwarfs in the FDS were analyzed due to time constraints. 10 dwarf galaxies were chosen as a sample to perform our analysis on. These were chosen by looking for isolated dwarf galaxies in the entire survey. This is because in those galaxies the background is less disturbed by other objects in the neighbourhood which makes doing the analysis easier. The chosen dwarf galaxies are: FDS2_DWARF000, FDS7_DWARF326, FDS10_DWARF189, FDS11_DWARF069, FDS11_DWARF279, FDS11_DWARF283, FDS11_DWARF458, FDS14_DWARF144, FDS16_DWARF417 and FDS20_DWARF334.

3.1   Background distributions

In the Background distributions in appendix 5, the shown Gaussian distributions give the error in the background. It can be seen that in almost all of the cases a single Gaussian profile fits very well to the background distribution. The only galaxy for which this is not the case is FDS11_DWARF458. For this galaxy, the method of determining its surface brightness and colour profiles is described in appendix 5.

3.2   Surface brightness

All of the surface brightness and colour profiles can be found in appendix 5. For the colour profiles, the g'-r' colours are highlighted because the g' and r' filters are the most accurate, as discussed in section 1. In the surface brightness profiles, the measurements with an error larger than 0.5 magnitudes are not displayed. The same goes for the colour profiles, but with a cutoff error of 0.333 magnitudes. In general, a depth of 28 to 30 magnitude/square arcsec was reached in the surface brightness profiles for any band.

The surface brightness profiles for all of the galaxies in this thesis decrease at a roughly constant pace within error bars, which means that the profiles are given by a power law. The g', r' and u' passband surface brightness profiles could reach a depth of 30 mag/square arcsec. On the other hand, the i' passband surface brightness profiles could generally reach a depth of 26 magnitudes/square arcsec. The reason why the i' band couldn't probe quite as deep is partly due to the cutoff imposed on this passband as described in section 2.

Almost all of the colour profiles for every galaxy have a global positive value. In many cases bumps in the colour profiles can be seen. Most of the colour profiles also seemed to be rather flat within error bars as a function of radial distance and g' band magnitude. In some cases, the profiles seem to drop or rise at higher distances or g' band magnitudes. For which galaxies that is the case is described in the section below. The g'-r' colour profiles were generally able to probe the furthest reaches of the galaxy. This profile is usually defined down to a g' band magnitude of 28 magnitudes/square arcsec, but was in some cases able to go deeper.

3.3   Individual dwarfs

In some of the profiles some interesting phenomena can be seen that deviate from a flat profile, those are described below.

In dwarf galaxy FDS7_DWARF326 the g'-r' colour profile is defined down to a depth of 29.5 magnitude/square arcsec, which is quite deep compared to the profiles of the other galaxies.

In dwarf galaxy FDS11_DWARF069 the g'-i' colour profile shows a small upward slope while the u'-g', u'-r' and u'-i' profiles show a small downward slope. This behaviour is not significantly deviating from a flat

profile but it should still be noted.

In dwarf galaxy FDS11_DWARF279 the surface brightness profile in the u' passband has a different behaviour from the rest of the surface brightness profiles in the different passbands. Furthermore the g'-i' and g'-r' colour profiles show a flat profile while the u'-g', u'-r' and u'-i' profiles show a small downward slope. It could be possible that the amount of ultraviolet grows compared to the other passbands as a function of radius. It is strange that this is not reflected in the g' band magnitude though and this behaviour is not seen in any of the other considered galaxies.

In dwarf galaxy FDS11_DWARF458 most of the colour profiles did not reach a depth greater than 26 magnitudes/square arcsec. This is because the residual background value for this galaxy had some issues in the i' and r' band as explained in appendix 5. The u'-g' colour was able to reach comparable depth to the other galaxies and shows a slight downward slope.

4 Comparison to literature

In this section I will compare the results produced by the script developed in this thesis with similar analysis produced by different research on other (dwarf) galaxies. By doing this, possible coherent or incoherent phenomena can be pointed out and the quality of the profiles created in the research can be discussed. Furthermore, by considering various research a statement can be made about the status of (dwarf) galaxy surface brightness profiles. The main comparison will be performed between the shape of the surface brightness and colour profiles and their errors. The profiles created in this thesis will be compared to the radially extended profiles found in Rathi's thesis, the dwarf galaxy profiles observed in a survey by van Zee in 2000 [5], the spiral galaxy profiles observed by Bakos et al. in 2018 [2], the Milky Way-like galaxy profiles created by Martinez-Lombilla et al. in 2018 [3] and the colour profile of M87 created by Rudick et al. in 2010 [4]. Comparisons of the results produced in this thesis to non-dwarf galaxies is done such that the quality of the profiles can be discussed even if the galaxies can't be compared. The main focus here is the comparison between the photometry and the way that the errors are produced if at all.

4.1 Comparison to Rathi

By comparing the brightness and colour profiles produced in this thesis to the ones produced by Rathi it can be found out if the methods used in this thesis will lead to surface brightness and colour profiles with more sensible errors. The surface brightness profiles that were created in this thesis can be directly compared to the the ones Rathi created since the same data was used. Rathi was not able to create surface brightness and colour profiles for every dwarf galaxy in the survey, so the galaxies that will be compared are: FDS2_DWARF000, FDS7_DWARF326, FDS11_DWARF069 and FDS11_DWARF279. Rathi did not create surface brightness profiles in every passband that is available for every dwarf galaxy, this also means that not every colour profile that was created in this thesis was created by Rathi, so of course only the ones that she did make are compared. From comparison we can draw the conclusions that both methods agree on the general behaviour and shape of the surface brightness profiles at low radius. The g' band profiles produced in this thesis could probe the surface brightness profiles to a similar radius as Rathi's profiles while the other passbands came slightly short. Additionally, the errors in the values of the surface brightness produced by Rathi are rather large compared to the ones produced in this thesis. When it comes to colour, the profiles again show the same behaviour at small radius with larger errors in Rathi's results. Rathi's profiles show the profiles at larger radius, but their accuracy becomes a lot worse at that point. The comparison of colour profiles is shown in figure 9 in appendix 5.

To conclude, the surface brightness and colour profiles produced using the method explained in section2 are consistent with the results obtained by Rathi. The depth that could be reached by the g' band surface brightness profiles was about the same for both methods but the uncertainty of the profiles produced in this thesis is better in all cases. Another improvement made in this thesis is that by using this method all passbands could be analysed for every dwarf, which was not the case using Rathi's method.

4.2 Comparison to van Zee

Van Zee's survey was performed using the Kitt Peak National Observatory (KPNO) 0.9 m telescope and consists of 58 isolated dwarf galaxies. Van Zee made use of the UBV photometric system, which consists of the U, B and V band. Their central wavelengths are 364 nm for the U band, 442 nm for the B band and 540 nm for the V band. This means that the U band is comparable to the u' band, the B band is comparable to the g' band and the V band is in between the g' and r' band. Van Zee produced B-band surface brightness profiles, B-V and U-B colour profiles all as a function of radial distance (in arcsec). The B band surface brightness profiles produced by van Zee could reach a surface brightness of 27 mag/square

arcsec, while the g'-band surface brightness profiles obtained using the FDS could reach a surface brightness of 30 mag/square arcsec. Van Zee's profiles did not show any error bars, so it is not easy to say how reliable every observation is. As mentioned previously in section 3, the surface brightness profiles produced in this thesis show a roughly constant power law behaviour. The colour profiles in most cases are roughly flat as well. This is comparable to the profiles produced by van Zee, although there are exceptions. In some cases, the slope of the B band surface brightness profiles either increases or decreases at a certain radius. For the galaxies in which the changing surface brightness slope is seen. None of the g' band surface brightness profiles created for the dwarf galaxies in this thesis showed a changing slope, within error. The B-V and U-B colour of van Zee can be compared to the g'-r' and u'-g' colour used in this thesis respectively. Some of the colour profiles in van Zee's survey show the same rather flat shape that is also seen in the colour profiles produced in this thesis, especially in the low radius/surface brightness regime which is probed by van Zee. However in the cases where the slope of the B band surface brightness profiles changes, the colour profiles are not flat but rather oscillate sporadically. Similar to the surface brightness profiles, the colour profiles did not show any error bars either which makes it hard to say if the colour profiles produced by van Zee can actually be considered flat or if the data is inconclusive.

To conclude, the profiles created in this thesis are somewhat consistent with a subset of the profiles found in van Zee's survey. There are several profiles in van Zee's survey though whose behaviour is not comparable to the behaviour of the galaxies analyzed in this thesis. Some examples of profiles that are and are not consistent with the profiles produced in this thesis are shown in figure 5. Since van Zee did not report any errors in her findings it is hard to say how accurate her findings are, especially for the galaxies where the slope changes in the fainter parts of the surface brightness profile. The profiles in this thesis were able to go several mag/square arcsec deeper than the profiles van Zee created and generated accurate error bars, so the results in this thesis can be seen as a significant improvement.

4.3   Comparison to van Bakos et al.

Van Bakos et al. created surface brightness and colour profiles of seven late type spiral galaxies using data from the Sloan Digital Sky Survey (SDSS) *Stripe82* [14]. The data in *Stripe82* is one of the deepest subsets of the SDSS because its regime has been observed rather often, so by stacking the observations the images can become very deep. The drift scanning technique that is used by Bakos et al. also makes sure that the background is very flat. The quality of the standard coaddition process performed by the SDSS archive was not high enough, so Bakos et al. created their own pipeline to stack the observations and create high quality images. They achieved this in the following way. First, the background in each observation was determined by randomly choosing 10 thousand 5 pixel wide apertures and taking the resistant mean as the background value, the scatter is also recorded. This method is also known as the box method. This was done in several iterations as to reduce the effect of background objects. Based on these background values, some of the observations are rejected due to outlying background value, background scatter or PSF. Finally, the accepted observations are added by first making mosaics by stacking the observations made in the same run and then median adding these mosaics to create the final mosaic. Masks are also created using a combination of SExtractor and improvements made by eye. Using the final mosaics and the masks, the surface brightness profiles could be obtained in the usual way. No errors are calculated at a certain radius but instead the 3-σ rejected mean of the flat part of the surface brightness profile at a far out part from the galaxy is taken as a residual background. If adding or subtracting the residual background would cause the surface brightness at a certain distance to change by 0.2 magnitude/square arcsec the datapoint is rejected. Due to the method that was used to generate the images, the images are about 2 magnitudes deeper than normal SDSS images. This is especially true for the g' and r' bands, where the observations were of the highest quality. In all cases, the g' band was able to probe the deepest and reach a depth of around 30 magnitudes/square arcsec. The surface brightness profiles show various different behaviour. Furthermore, the colour profiles show a flat
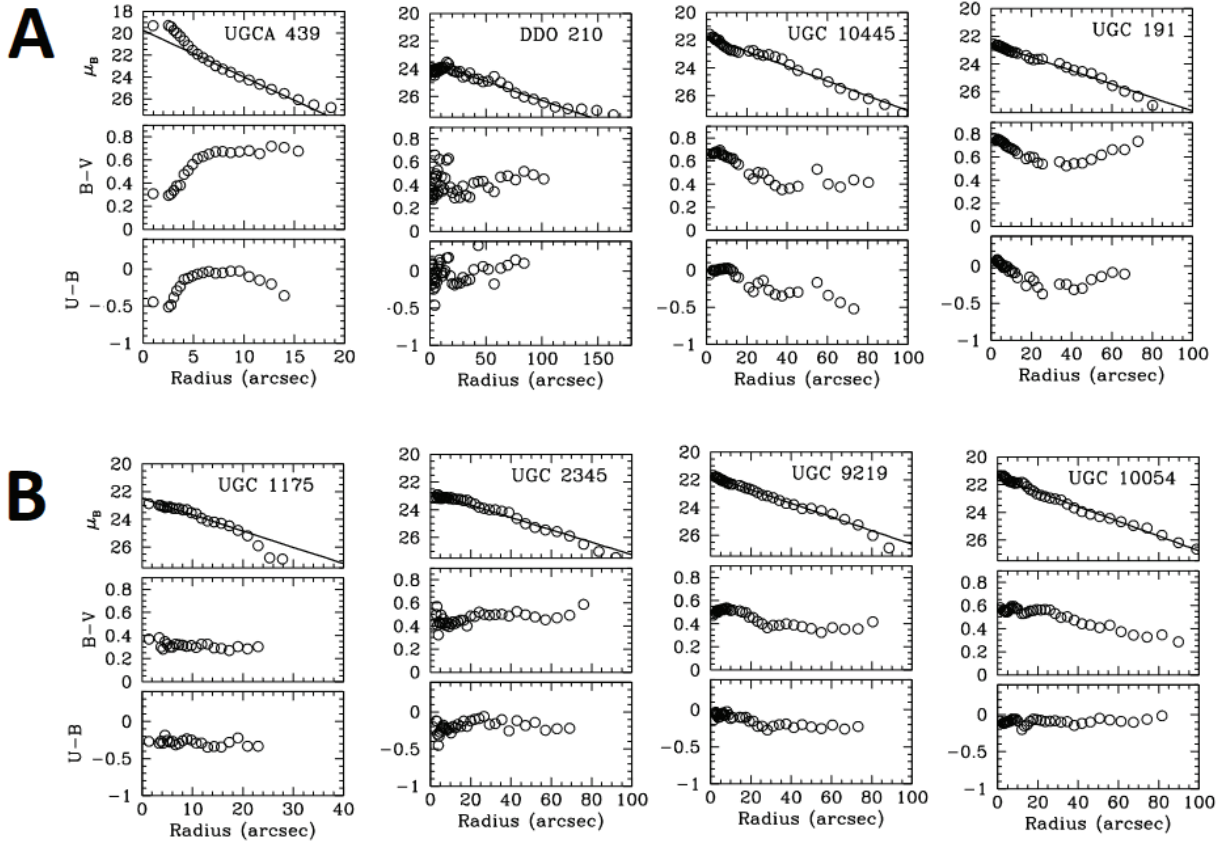
Figure 5: Row A: examples of profiles produced by van Zee that show behaviour that is not seen in the profiles produced in this thesis. Row B: examples of profiles produced by van Zee that show behaviour which is seen in the profiles produced in this thesis.

behaviour at small radii, while they start to trail off at larger radii.

Bakos et al. produce similarly deep surface brightness profiles as the ones produced in this thesis. This is not unexpected, as both use a similar method of creating very deep images, namely by stacking multiple high quality observations and creating mosaics. The reason why the shapes of the produced surface brightness and colour profiles that Bakos et al. produce is very different from the surface brightness and colour profiles produced in this thesis because different galaxy types are considered. Dwarf galaxies in this thesis and spirals for Bakos et al. Only the spiral NGC 1087 shows a surface brightness profile similar to the dwarf galaxies as can be seen in figure 6.

4.4 Comparison to Martinez-Lombilla et al.

The goal of Martinez-Lombilla et al. was to investigate the disc truncation of two spiral galaxies, NGC 4565 and NGC 5907. They did this by observing the galaxies in wavelengths from the near ultraviolet and optical to 3.6 μm using the 0.6m CWRU Burrell Schmidt Telescope at Kitt Peak National Observatory. In the process of investigating this, very deep surface brightness profiles with well defined errors are created. These surface brightness profiles were created using mosaics created from the original exposures. The total amount of exposure time that was used to generate the mosaics for NGC 4565 was 12050.15 seconds and 15118.45 seconds for NGC 5907. This leads to a surface brightness depth of 30.5 mag/square arcsec at a
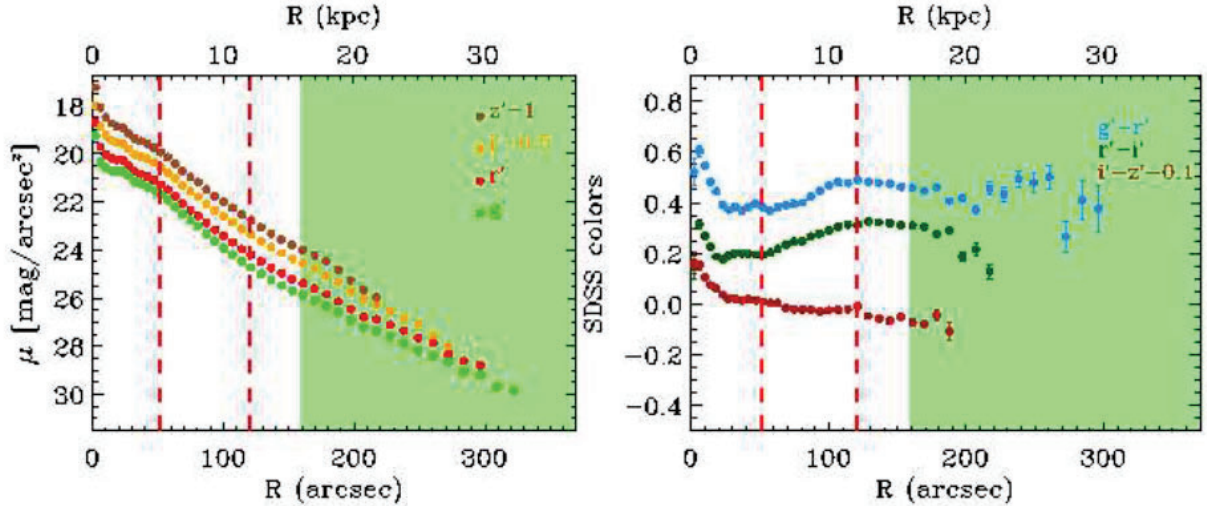
14

Figure 6: Surface brightness profiles (left) and colour profiles (right) of the galaxy NGC 1087 produced by Bakos et al. The surface brightness profiles go to a depth comparable to the surface brightness profiles produced in this thesis.

1σ error in the background. Before the images are mosaiced together, the background is determined and subtracted in each exposure. Because the optics used by Martinez-Lombilla et al. are less complicated than the ones used by the FDS, the sky background of Martinez-Lombilla et al. is flatter than the one in the FDS. Then after this background is subtracted an additional second background value is subtracted. This was done in two steps, first a mask of the foreground objects is applied to the images. After this a gradient of the surface brightness profile of the main galaxy is created until a large radius of about 1.5 times the size of the galaxy. The mean value of a flat region of the gradient at the outer parts of the galaxy is taken as the background value and subtracted from the image. The advantage of this method is that it allows for a very clear identification of the outer bounds of the galaxy. Surface brightness profiles were created from these final double background corrected mosaics. The galaxies investigated in the paper are edge-on, which allowed Martinez-Lombilla et al. to create the surface brightness profiles at different heights from the central plane and with that investigate disc truncation. The error in the surface brightness values is given by the combination of Poisson error and the sky error in each of the bins. The surface brightness profiles could reach a depth of roughly 28 magnitudes/square arcsec in optical passbands as shown in figure 7 and 30 magnitudes/square arcsec in near ultraviolet passbands. The method used by Martinez-Lombilla et al. is slightly different from the method used in this thesis. Instead of determining the residual background of the mosaiced image in a similar way to the background in the original exposures their method used the surface brightness values of the very outer reaches of the galaxy as the residual background. Their method works great as evident from the depth that was reached in the images, it does not seem to be a straight improvement over the method used in this thesis especially considering the fact that their method is harder to use with a less flat background. It might be worthwhile to check both methods if possible to see which one results in the greatest accuracy in the surface brightness values when creating them in the future.

4.5   Comparison to Rudick et al.

The goal of Rudick et al. was to investigate the low surface brightness features in the core of the Virgo cluster.They did this by performing deep observations of the core of the Virgo cluster and in the process created a colour profile for the elliptical galaxy M87 which is located in the core of the cluster. The observations were made using the 0.6m CWRU Burrell Schmidt telescope at Kitt Peak National Observatory
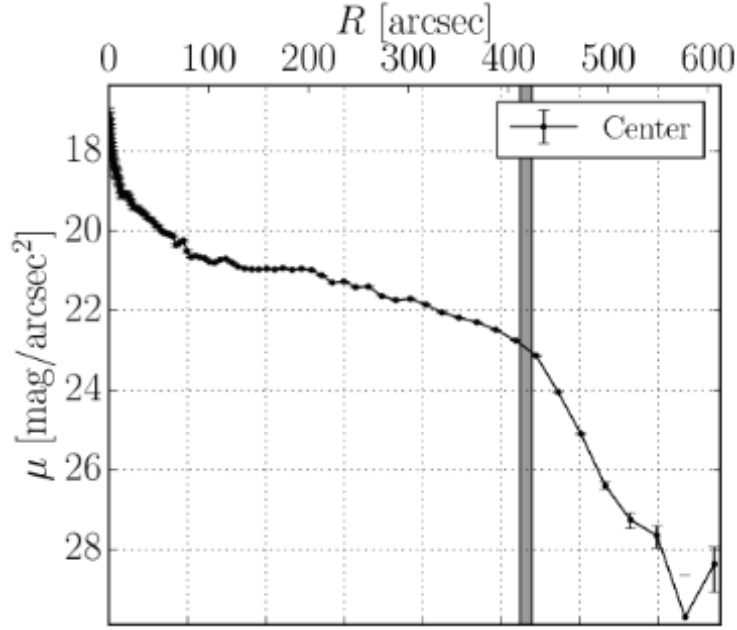
15

Figure 7: Surface brightness profile of NGC 4565 in the optical regime as produced by Martinez et al. The profile goes to a depth of approximately 28 magnitudes/square arcsec.

in the B band and the B-V colour profile was created using additional data in the V band from Mihos et al. [15]. The B band images were sky background value subtracted in the following way. The bright objects were masked out of the images, after which the images were binned. The median values of the bins were then collected and a plane is fitted to these median values. This plane is taken as the position dependent background. Applying this method is not without problem, since the exposures that were pointed at the center of the Virgo cluster contain a lot of low intensity intracluster light. It is therefore hard to find pixels with purely background and because the intracluster light varies in a similar way to the sky background it is hard to differentiate between them. Despite this a background was able to be fitted and subtracted from the images. After this, the images can be mosaiced on top of eachother in a way similar to what was done with the FDS. After this a residual background is removed in the same way as the sky background described above. Due to the initial background subtraction of the original sky background in the exposures, the sky error in the surface brightness values of the final mosaic is rather large at 1 analog-to-digital unit (ADU). In contrast, this means that a surface brightness value of 28 mag/square arcsec will have an error of 0.4 mag/square arcsec. Despite this, the B-V colour profiles could be produced with ±1 ADU error bars which is shown in figure 8. A small blue-ward slope is observed in the profile by the writers although it is hard to say how far this behaviour continues due to the huge error bars at large radii. The source of error of the colour profile in the paper by Rudick et al. is the same as the source of error for the colour profiles in this thesis. The main difference though is that the depth of the profiles in this thesis is greater than the depth that was reached by Rudick et al. The reason for this is of course that the background of the images that were used to generate the profiles in this thesis are not filled with intracluster light or any other form of noise which allows for an easier determination of background values.
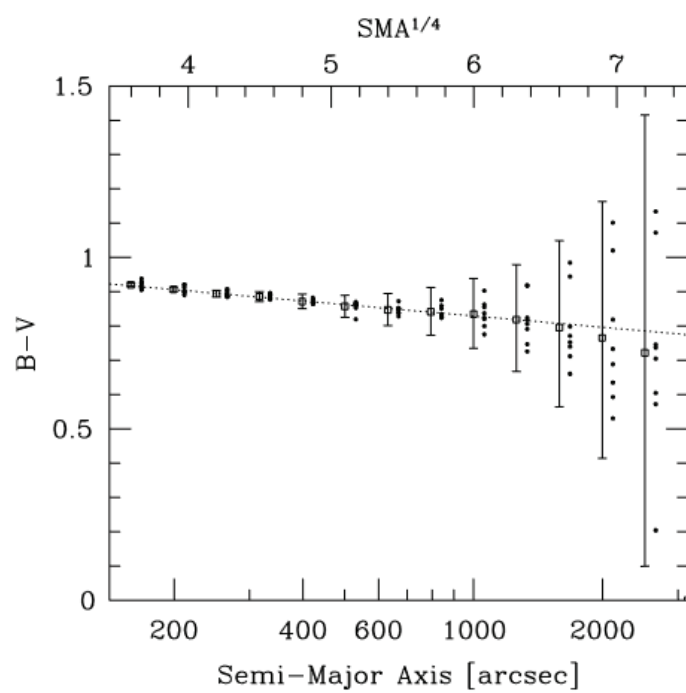
Figure 8: Colour profile in the B-V colour of M81 as produced by Rudick et al.

5 Discussion and conclusions

In this thesis the data generation process of the FDS is described and a method to determine the residual background values together with sensible errors is developed for 10 dwarf galaxies in the Fornax cluster. This method creates a single background value for an entire image, in contrast to the work of Shivangee Rathi where a 2D polynomial background is fitted to the residual background and applied to the images. The results shown in appendix 5 generally show a power law behaviour for the different surface brightness profiles and a flat colour profile for the different colours. There are cases though where the colour profiles show a blueish or reddish shift as the distance increases. This is similar to the results found by van Zee [5]. The bumps that can be found on some of the colour profiles could be explained by the way that the masks are created. When masking, some bright sources in the regime of the dwarf galaxy are also masked. This is sometimes useful as a bright source can be in front or behind the dwarf and cause interference because of that, however if the source belongs to the galaxy a portion of its light is masked away, which would decrease the observed amount of light at that point in the galaxy and cause a bump. Improved masks might fix this problem by excluding all objects that belong to the dwarf galaxy.

Compared to previous research into galaxies the surface brightness depth reached in this thesis is comparable if not better. Not much research has been done into dwarf galaxies, so reaching a depth of 30 mag/square arcsec when analyzing their surface brightness and colour profiles is a great development. Another great advantage of the profiles created in this thesis compared to others is that the error in the residual background values have been carefully and sensibly created in contrast to previous research where that is often not the case. By using the methods described in this thesis, many other dwarf galaxies found in the FDS or similar surveys can be properly analyzed.

References

[1] Shivangee Rathi. "The stellar lives of dwarf galaxies : photometric analysis of simulated and observed dwarf galaxies". PhD thesis. Gent U., Krijgslaan 281, S9, 9000, Gent, Belgium, 2021.

[2] Judit Bakos and Ignacio Trujillo. *Deep Surface Brightness Profiles of Spiral Galaxies from SDSS Stripe82: Touching Stellar Halos*. 2012. DOI: 10.48550/ARXIV.1204.3082. URL: https://arxiv.org/abs/1204.3082.

[3] Cristina Martinez-Lombilla, Ignacio Trujillo, and Johan H Knapen. "Discovery of disc truncations above the galaxies' mid-plane in Milky Way-like galaxies". In: *Monthly Notices of the Royal Astronomical Society* 483.1 (Oct. 2018), pp. 664–691. ISSN: 0035-8711. DOI: 10.1093/mnras/sty2886. eprint: https://academic.oup.com/mnras/article-pdf/483/1/664/27012464/sty2886.pdf. URL: https://doi.org/10.1093/mnras/sty2886.

[4] Craig S. Rudick et al. "OPTICAL COLORS OF INTRACLUSTER LIGHT IN THE VIRGO CLUSTER CORE". In: *The Astrophysical Journal* 720.1 (Aug. 2010), pp. 569–580. DOI: 10.1088/0004-637x/720/1/569. URL: https://doi.org/10.1088%5C%2F0004-637x%5C%2F720%5C%2F1%5C%2F569.

[5] Liese van Zee. "The Evolutionary Status of Isolated Dwarf Irregular Galaxies. I. UBV and Hα Imaging Observations". In: *The Astronomical Journal* 119.6 (June 2000), pp. 2757–2779. DOI: 10.1086/301378. URL: https://doi.org/10.1086/301378.

[6] M. G. Watson et al. "The XMM-Newton serendipitous survey. V. The Second XMM-Newton serendipitous source catalogue". In: *Astronomy and Astrophysics* 493.1 (Jan. 2009), pp. 339–373. DOI: 10.1051/0004-6361:200810534. arXiv: 0807.1067 [astro-ph].

[7] O. G. Nasonova, J. A. de Freitas Pacheco, and I. D. Karachentsev. "Hubble flow around Fornax cluster of galaxies". In: *Astronomy and Astrophysics* 532, A104 (Aug. 2011), A104. DOI: 10.1051/0004-6361/201016004. arXiv: 1106.1291 [astro-ph.CO].

[8] Aku Venhola et al. "The Fornax Deep Survey with the VST. IV. A size and magnitude limited catalog of dwarf galaxies in the area of the Fornax cluster". In: *Astronomy & Astrophysics* 620, A165 (Dec. 2018), A165. DOI: 10.1051/0004-6361/201833933. arXiv: 1810.00550 [astro-ph.GA].

[9] Henry C Ferguson. "Population studies in groups and clusters of galaxies. II-A catalog of galaxies in the central 3.5 deg of the Fornax Cluster". In: *The Astronomical Journal* 98 (1989), pp. 367–418.

[10] Andrés Jordán et al. "The ACS Fornax Cluster Survey. I. Introduction to the Survey and Data Reduction Procedures". In: *The Astrophysical Journal Supplement Series* 169.2 (Apr. 2007), pp. 213–224. DOI: 10.1086/512778. arXiv: astro-ph/0702320 [astro-ph].

[11] K. Kuijken et al. "OmegaCAM: the 16k×16k CCD camera for the VLT survey telescope". In: *The Messenger* 110 (Dec. 2002), pp. 15–18.

[12] Pietro Schipani et al. "VST: from commissioning to science". In: *Ground-based and Airborne Telescopes IV*. Ed. by Larry M. Stepp, Roberto Gilmozzi, and Helen J. Hall. Vol. 8444. Society of Photo-Optical Instrumentation Engineers (SPIE) Conference Series. Sept. 2012, 84441C, p. 84441C. DOI: 10.1117/12.925481.

[13] Reynier Peletier et al. *The Fornax Deep Survey data release 1*. 2020. DOI: 10.48550/ARXIV.2008.12633. URL: https://arxiv.org/abs/2008.12633.

[14] Kevork N. Abazajian et al. "The Seventh Data Release of the Sloan Digital Sky Survey". In: *The Astrophysical Journal Supplement* 182.2 (June 2009), pp. 543–558. DOI: 10.1088/0067-0049/182/2/543. arXiv: 0812.0649 [astro-ph].

[15] J. Christopher Mihos et al. "Diffuse Light in the Virgo Cluster". In: *The Astrophysical Journal* 631.1 (Sept. 2005), pp. L41–L44. DOI: 10.1086/497030. arXiv: astro-ph/0508217 [astro-ph].

Appendix A: Profile comparisons with Rathi

Comparisons between profiles produced in this thesis and other research
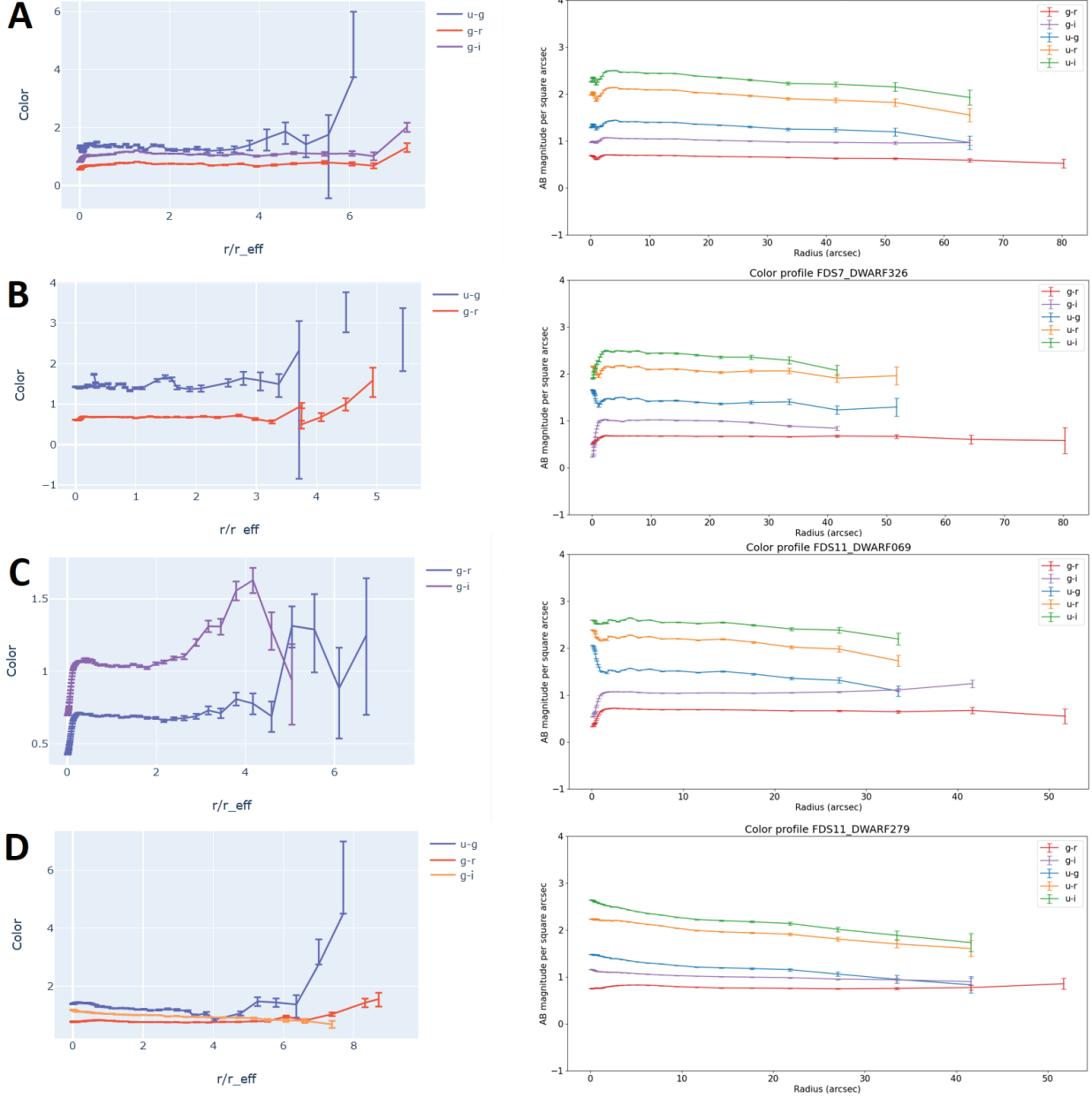

Figure 9: Comparison between colour profiles produced by Rathi [1] and colour profiles produced in this thesis. The profiles in the graphs in row A correspond to FDS2_DWARF000 where $r_{eff} = 14.5$ arcsec, the profiles in the graphs in row B correspond to FDS7_DWARF326 where $r_{eff} = 20.8$ arcsec, the profiles in the graphs in row C correspond to FDS11_DWARF069 where $r_{eff} = 11.1$ arcsec and the profiles in the graphs in row D correspond to FDS11_DWARF279 where $r_{eff} = 9.8$ arcsec. It can be seen that the profiles produced have more consistent shapes and error bars although they don't probe quite as far away from the center of the galaxy.

Appendix B: Dwarf galaxy FDS11_DWARF458

There is one exception to the method of determining the background described in section 2. One of the dwarf galaxies, FDS11_DWARF458 , had a badly defined background in the r' and i' bands. This resulted in a background that consisted of two bell curves. This distribution was simply fitted to a double Gaussian profile which gave two different background values and errors in those cases. It is not certain which pixel belongs to which background value. To still be able to derive some results from these images, the script subtracts checks the value of the pixel and compares it to the value at which both Gaussian profiles are equally represented, X. If the pixel value is below the value X, the lower background is subtracted and if the pixel value is above the value X, the larger background is subtracted. This is of course not entirely accurate since there will be cases where the wrong background is subtracted, especially for pixels closer to the center of the galaxy where there is no longer empty space. Because of this the error that is give to the pixels is equal to the difference between the peaks plus the error of the subtracted background. The fact that the wrong background might be subtracted does not have a huge influence on the pixels in the center of the galaxy since the counts there are large compared to the background value.

The result of fitting the background profile to a double Gaussian profile can be seen in figure 40. It is possible that for other galaxies a double Gaussian could also fit better, however if a single Gaussian fits well enough it is easier and often better to use that instead. This is because the method described above generates larger errors compared to the method described in section 2.

Appendix C: Results

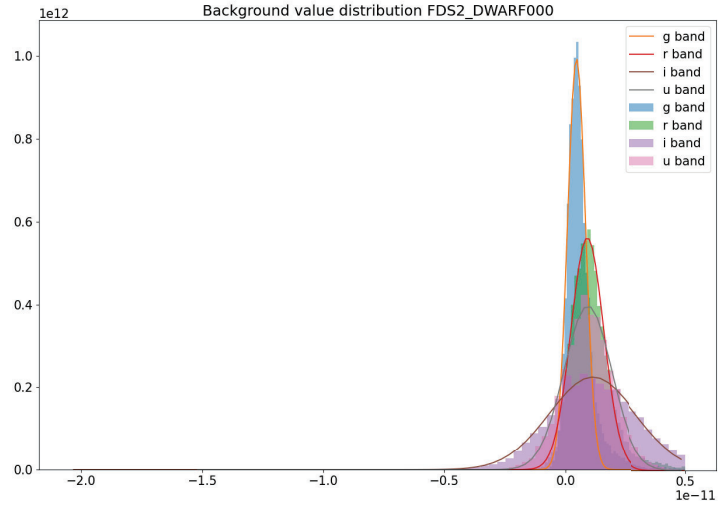Background distribution graphs and graphs containing the surface brightness profiles.

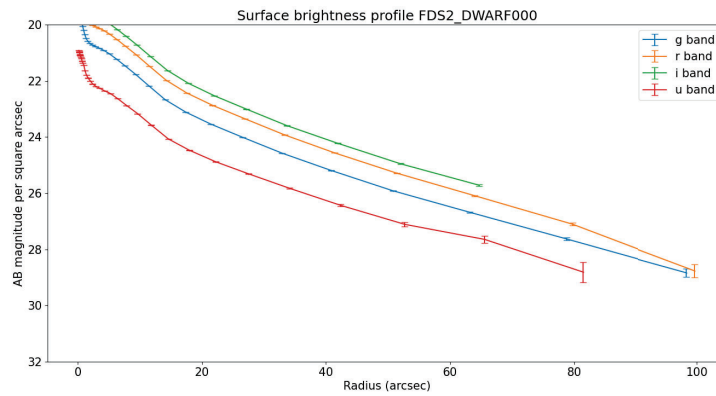Figure 10: Background distribution graph for galaxy FDS2_DWARF000

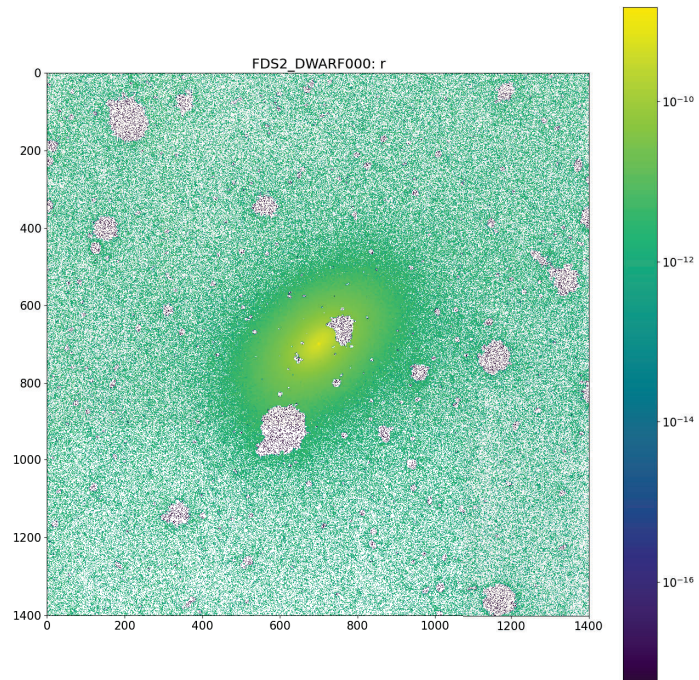Figure 11: Surface brightness profile as a function of distance for galaxy FDS2_DWARF000

Figure 12: Masked image in the r' band for galaxy FDS2_DWARF000
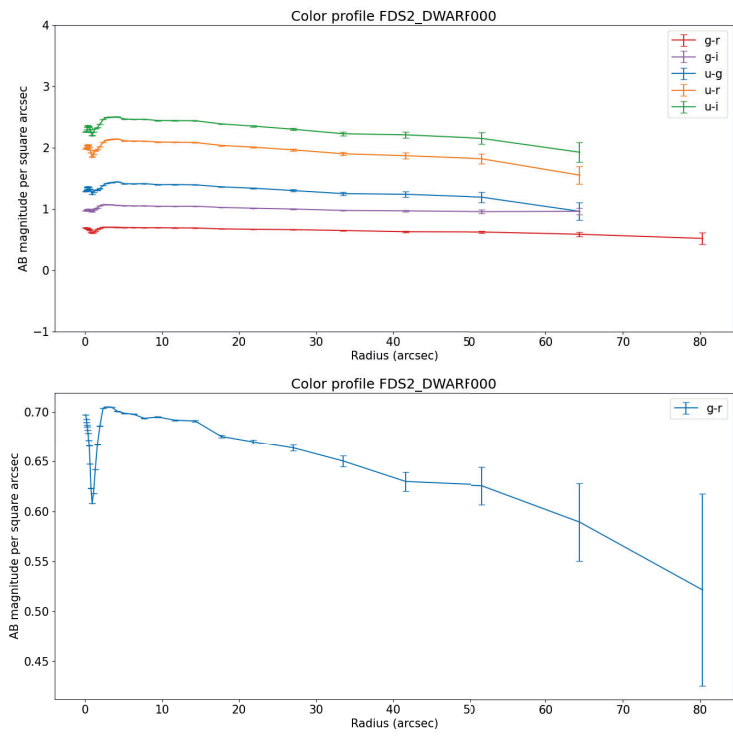
Figure 13: Color profiles as a function of distance for galaxy FDS2_DWARF000
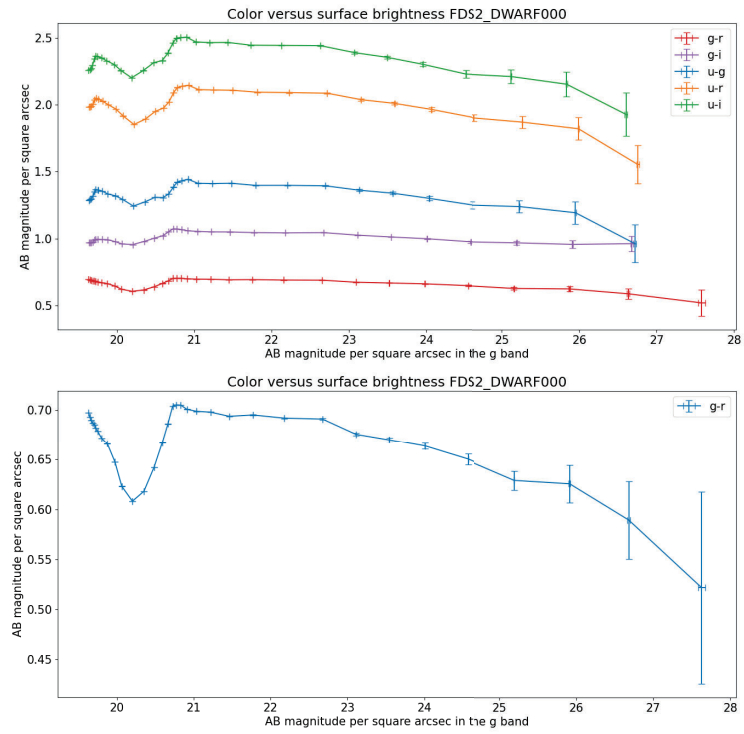
Figure 14: Color profiles as a function of g'-band magnitude for galaxy FDS2_DWARF000

Figure 15: Background distribution graph for galaxy FDS7_DWARF326

25

Figure 16: Surface brightness profile as a function of distance for galaxy FDS7_DWARF326

Figure 17: Masked image in the r' band for galaxy FDS7_DWARF326

Figure 18: Color profiles as a function of distance for galaxy FDS7_DWARF326

Figure 19: Color profiles as a function of g'-band magnitude for galaxy FDS7_DWARF326

Figure 20: Background distribution graph for galaxy FDS10_DWARF189

Figure 21: Surface brightness profile as a function of distance for galaxy FDS10_DWARF189

Figure 22: Masked image in the r' band for galaxy FDS10_DWARF189

Figure 23: Color profiles as a function of distance for galaxy FDS10_DWARF189

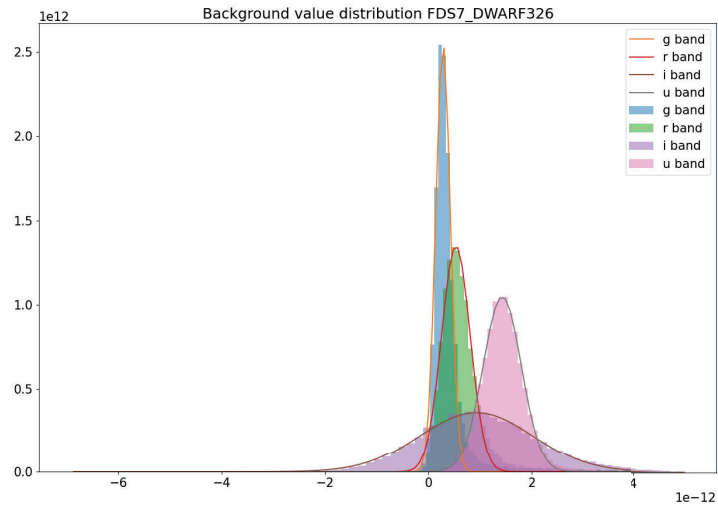Figure 24: Color profiles as a function of g'-band magnitude for galaxy FDS10_DWARF189

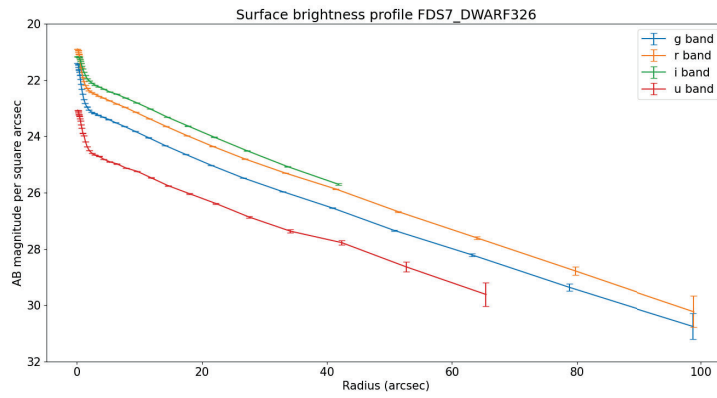Figure 25: Background distribution graph for galaxy FDS11_DWARF069

Figure 26: Surface brightness profile as a function of distance for galaxy FDS11_DWARF069

Figure 27: Masked image in the r' band for galaxy FDS11_DWARF069

Figure 28: Color profiles as a function of distance for galaxy FDS11_DWARF069

Figure 29: Color profiles as a function of g'-band magnitude for galaxy FDS11_DWARF069
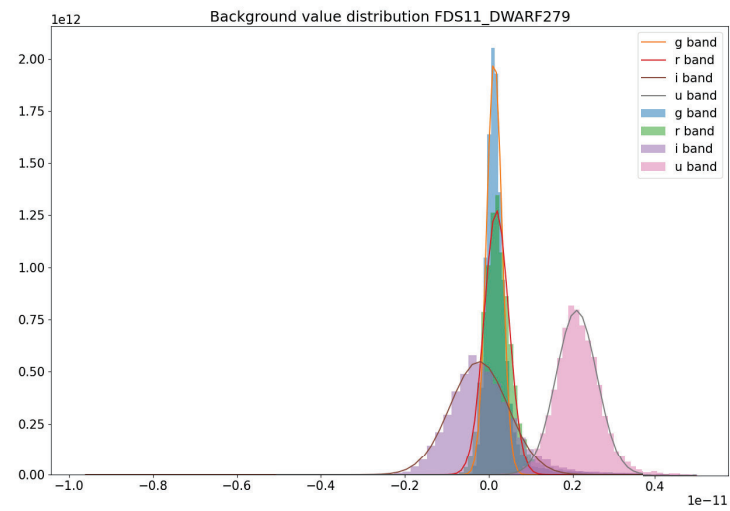
Figure 30: Background distribution graph for galaxy FDS11_DWARF279
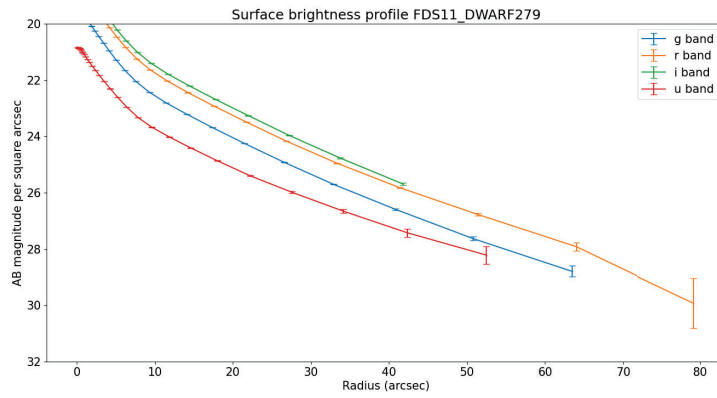
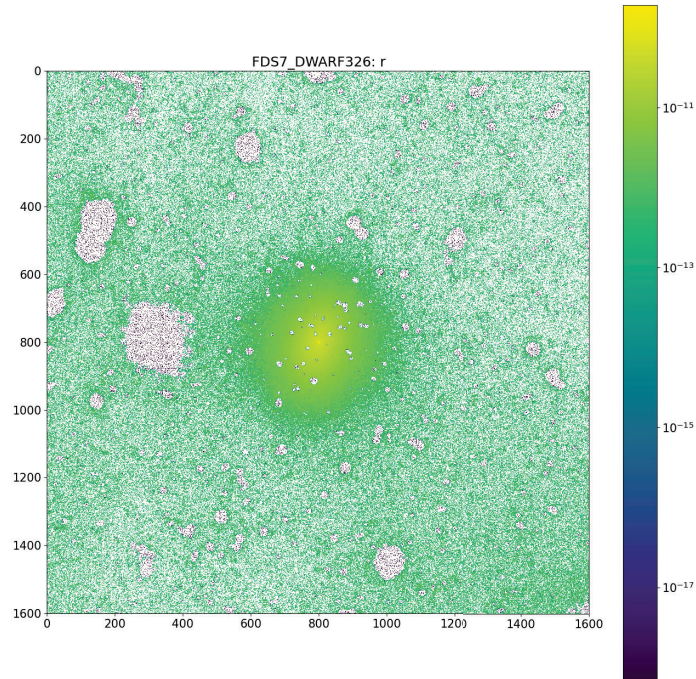Figure 31: Surface brightness profile as a function of distance for galaxy FDS11_DWARF279
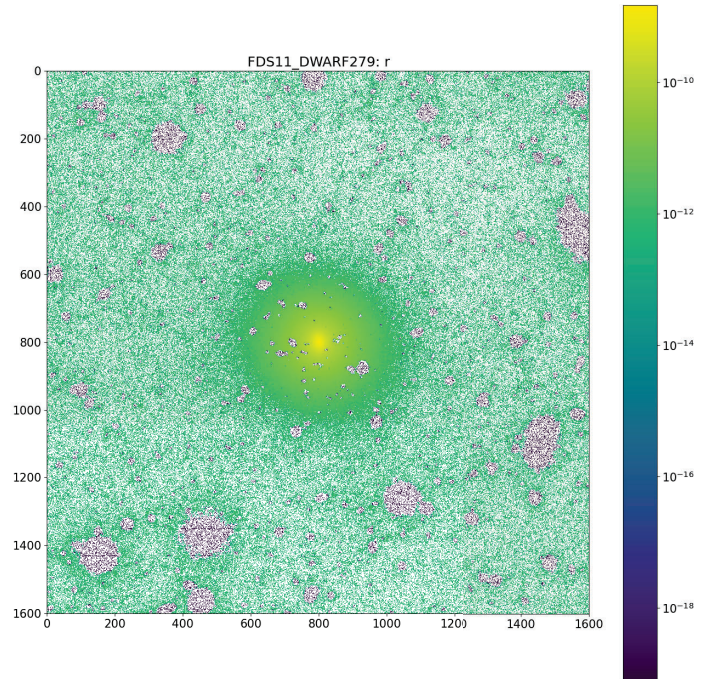
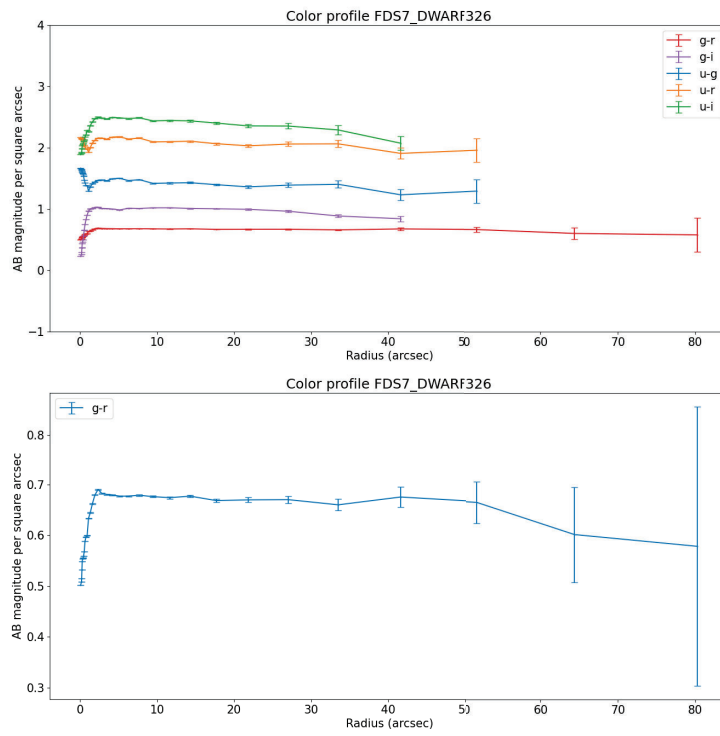Figure 32: Masked image in the r' band for galaxy FDS11_DWARF279
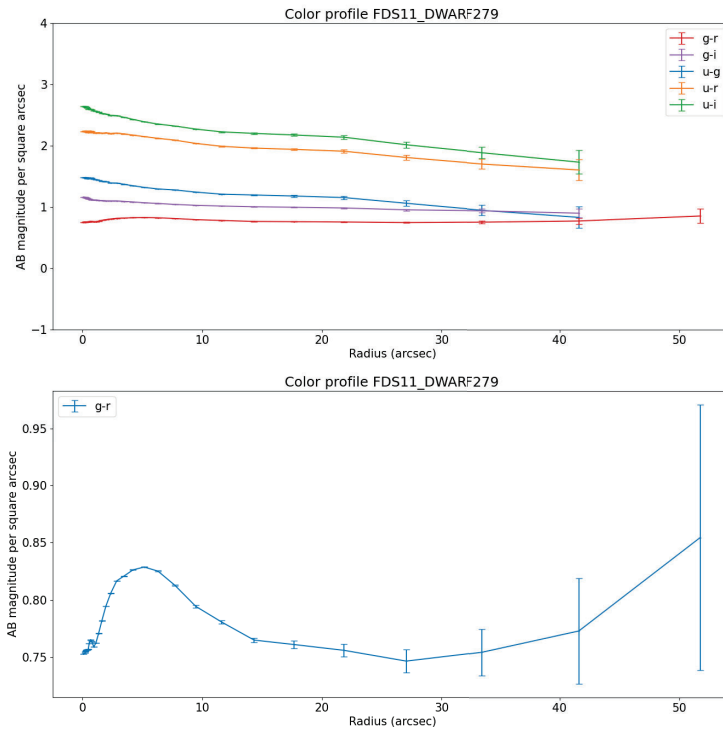
Figure 33: Color profiles as a function of distance for galaxy FDS11_DWARF279
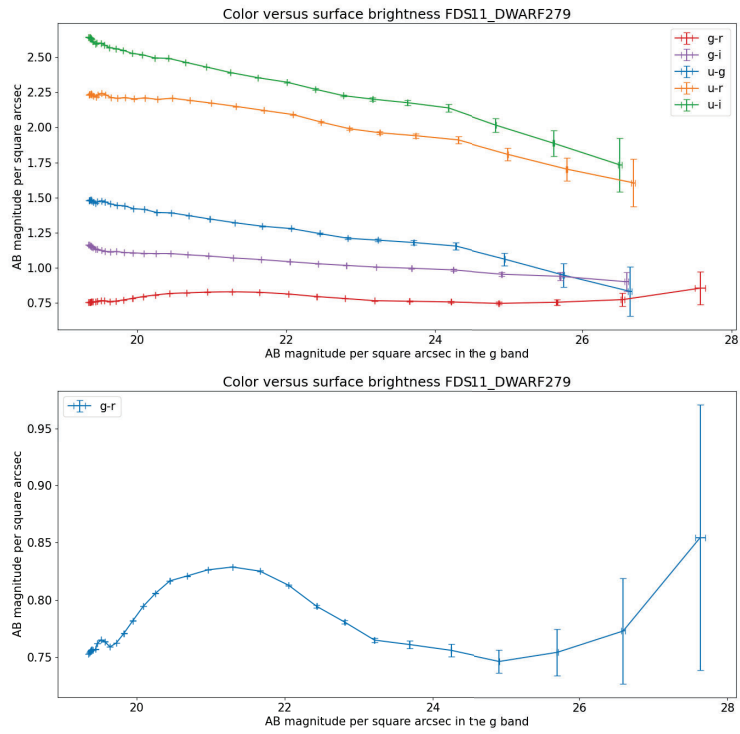
Figure 34: Color profiles as a function of g'-band magnitude for galaxy FDS11_DWARF279
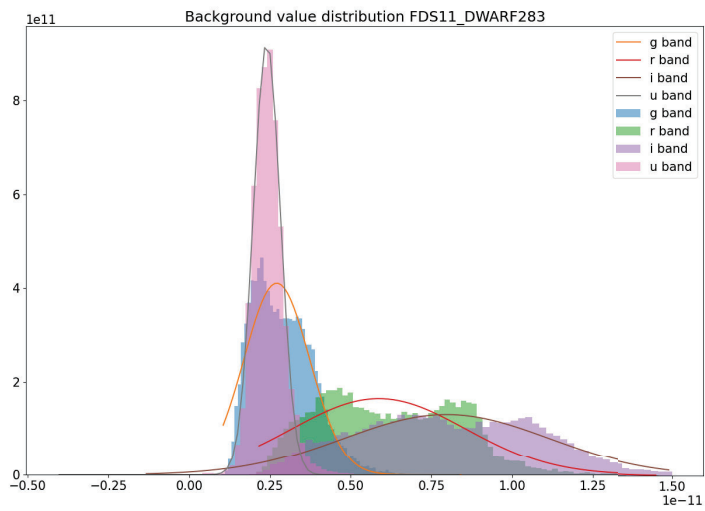
Figure 35: Background distribution graph for galaxy FDS11_DWARF283
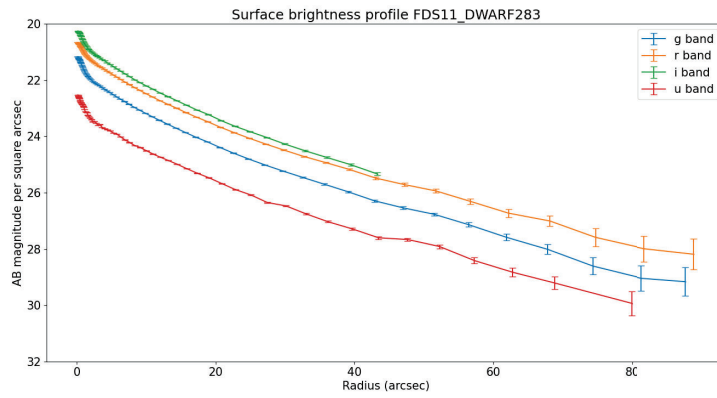
Figure 36: Surface brightness profile as a function of distance for galaxy FDS11_DWARF283
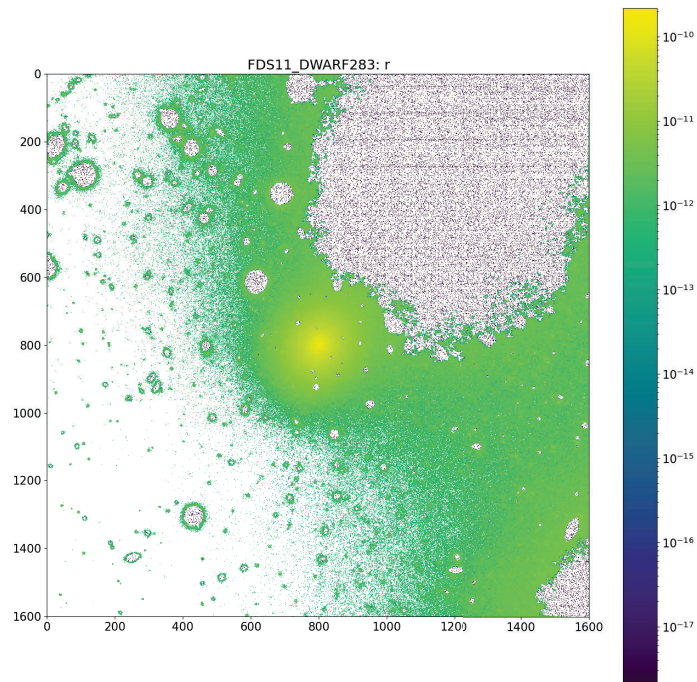
Figure 37: Masked image in the r' band for galaxy FDS11_DWARF283
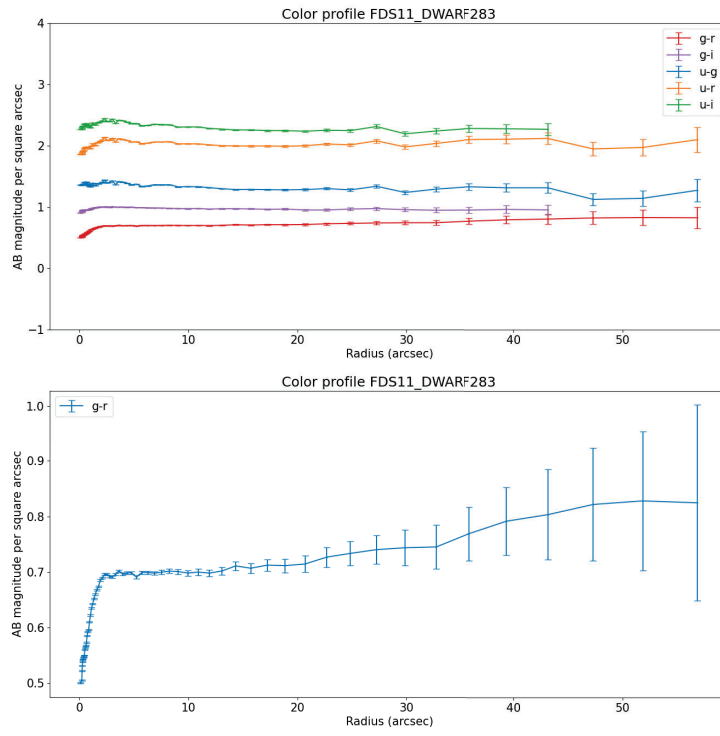
Figure 38: Color profiles as a function of distance for galaxy FDS11_DWARF283
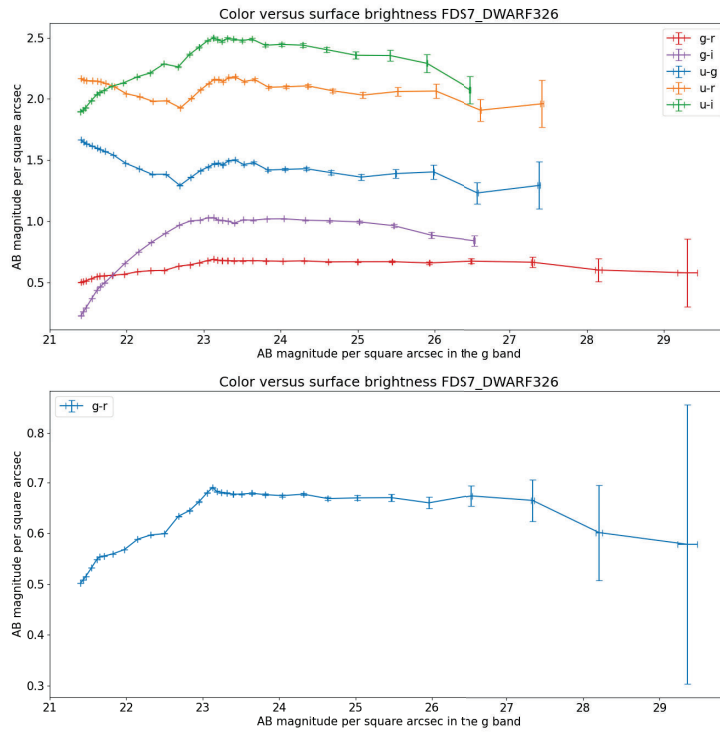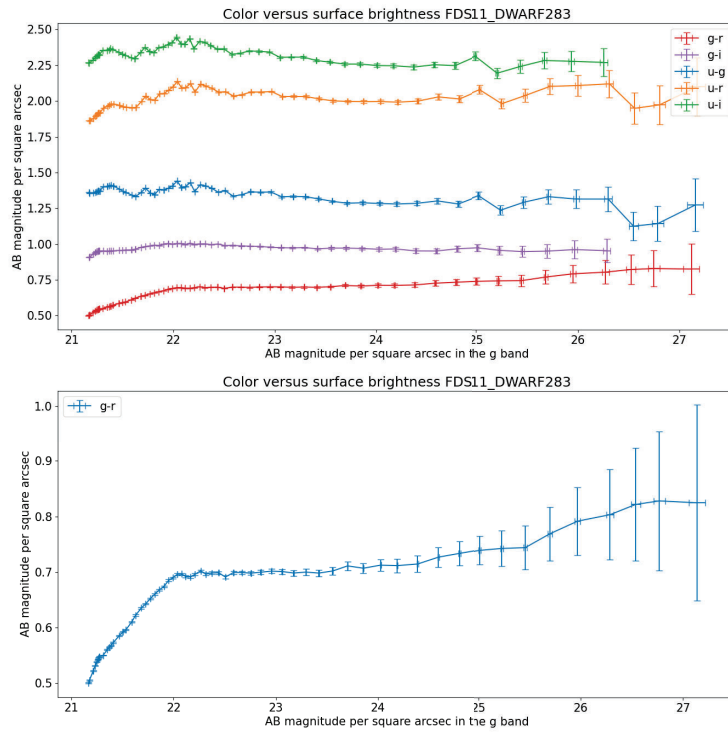
Figure 39: Color profiles as a function of g'-band magnitude for galaxy FDS11_DWARF283
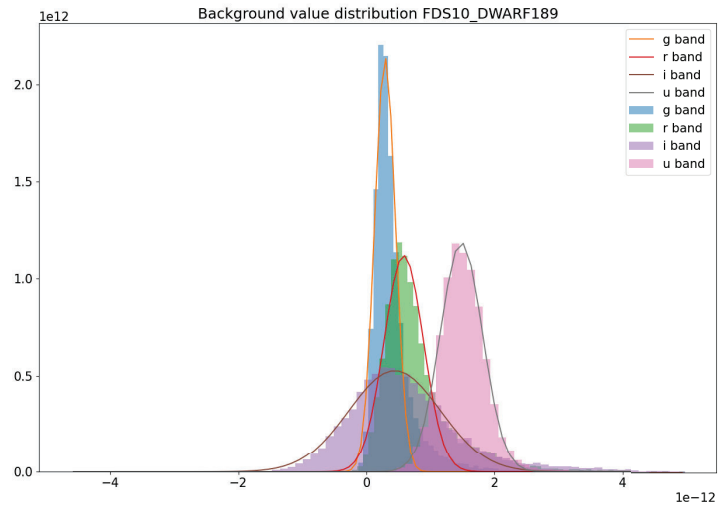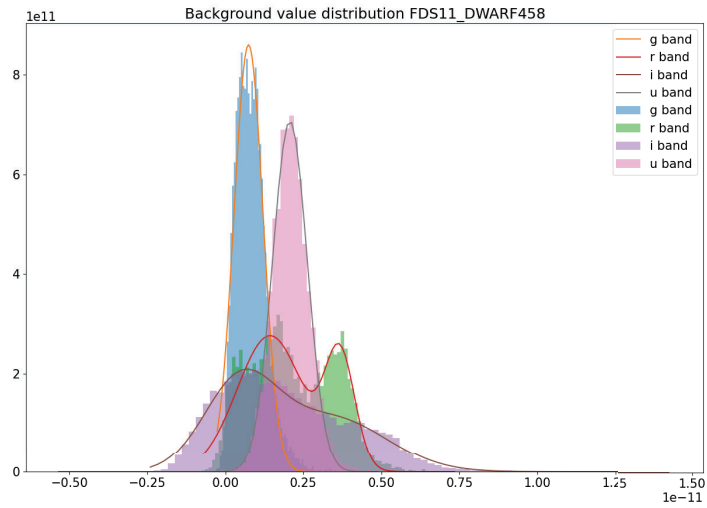

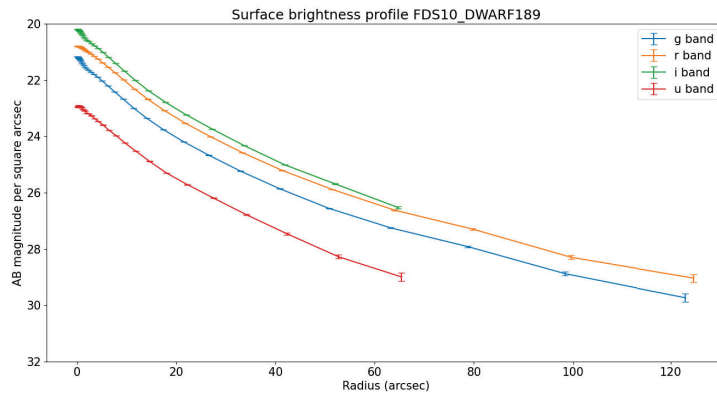Figure 40: Background distribution graph for galaxy FDS11_DWARF458
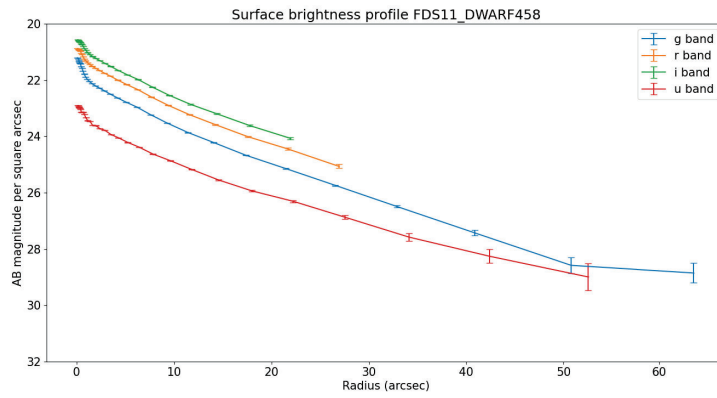
Figure 41: Surface brightness profile as a function of distance for galaxy FDS11_DWARF458
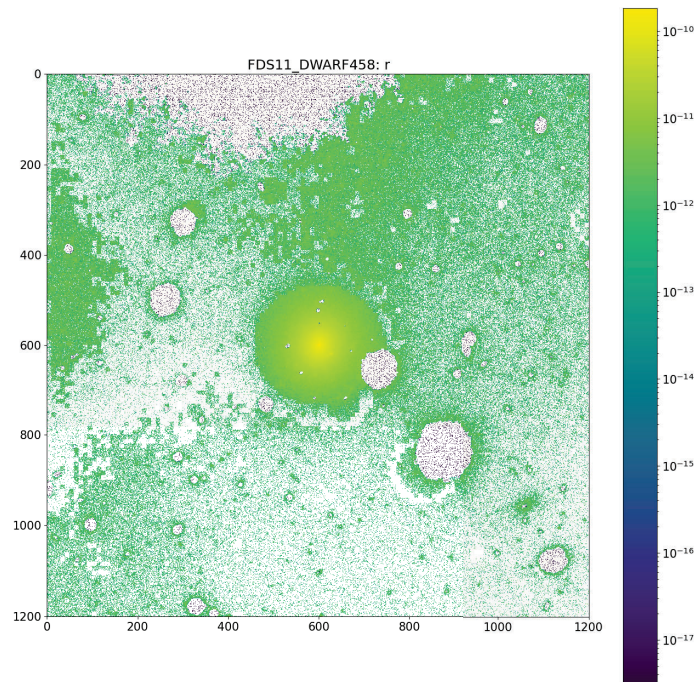
Figure 42: Masked image in the r' band for galaxy FDS11_DWARF458
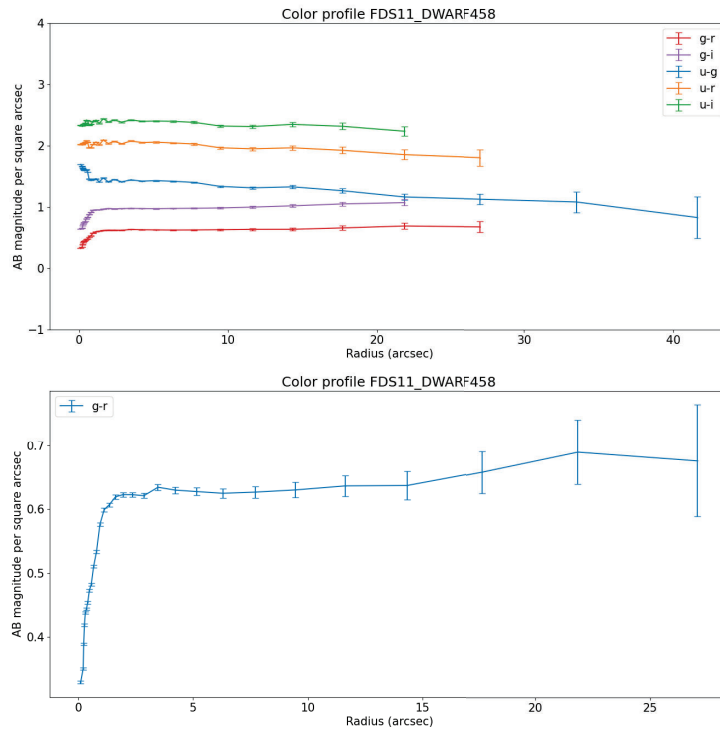
Figure 43: Color profiles as a function of distance for galaxy FDS11_DWARF458
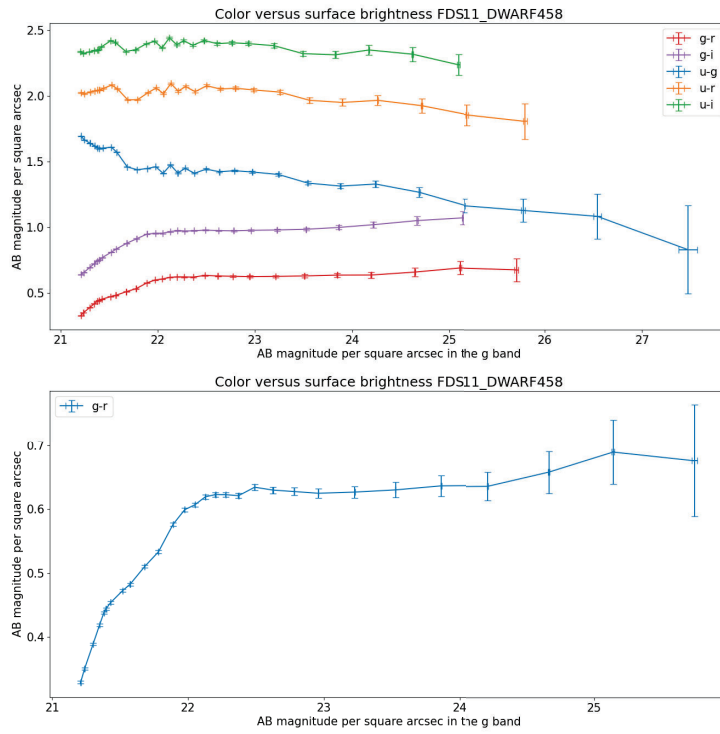
Figure 44: Color profiles as a function of g'-band magnitude for galaxy FDS11_DWARF458
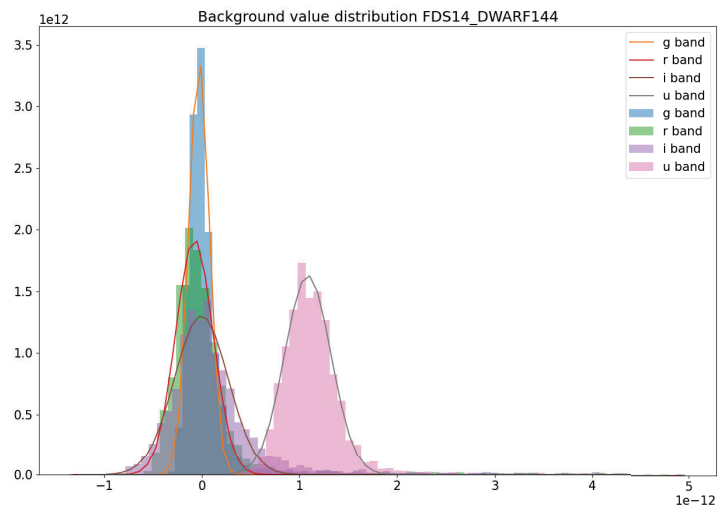
Figure 45: Background distribution graph for galaxy FDS14_DWARF144
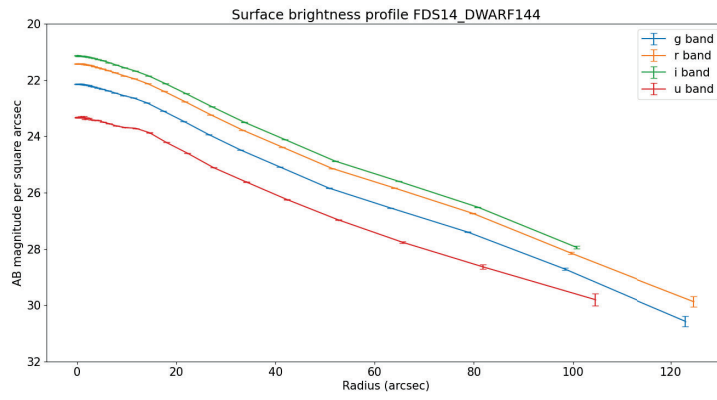
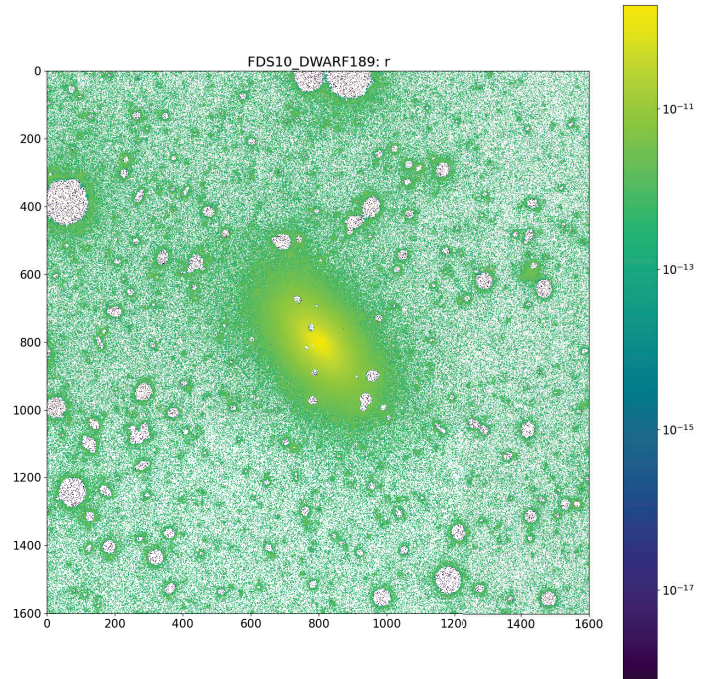Figure 46: Surface brightness profile as a function of distance for galaxy FDS14_DWARF144
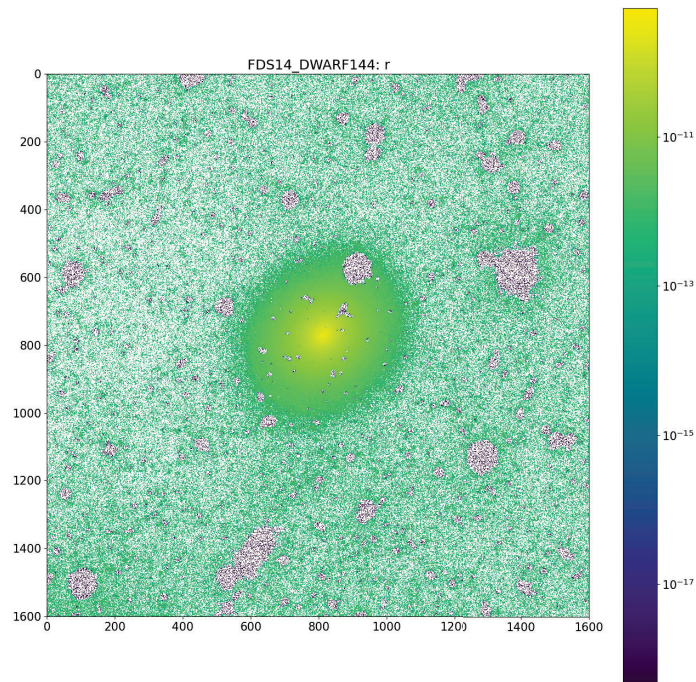
Figure 47: Masked image in the r' band for galaxy FDS14_DWARF144
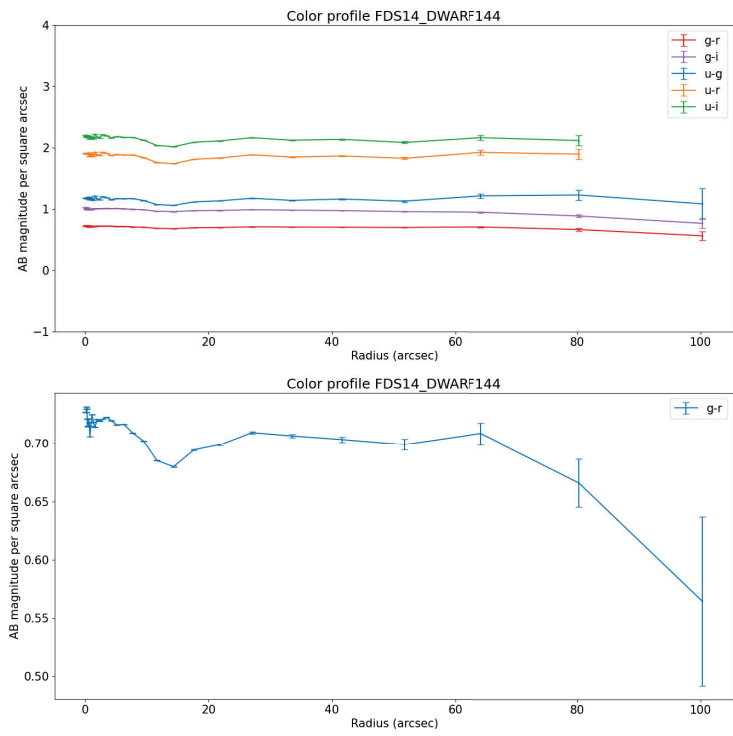
Figure 48: Color profiles as a function of distance for galaxy FDS14_DWARF144
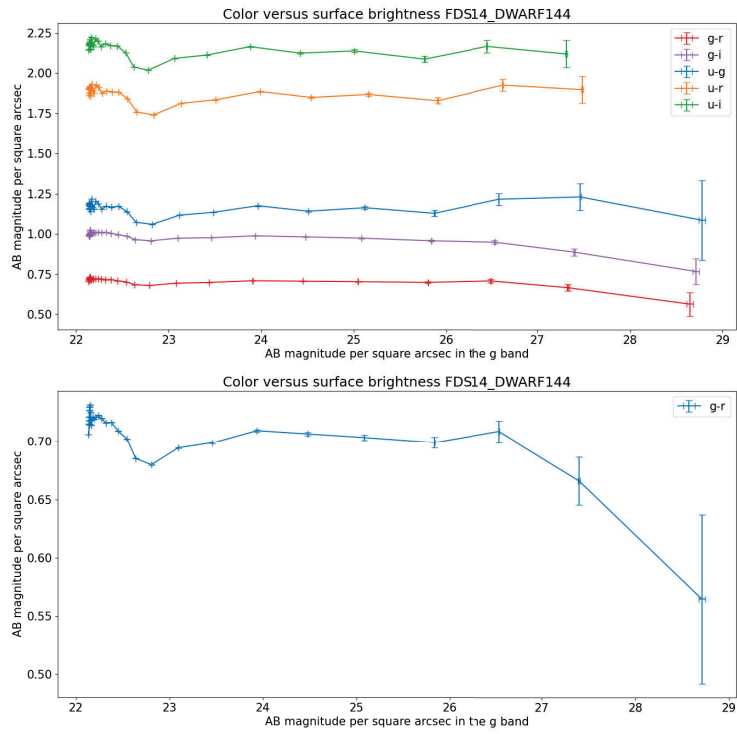
Figure 49: Color profiles as a function of g'-band magnitude for galaxy FDS14_DWARF144
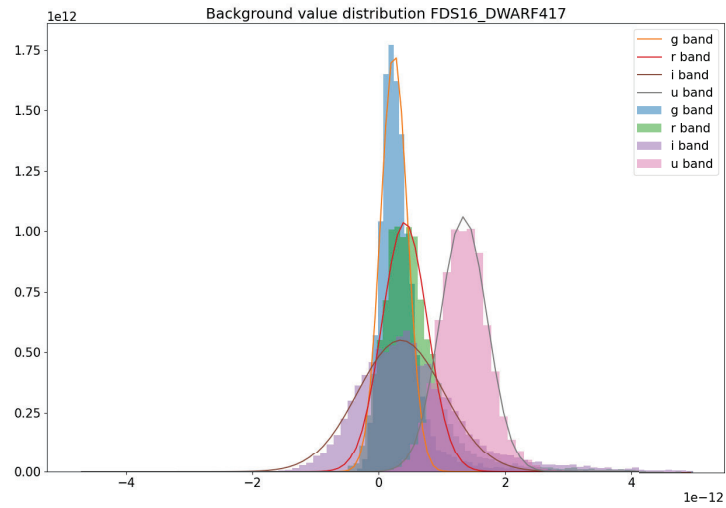
Figure 50: Background distribution graph for galaxy FDS16_DWARF417
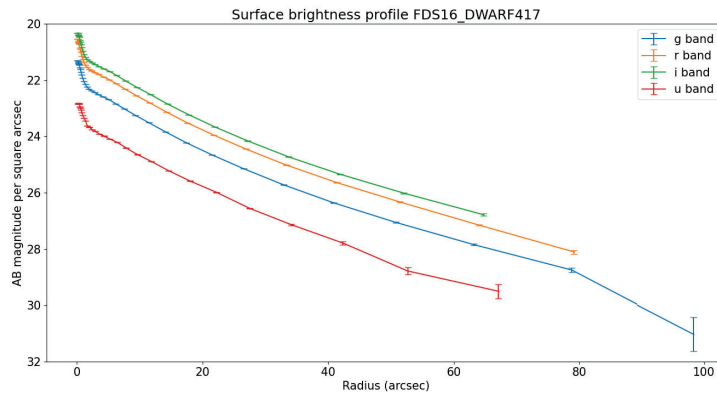
Figure 51: Surface brightness profile as a function of distance for galaxy FDS16_DWARF417
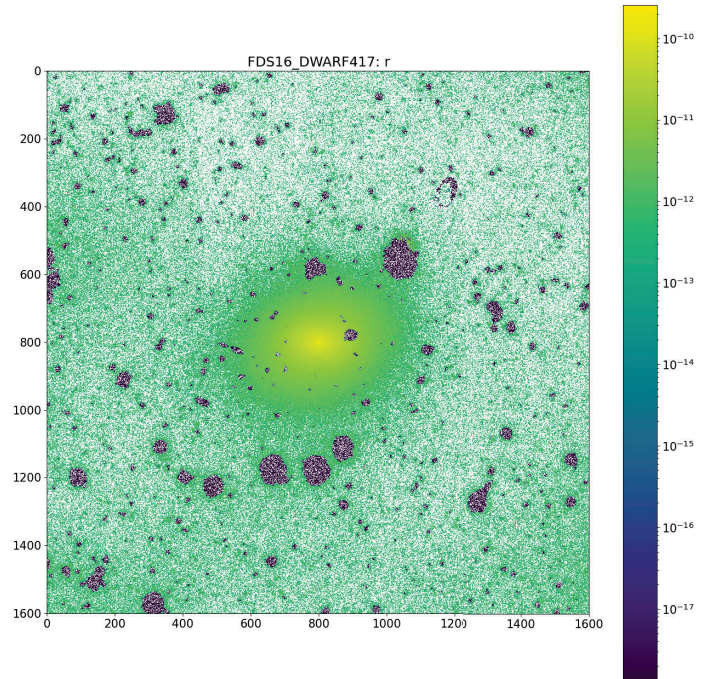
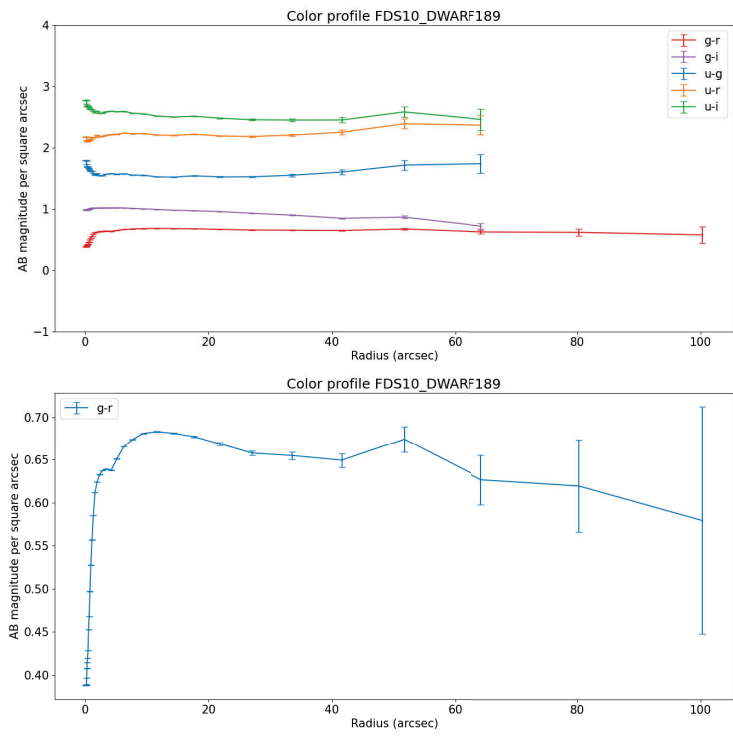Figure 52: Masked image in the r' band for galaxy FDS16_DWARF417
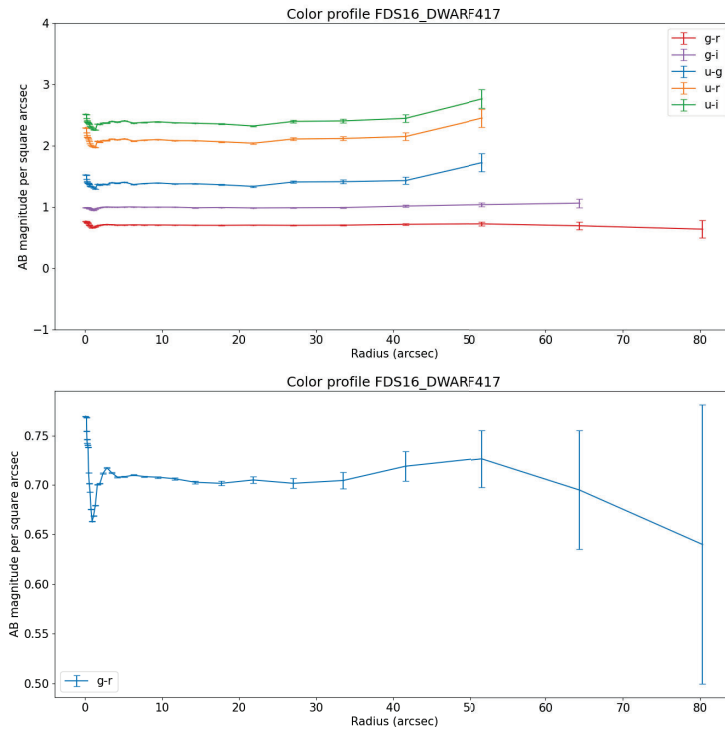
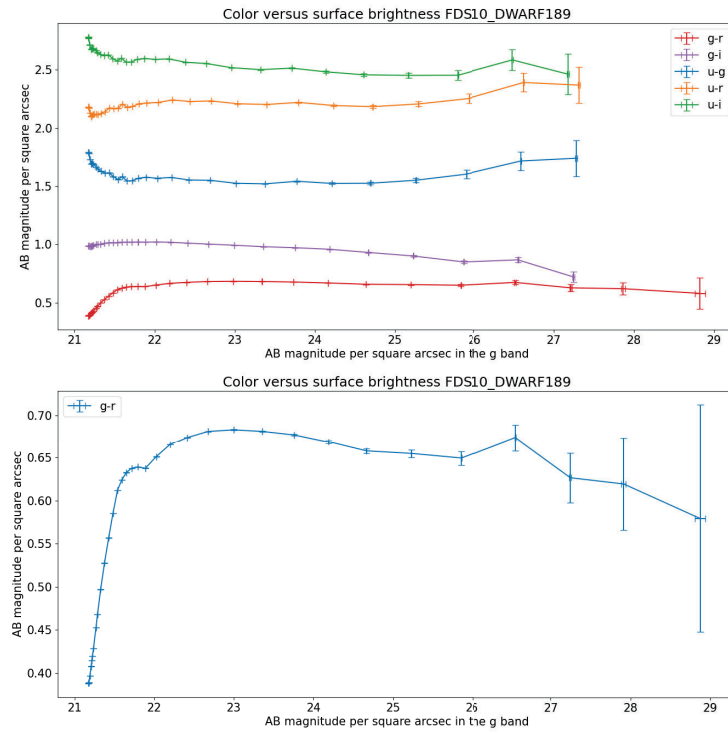Figure 53: Color profiles as a function of distance for galaxy FDS16_DWARF417
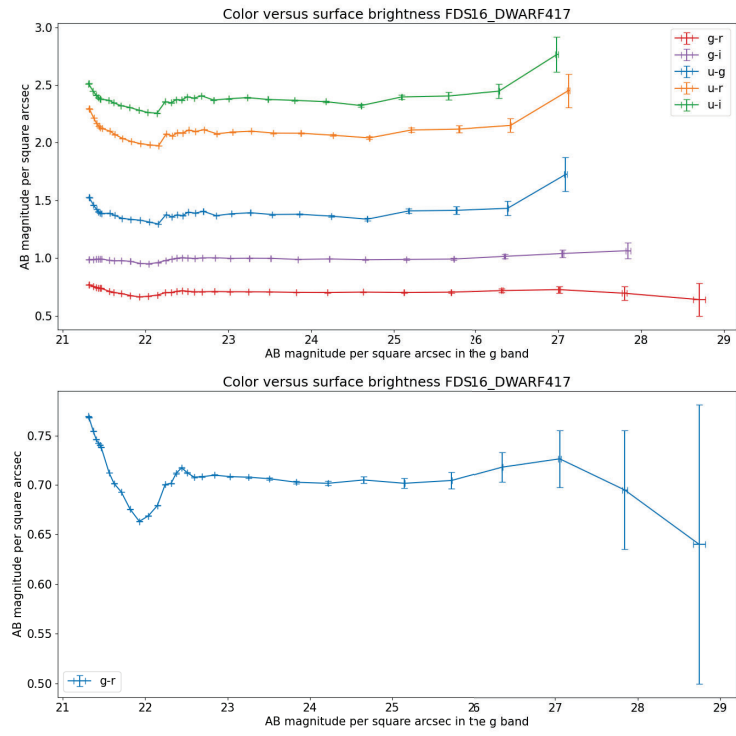
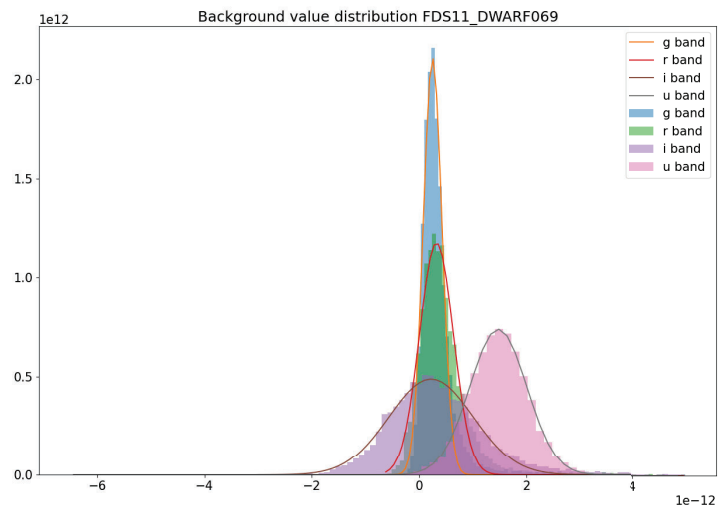Figure 54: Color profiles as a function of g'-band magnitude for galaxy FDS16_DWARF417
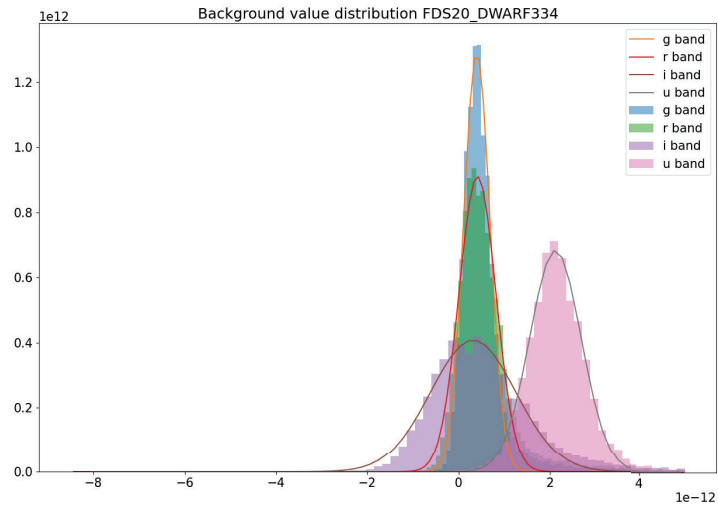
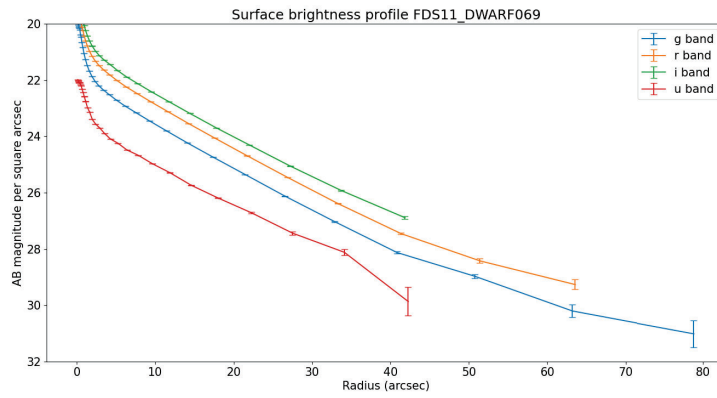Figure 55: Background distribution graph for galaxy FDS20_DWARF334
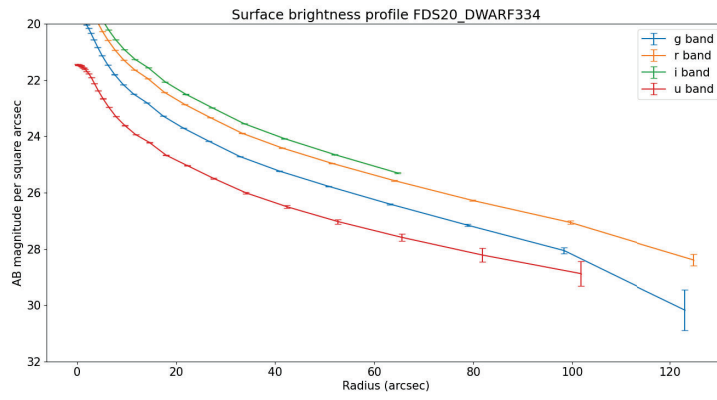
Figure 56: Surface brightness profile as a function of distance for galaxy FDS20_DWARF334
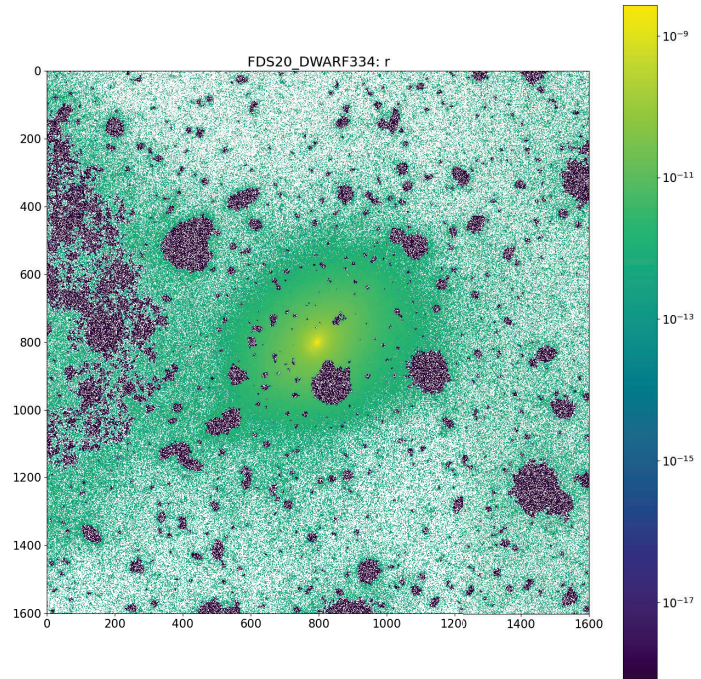
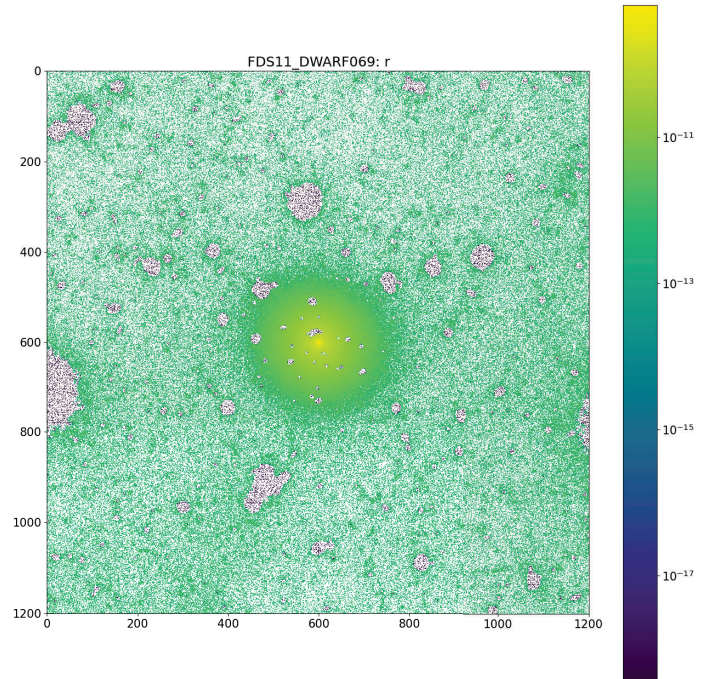

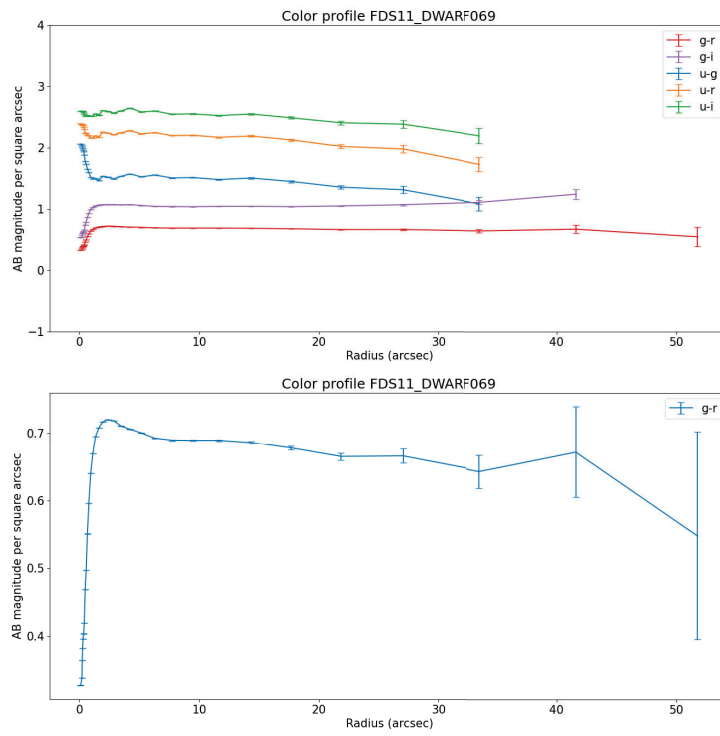Figure 57: Masked image in the r' band for galaxy FDS20_DWARF334

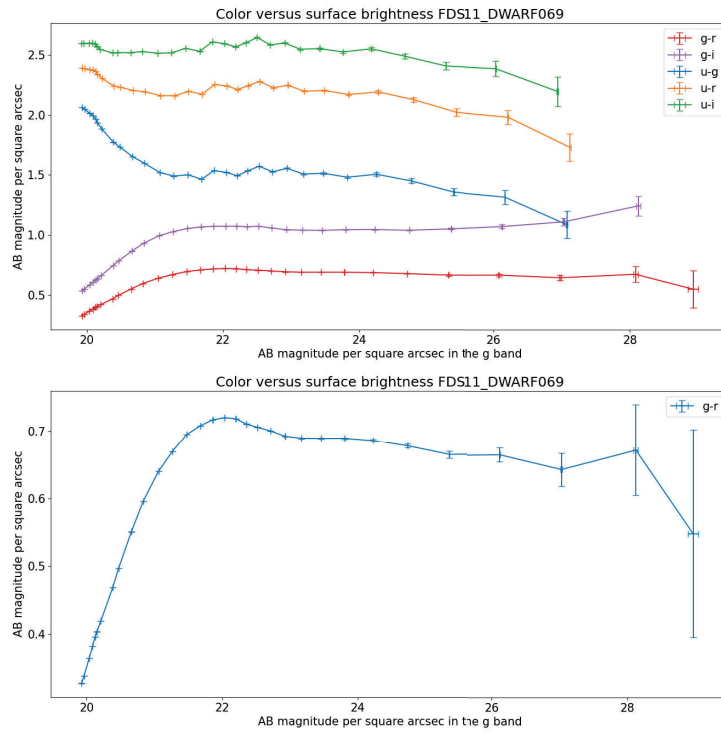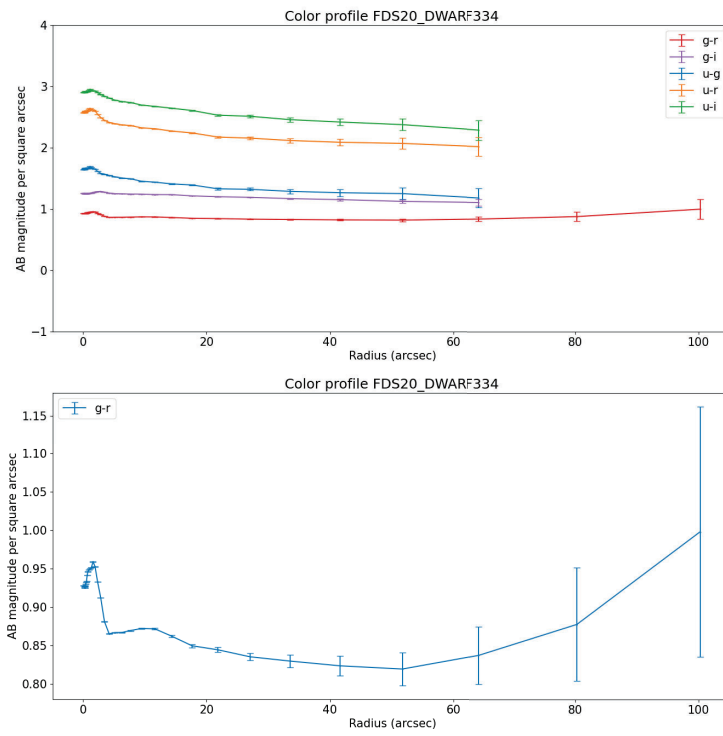Figure 58: Color profiles as a function of distance for galaxy FDS20_DWARF334
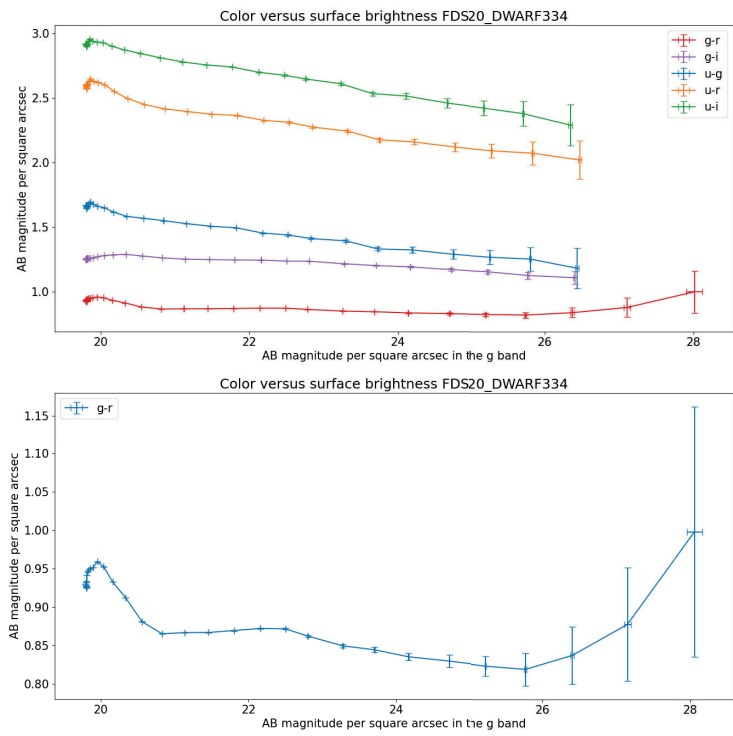
Figure 59: Color profiles as a function of g'-band magnitude for galaxy FDS20_DWARF334

Intermission

This full master thesis has been divided into two parts/projects. This is because my first project about the creation of 3D models was deemed to have too little of an astronomy research component to count for an astronomy masters project. The second (smaller) project about the creation of colour profiles for dwarf galaxies was therefore performed. Both projects have different first and second examiners. In order to create a connection between the two projects a piece of both was used to create a 3D model of the dwarf galaxy FDS16_DWARF417. This was done by using the methods described in both projects. Some pictures of this model in a 3D model viewer are shown below.
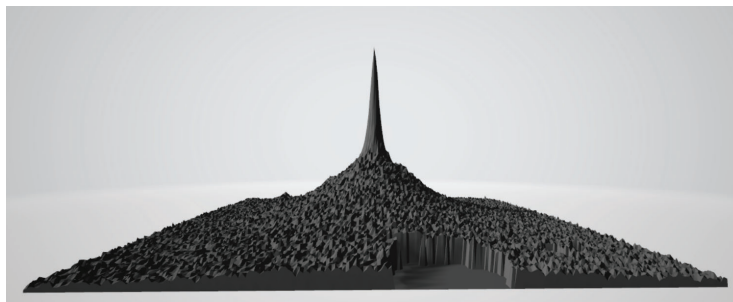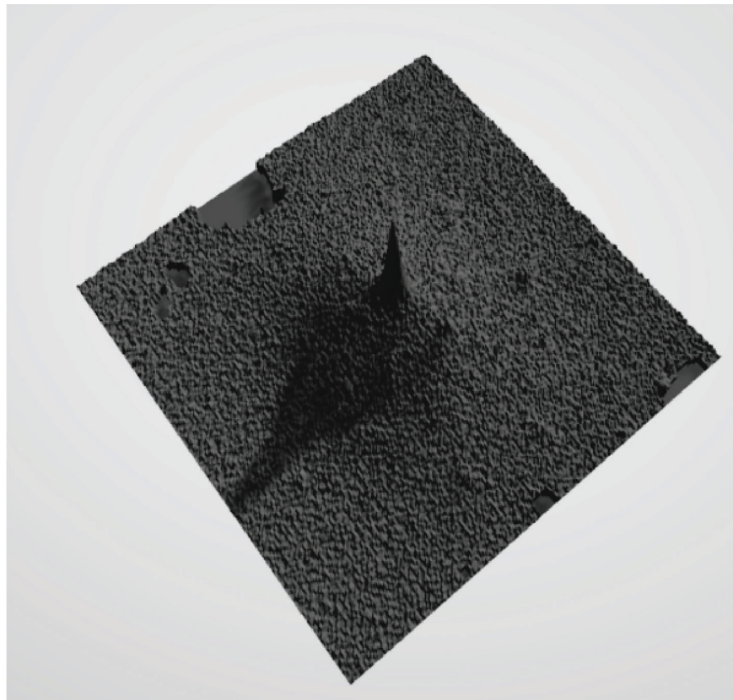
Master Research Project

Improving inclusivity in astronomy education with the help of 3D physical models

Jasper Jacob Postema

s3164063

Supervised by:

J. Noel-Storr

June 28, 2022

Abstract

Astronomy education is currently dominated by and catered to students with a visual learning style. A student with a visual learning style tends to understand subjects better by reading text or looking at figures. This means that students with different learning styles can have a harder time participating in astronomy education. The goal of this thesis is to improve the inclusion in astronomy education by making astronomy education more accessible to tactile learners. Tactile learners tend to learn more easily by touching or trying things out. To improve this inclusion I designed 3 sets of 3D models for first year astronomy students that follow the observational astronomy course. The 3D models are made to explain the topics of galaxies, variable stars and point spread functions. To test if the models are intuitive to handle, have a positive effect on the understanding of the topic of the user and have an especially positive influence on the understanding of the topic of tactile learners, a survey was made. A group of students responded to the survey after using the models, and with these results I conclude that most of the models were intuitive to use, that most of the models improved the understanding of the students, that the models were more intuitive for tactile learners than visual learners and that the models helped the tactile learners understand the topics better than the visual learners. Because of the small number of students that answered the survey, there are not yet quantitative results for a statistical sample, but the qualitative evidence is compelling. With this thesis I hope to convince and allow other teachers to use physical models during their courses as well.

Contents

1 Introduction

In this thesis I will address a problem in astronomy education and I will create physical 3D models that may help to solve this problem in the context of the observational astronomy course at the Rijksuniveristeit Groningen (RUG). I will also show how these 3D models were made so that the reader has an easier time to recreate these models for their own courses. The problem in question is the exclusion of some types of learners in astronomy education. Astronomy education as a whole is aimed towards students with an abstract mindset, also known as visual learners. This is evident by the heavy reliance on images and figures in astronomy courses. Students with different mindsets have therefore a harder time to grasp the subjects taught in those courses. For instance students with a tactile mindset, who learn better by interacting with objects rather than looking at pictures. Not only students with a different mindset are hindered by the large amount of images used in astronomy education, student with a visual impairment are also excluded due to this. It is hard or even nearly impossible to imagine astronomy without the use of pictures, however we can include more students by showing the contents of these images in different formats as well. This way we don't start excluding abstract learners. The way I will try to achieve this is by creating physical 3D models that can be used to help teach the observational astronomy course that all first year astronomy students at the RUG have to follow. These models will help tactile learners and students with a visual impairment to better understand the topic.

The layout of my thesis is as follows: first I will discuss some theory about inclusion of tactile learners and visual impaired students in STEM education. For different topics in astronomy I will also imagine different kinds of models that can be made to improve inclusion while teaching those topics. Next I will discuss the journey of creating my own models for observational astronomy from the ground up. My hope is that this can be a guide for others who are interested in creating their own custom models for astronomy education. After this I will show the models and discuss their intended use. Finally I will discuss a survey that was made to test if the models are easy to understand and if they actually have a positive effect on the students that used them.

2 Definitions for tactile astronomy

Education in astronomy is a vital part of ensuring that the scientific community keeps expanding. It is therefore of great import that as many students as possible can benefit as much as possible from this education. Currently, much of the astronomy education is aimed at students with an abstract, or visual, mindset and those with a preference for spatial learning (A. Yerlikaya and M. Yerlikaya 2016). This can be seen by the (over)reliance on figures and graphs in the classes. Students with an abstract mindset are able to understand difficult astronomical subjects like layers inside stars by looking at figures and graphs in a book. The field of astronomy consists of many topics that are most easily understood with an abstract mindset (Cole et al. 2018). Not every student that starts astronomy education has an abstract mindset. I will call the students that understand and learn more effectively using hands on science and with the help of interactable models tactile learners. The tactile learners will have a harder time understanding astronomy, however it is possible for tactile learners to adopt a more abstract mindset (Cole et al. 2018). Not only tactile learners are hindered in their astronomy education, but also the group of visually impaired students. The number of visually impaired students who are willing to enrol in STEM (science, technology, engineering and maths) fields is small, this is possibly due to its great reliance on data (A. Yerlikaya and M. Yerlikaya 2016). The focus of astronomy education on abstract learners decreases the amount of students that would be willing to pursue a further career in astronomy, which is bad for the diversity of the field as a whole. In this paper I aim to help to make astronomy education more inclusive for both tactile learners and visually impaired students. I will do this by recommending the use of appropriate interactable models that can help these students understanding various topics during their astronomy education. These models range from 3 dimensional objects that can be made by a 3D printer to sound files that can help blind students to picture images using their ears.

2.1 Methods

Physical models can be a great help for blind or visually impaired students to improve their understanding of STEM fields (Aldajani 2016). However they not only help them, but their unimpaired students as well (Hasper et al. 2015). This means that the use of models in astronomy education can not only help to make it more favourable for blind or visually impaired students, but other students, for instance tactile learners, as well. The goal of this paper is to improve the diversity in the astronomy bachelor education, by defining models (physical and more abstract) that can be used during the first three years of astronomy education. These models can encourage blind and visually impaired students, as well as tactile learners, to stick with astronomy for longer than they would otherwise and eventually finish their education. To organise the proposed solutions, a table is made. This table lists examples of different types of models that can be used to explain topics in astronomy. The topics that I considered are: Intensity of light, colour, composition and taxonomy, topography, morphology, scale, structure, timescale, invisible fields, atoms and molecules, spectra and waves. In the table, these topics are linked to some fields in astronomy that

they appear in. These fields are: galaxy formation, planets, meteorites, interior of stars, Earth atmosphere, light emission and reflection/absorption, nuclear physics, exterior of stars, gas clouds, radio waves. These fields were chosen based on the first years curriculum of astronomy at the Rijksuniversiteit Groningen. For each topic examples of models that can help explain the topic are presented. Each example corresponds to a certain type of model. The considered model types are: physical models, embellished tiles, embossed tiles, real examples, video animations, sound and haptic models. Examples of a physical model, embellished tile model and embossed tile model are shown in figure 1.

(a) Physical model example   (b) Embellished tile example   (c) Embossed poster example
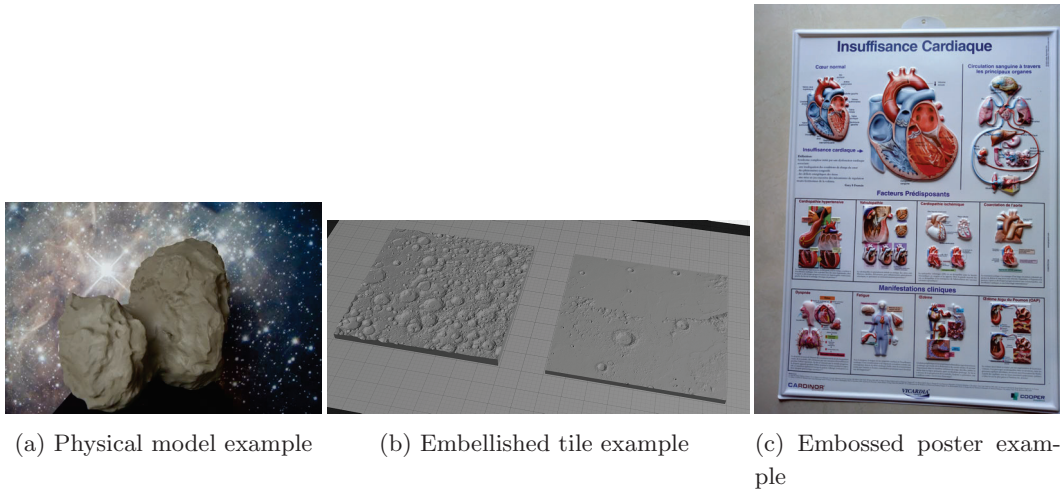
Figure 1: Examples of the physical model, embellished tile and embossed tile/poster. The physical model shows the 67P/Churyumov–Gerasimenko comet from the Rosetta mission (DigitalEngineering247 2021). The embellished tile shows the surface of the Moon (News 2021). The embossed poster shows the human anatomy (group 2022).

Physical models are the 3D models that can be created using 3D printers, they can have any shape and size. The shape and features on the surface of the model can represent an actual object, or they can explain the dependence on some parameter over a 3 dimensional space. These models can often cheaply be made using 3D printers. They can help tactile learners better visualise relations and shapes of astronomical objects. Visually impaired students will be able to feel the model, which allows them to find out information by themselves. Together with explanations from the teacher this should allow students with both learning types to more quickly understand the topic at hand. Without explanation though it can be hard for inexperienced students to make sense of the models.

Embellished tiles are also 3D models, however they are more restricted in the sense that they consist of a thin tile that can have any height which varies over the tile. This height difference between positions on the tile can show the dependence on some parameter over a 2-dimensional space. This type of model has the same advantages and disadvantages as physical models, where it is rather cheap to produce and can help tactile learners

and visually impaired students to understand the corresponding astronomical subject more quickly provided that there is explanation from teachers. It can sometimes be preferable to use embellished tiles over physical models, since the embellished tiles are even easier to produce using small 3D printers. Embossed tiles are similar to embellished tiles, with the difference being that the features on the surface can only have 2 different heights, high and low. Because of this embossed tiles can't describe a relation between any parameter and a 2-dimensional space but it can describe the relation between a binary parameter and a 2-dimensional space. Again, the embossed tiles have the same advantages and disadvantages as physical models and embellished tiles. However in some situations you might prefer to use an embossed tile model over the others. Embossed posters for example can be made without the use of a 3D printer, so they can be easier to produce than the previous two model types.

Real examples are simply real life objects that can be touched and handled. It is often preferable to use real examples as a means to explain a certain subject. This is because a tangible example of the theory that was explained can be very helpful for tactile learners. For blind or visually impaired students it is always helpful to be able to touch objects related to the subject at hand. Unfortunately it is often the case that it is impossible to use real examples when dealing with astronomical subjects. In the very few cases we can use real examples, the examples are often difficult or expensive to obtain. This is the case with meteorites or moon rocks for example. Video animations are also simply animations that can show a process or relation using a screen. It can be difficult to create video animations for yourself, so this type of method is reliable on the availability of the animations you are looking for. It is also not a method that you can use to explain topics to blind or visually impaired students. For tactile learners though, animations may be extremely helpful. These videos can often be understood without additional explanation from a teacher. They can also be replayed by the student in their free time, especially in the case of alternate reality (AR) or virtual reality (VR) simulations that students can manipulate themselves. Which makes this method more flexible of a tool depending on the learning program.

Sound can also be a useful way to display images, especially for blind or visually impaired students. In this paper by sound I mean a sonified image which can be created from a normal image to make it understandable for blind or visually impaired students. Some great examples of these sonified images are shown by NASA, the Pillars of creation can be found using the following url for example: (`https://www.youtube.com/watch?v=EnysNELH2uc`) Vogel 2020.

Finally haptic models are models that can not only be touched and handled, but also give feedback in response. These models usually consist of electronic devices that can both be helpful for blind or visually impaired students and tactile learners alike. Haptic models are the most versatile of the considered models, as one device can be used to help students in many topics if reprogrammed the right way. They can also be used autonomously, as the models can be created in such a way that a teachers explanation is not needed to understand the topic. Unfortunately though haptic devices are really expensive and acquiring only one would take a significant part of the school's budget. However if a blind or visually impaired

student takes part in your class, it might still be worthwhile considering using a haptic device as it can really help these students to discover and understand astronomical subjects on their own (M. G. Jones et al. 2006). The above models were chosen, because they cover a wide range of accessibility and degree of sophistication. The physical and tile models can be created using a 3D printer, which nowadays is not a very large hurdle to overcome. It is a bit more difficult to find or make images that are transformed into sound files, but they can be extremely helpful for blind or visually impaired students. Similarly, video animations can also be hard to find or make but they can help to explain difficult astronomical subjects to tactile learners and other not visually impaired students as well. The haptic devices can be the most useful kinds of models out of all of the ones mentioned, however they are also the most expensive. Other types of models could have been considered, however the ones considered in this paper are enough to achieve the ranges of accessibility and sophistication that I wanted, so no more were needed.

2.2 Results

Using the considered methods and topics in the previous section, I created a table which gives examples of models to help explain topics in astronomy. This table is shown in Figure 2. Two additional tables were created as well. The first additional table, shown in Figure 4, shows how very general topics that do not belong to a single subject in astronomy can be explained using the previously mentioned models. This concerns 2D plots, 3D plots and tables. The second additional table, shown in Figure 5, lists different types of supporting devices and methods that blind or visually impaired students can use to advance their studies. These methods and devices are structured based on their goals. The considered goals are: Interpreting study material, doing measurements and communication between students. Communication between students here means between blind or visually impaired students and/or their visually unimpaired classmates. In this section I will explain the contents of each table and the reason as to why it is chosen.

2.2.1 Diagram of topics

The first diagram that will be explained is shown in Figure 2. This diagram contains models that can explain various topics in astronomy. The first row shows different subjects that appear during an astronomy bachelor's education and the second row shows topics that are treated during one or more of the subjects. The relation between topics and subjects is shown by lines between them. For each topic, different models that can help to explain the topic are shown. These models each belong to a different model type discussed in section 2.1. Each model also has a colour, green, yellow or red. This colour signifies how good this model is at explaining the topic. What follows is an explanation of every model that is present in Figure 2 in order of the topic they appear in.

Intensity (of light) distribution

Topic categories (left): Galaxy formation, Planets, Meteorites, Interior of stars, Earth atmosphere, Gas clouds, Light emission and reflection/absorption, Nuclear physics, Exterior of stars, Radio waves

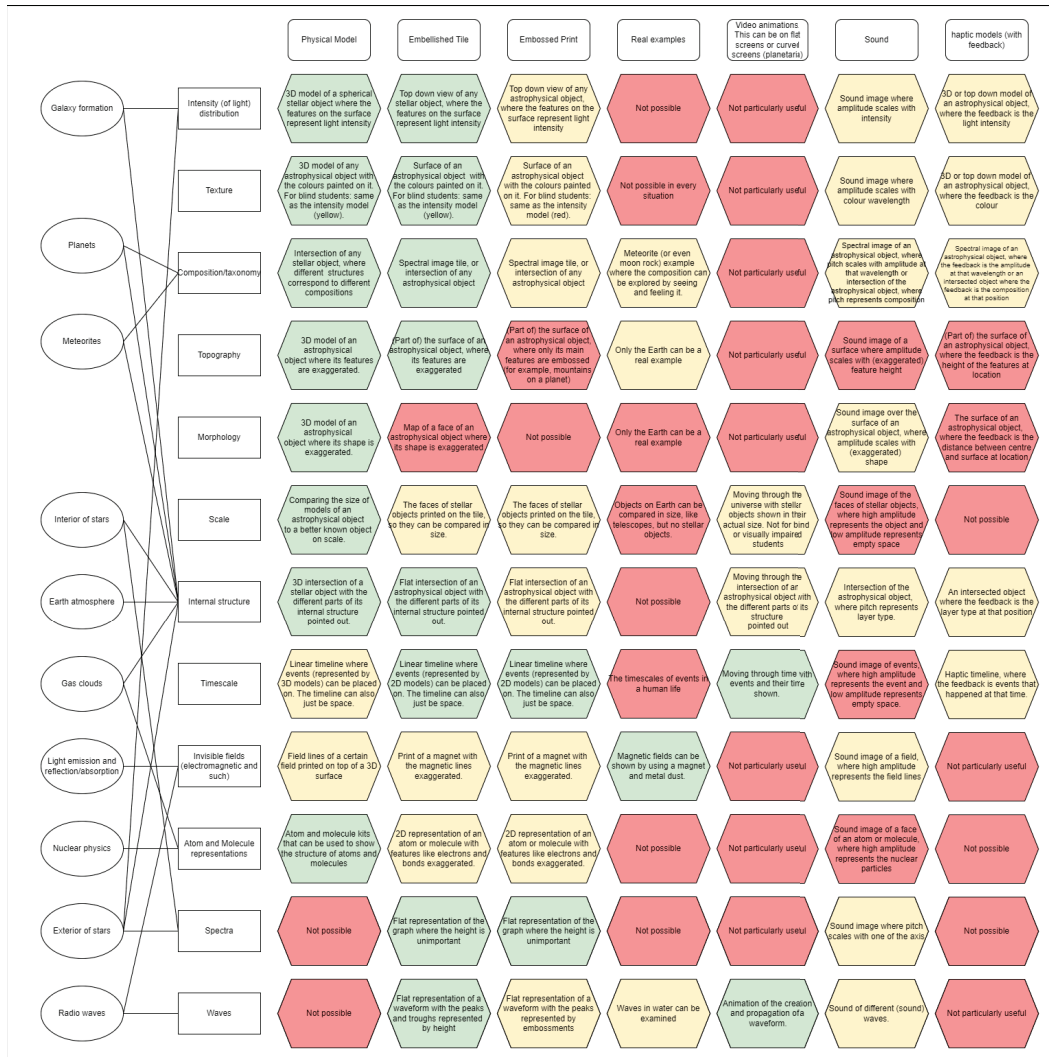| Feature	Physical Model	Embellished Tile	Embossed Print	Real examples	Video animations (This can be on flat screens or curved screens (planetaria))	Sound	haptic models (with feedback)
Intensity (of light) distribution	3D model of a spherical stellar object where the features on the surface represent light intensity	Top down view of any stellar object, where the features on the surface represent light intensity	Top down view of any astrophysical object, where the features on the surface represent light intensity	Not possible	Not particularly useful	Sound image where amplitude scales with intensity	3D or top down model of an astrophysical object, where the feedback is the light intensity
Texture	3D model of any astrophysical object with the colours painted on it. For blind students: same as the intensity model (yellow).	Surface of an astrophysical object with the colours painted on it. For blind students: same as the intensity model (yellow).	Surface of an astrophysical object with the colours painted on it. For blind students: same as the intensity model (red).	Not possible in every situation	Not particularly useful	Sound image where amplitude scales with colour wavelength	3D or top down model of an astrophysical object, where the feedback is the colour
Composition/taxonomy	Intersection of any stellar object, where different structures correspond to different compositions	Spectral image tile, or intersection of any astrophysical object	Spectral image tile, or intersection of any astrophysical object	Meteorite (or even moon rock) example where the composition can be explored by seeing and feeling it.	Not particularly useful	Spectral image of an astrophysical object, where pitch scales with amplitude at that wavelength or intersection of the astrophysical object, where pitch represents composition	Spectral image of an astrophysical object, where the feedback is the amplitude at that wavelength or an intersected object where the feedback is the composition at that position
Topography	3D model of an astrophysical object where its features are exaggerated.	(Part of) the surface of an astrophysical object, where its features are exaggerated	(Part of) the surface of an astrophysical object, where only its main features are embossed (for example, mountains on a planet)	Only the Earth can be a real example	Not particularly useful	Sound image of a surface where amplitude scales with (exaggerated) feature height	(Part of) the surface of an astrophysical object, where the feedback is the height of the features at location
Morphology	3D model of an astrophysical object where its shape is exaggerated.	Map of a face of an astrophysical object where its shape is exaggerated.	Not possible	Only the Earth can be a real example	Not particularly useful	Sound image over the surface of an astrophysical object, where amplitude scales with (exaggerated) shape	The surface of an astrophysical object, where the feedback is the distance between centre and surface at location
Scale	Comparing the size of models of an astrophysical object to a better known object on scale.	The faces of stellar objects printed on the tile, so they can be compared in size.	The faces of stellar objects printed on the tile, so they can be compared in size.	Objects on Earth can be compared in size, like telescopes, but no stellar objects.	Moving through the universe with stellar objects shown in their actual size. Not for blind or visually impaired students	Sound image of the faces of stellar objects, where high amplitude represents the object and low amplitude represents empty space	Not possible
Internal structure	3D intersection of a stellar object with the different parts of its internal structure pointed out.	Flat intersection of an astrophysical object with the different parts of its internal structure pointed out.	Flat intersection of an astrophysical object with the different parts of its internal structure pointed out.	Not possible	Moving through the intersection of an astrophysical object with the different parts o its structure pointed out	Intersection of the astrophysical object, where pitch represents layer type.	An intersected object where the feedback is the layer type at that position
Timescale	Linear timeline where events (represented by 3D models) can be placed on. The timeline can also just be space.	Linear timeline where events (represented by 2D models) can be placed on. The timeline can also just be space.	Linear timeline where events (represented by 2D models) can be placed on. The timeline can also just be space.	The timescales of events in a human life	Moving through time with events and their time shown.	Sound image of events, where high amplitude represents the event and low amplitude represents empty space.	Haptic timeline, where the feedback is events that happened at that time.
Invisible fields (electromagnetic and such)	Field lines of a certain field printed on top of a 3D surface	Print of a magnet with the magnetic lines exaggerated.	Print of a magnet with the magnetic lines exaggerated.	Magnetic fields can be shown by using a magnet and metal dust.	Not particularly useful	Sound image of a field, where high amplitude represents the field lines	Not particularly useful
Atom and Molecule representations	Atom and molecule kits that can be used to show the structure of atoms and molecules	2D representation of an atom or molecule with features like electrons and bonds exaggerated.	2D representation of an atom or molecule with features like electrons and bonds exaggerated.	Not possible	Not particularly useful	Sound image of a face of an atom or molecule, where high amplitude represents the nuclear particles	Not possible
Spectra	Not possible	Flat representation of the graph where the height is unimportant	Flat representation of the graph where the height is unimportant	Not possible	Not particularly useful	Sound image where pitch scales with one of the axis	Not possible
Waves	Not possible	Flat representation of a waveform with the peaks and troughs represented by height	Flat representation of a waveform with the peaks represented by embossments	Waves in water can be examined	Animation of the creation and propagation of a waveform.	Sound of different (sound) waves.	Not particularly useful

Figure 2: Diagram containing various types of models that can explain topics in astronomy and how well suited they are to explain the topic. DOI: 10.13140/RG.2.2.13881.85606

Physical model: A 3D model of a spherical astronomical object where the features on the surface represent light intensity. This 3D model represents the real shape of the object in question, which can be a star, planet asteroid or other kind of astronomical object. The intensity of this object is different at different positions on the surface, which must become clear from the model. This can be done by modifying the surface on the model in such a way that modification is a scale for the intensity. There are many possible features on the surface that you can choose from. Some examples are: texture, colour and height variation. The texture of the surface can be changed by adding little elevations to the surface. This feature might be hard to implement if the 3D printer that you are using is not sophisticated enough. More elevations can be placed at positions where the intensity is high and fewer where the intensity is low. Colour can of course easily be used to represent intensity. This colour can then be applied to the surface of the model. This type of model can obviously not be applied to students with a visual impairment. If the object in question has a shape that is very spherical, which is the case for many astronomical objects, for instance the sun, you can also relate the intensity to the height of the surface with respect to the centre. In this case, the object will not look spherical, so you should give the information that the object is spherical in reality to the students. Which type of feature on the surface you choose is purely dependent on the topic, students that you are teaching to and the amount of sophistication of the 3D printer that you are using.

Embellished tile: Top down view of any astronomical object, where the features on the surface represent light intensity. The shape of this embellished tile represents (part of) the surface of the astronomical object, including height profile. We can use the same features as the physical model to show the intensity over the surface. Which type of feature to use still depends on the topic, students and the amount of sophistication of the 3D printer. If you want to examine a certain part of an object or if the object in question is rather symmetrical it can be preferable to use an embellished tile over a physical model. This is because embellished tiles are easier to create using 3D printers than physical models if you want the same amount of detail.

Embossed print: Top down view of any astronomical object, where the features on the surface represent light intensity. The embossed print model is quite similar to the embellished tile model. It can be used to represent (part of) the surface of an astronomical object. However in the embossed print model we can not express the intensity using height or texture variations. Out of the given examples this only leaves colour, which makes it difficult for blind or visually impaired students to interpret the model. So for those students the embossed print model can only be used if the astronomical object's surface is flat and the intensity is communicated as high or low.

Real examples: It is not quite possible to get a real example of an astronomical object with an intensity distribution. However if the intent of the lesson is to explain the way that light propagates from a radiating object like the sun, a light source like a light bulb can be used as an example, especially if the bulb is incandescent and can be felt.

Video animations: For almost every topic, it is possible to use video animations to explain the topic. However because it is hard to find or make these videos in every situation, it might not always be worthwhile to use them. When explaining the intensity distribution it can be useful to describe the intensity distribution using a video animation, however the

previously described models can achieve the same usefulness while being easier to create. The previous models are also more useful for blind or visually impaired students to use.

Sound: Sonified image where amplitude scales with intensity. Sonified images are hard to create but really helpful for blind or visually impaired student to understand the topic. Often the sonified images can replicate the embellished tile models, however in some situations they can not be used. In the situation of intensity distributions, the sonified image can show the intensity as the amplitude of the sound and the 2D position over the surface with pitch and time.

Haptic models (with feedback): 3D or top down model of an astronomical object, where the feedback is the light intensity. Haptic models are also very hard to create but can single-handedly make sure that a student understands the topic. Using a model that represents the object in question where the feedback is the intensity at a certain point a haptic model can be created. The feedback can be felt or heard depending on the way that the model is designed.

Textures

Physical model: 3D model of any astronomical object with the colours painted on it. To show the colour of an astronomical object it is easiest to just model the object and to have the colours painted on at the right position. However this kind of model can obviously not be used to teach blind or visually impaired students. So in those situations the model can be made similarly to the physical model for teaching intensity distributions. The features on the surface will be mapped to a property of colour like the wavelength. In any case, using a physical model is quite a good way to show the colour of an astronomical object.

Embellished tile: Surface of an astronomical object with the colours painted on it. For blind students: same as the intensity model. If the colour of the entire object is not important, but the colour at a certain part of the surface is, it is probably better to use an embellished tile than a physical model. The function of the embellished tile will be the same as the physical model, where the surface can be coloured. For blind or visually impaired students, previously discussed features can be made upon the surface.

Embossed print: Surface of an astronomical object with the colours painted on it. For blind students: same as the intensity model. The embossed print can be used in similar situations as the embellished tiles if the resolution of the surface height is not very important. For blind or visually impaired students, the embossed print can only be used if the surface is nearly flat and the colour is communicated as blue or red.

Real examples: It is hard to find astronomical objects that can be shown in a class. One of the few real examples that can be shown in class are meteorites. So if the topic of interest is the colour of meteorites, real examples can be shown. In other cases though it might be better to use one of the previous models.

Video animations: Similar to the intensity situation, it is most likely not worthwhile using video animations to explain colour. Video animations will not be able to explain colours of astronomical objects than an image in a book, which is exactly what we want to improve on.

Sound: Sonified image where amplitude scales with colour wavelength. In this situation we can use a sonified image to replicate the embellished tile model for blind or visually impaired students. The sonified image can show the colour wavelength as the amplitude of the sound

and the 2D position over the surface with pitch and time.

Haptic models (with feedback): 3D or top down model of an astronomical object, where the feedback is the colour. Using a model that represents the object in question where the feedback is the colour at a certain point a haptic model can be created. This haptic model represents the 3D physical model, but with feedback. The feedback can be felt or heard, depending on the way that the model is designed.

Composition/taxonomy

Physical model: Intersection of any astronomical object, where different features correspond to different compositions. If the composition or taxonomy of an astronomical object has to be explained, it is usually best to produce a model that shows an intersected object. This is because it allows us to look inside of the object to see the composition and explain the taxonomy. The different parts of the inside of the object can be expressed using the features I discussed earlier, especially colour and texture can be very helpful. This method can be used for both radiating objects like the Sun and cold objects like meteor(ites).

Embellished tile: Spectral image tile like the ones shown in figure 3 or an intersection of an astronomical object. For radiating objects, the spectral image tile can explain the way that composition is determined from Earth, especially to blind or visually impaired students. For any object, including radiating objects, the embellished tile can also represent an intersection, which can help to explain the composition or taxonomy in a similar way to the physical model.

Embossed print: Spectral image tile like the ones shown in figure 3 or an intersection of an astronomical object. An embossed print can also be used to make a spectral image tile, however they will have less resolution than their embellished tile counterparts unless they are made quite large. Spectral tiles like the one shown in figure 3 A are easier to create using embossed print than spectral tiles like tile B. Embossed print can also be used to create an intersection of an object, however due to its restrictions, the composition can only be communicated using colour. This makes embossed print not a good option if you want to teach the taxonomy of asteroids to blind or visually impaired students.

Real examples: Meteorite (or even moon rock) example where the composition can be explored by seeing and feeling it. There are some astronomical objects of which the composition or taxonomy is of interest and we have real examples. Meteorites and moon rocks fall into this category and if possible these models are great to explain composition or taxonomy of these specific objects to all students alike. This is of course because the composition can actually be seen or felt by the students.

Video animations: Again video animations are hardly better in this situation than pictures on this topic. It is therefore advised to spare the effort of using video animations to explain composition or taxonomy.

Sound: Spectral image of an astronomical object, where pitch scales with amplitude at that wavelength or intersection of the astronomical object, where pitch represents composition and amplitude and time position. In this situation we can use a sonified image to replicate the spectral image tile or the intersection of the astronomical object. The sonified image can show the spectral image with the amplitude at a colour wavelength as the pitch and the wavelength are addressed over time. Even the intersection can be shown if different
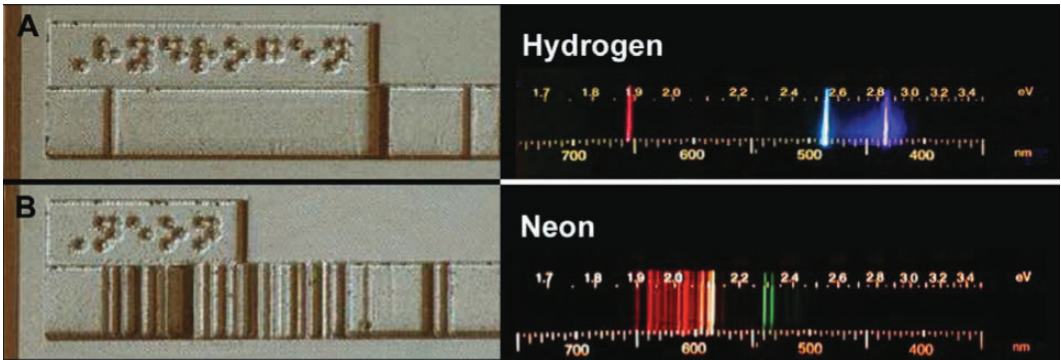
Figure 3: Embellished tile examples which can help to explain the spectroscopy of a star to blind or visually impaired students. Tile A shows hydrogen and tile B shows neon. From Hasper et al. 2015.

pitches represent different parts of the composition and the 2D position over the surface is represented by amplitude and time.

Haptic models (with feedback): Spectral image of an astronomical object, where the feedback is the amplitude at that wavelength or an intersected object where the feedback is the composition at that position. A spectral image of a radiating object can be shown where the feedback can be the amplitude (high or low) at a certain wavelength. A haptic model can also show an intersected astronomical object, like the physical model, where the feedback can be the composition of the astronomical object at that position.

Topography

Physical model: 3D model of an astronomical object where its features are exaggerated. In astronomy, topography refers to the study of surface features of astronomical objects. Think for instance about the study of mountains on Mars. A physical model can represent the global shape of the object and the features on the surface can be exaggerated so that they have significant height difference compared to the size of the object. This allows all students to be able to see or feel the surface features that are present on this (type of) astronomical object.

Embellished tile: (Part of) the surface of an astronomical object, where its features are exaggerated. The embellished tile model can be made similarly to the physical model, with the difference that it can only represent (a part of) the surface of the object. The embellished tile model allows the students to learn the general topography of the astronomical object that is discussed while being easier to produce than the physical model. The drawback of the embellished tile model compared to the physical model is that the physical model can show the entire astronomical object, which can be important when talking about specific objects like Mars.

Embossed print: (Part of) the surface of an astronomical object, where only its main features are embossed (for example, mountains on a planet). The embossed print model can be created similarly to the embellished tile model with the downside that only the mayor

features can be shown. Because of this, the embossed print model can only show the general surface features of the object. This is fine if we are talking about specific objects like Mars, but those are harder to show using tile models. So the Embossed print is not really a good model to use to explain topography.

Real examples: Only the Earth can be a real example if topography is to be explained. Earth topography is not often a subject in astronomy, however our planet can still serve a purpose as an example of a habitable planet.

Video animations: Again video animations are hardly better in this situation than pictures on this topic. It is therefore advised to spare the effort of using video animations to explain topography.

Sound: Sonified image of a surface where amplitude scales with (exaggerated) feature height. In this situation we can use the sonified image to represent the embellished tile model. The sonified image can show a feature map of the surface, where the amplitude of the sound represents the height of the feature and pitch and time represent the 2D position over the surface.

Haptic models (with feedback): (Part of) the surface of an astronomical object, where the feedback is the height of the features at location. A 3D image of the astronomical object or the surface of the astronomical object where the feedback can be the height or the type of feature that is at that position.

Morphology

Physical model: 3D model of an astronomical object where its shape is exaggerated. This is quite similar to how the physical model of the topography is described. This is because the topography and morphology both have to do with features on the surface of the object. The morphology means the global shape of the astronomical object while the topography means the local variations from the morphology. So to show the morphology of an astronomical object, it is important to show the entire object and therefore its shape. The proposed physical model does this and since the shape is exaggerated, small deviations from the norm can be discussed. This model can work for all types of astronomical objects.

Embellished tile: Model of a face of an astronomical object where its shape is exaggerated. It is hard to show an entire astronomical object using a tile model, since most of them don't have a flat shape. It is possible though to show one face of the object, which can be enough if the object in question is symmetrical. This is for instance the case for stars, planets or moons. However in those situations, the morphology is already quite simple and might not need models to be explained. For more morphologically interesting objects like asteroids, tile models can not be used.

Embossed print: Not possible. It is already hard to argue that tile models can be used to help explain morphology, since the embossed print models only have two different heights. It is not advisable to use embossed print models to explain the morphology of astronomical objects.

Real examples: Only the Earth can be a real example. Just like topography, only the Earth can help to explain morphology. It can be used to explain the shape of terrestrial planets. However, since the planets have quite a simple shape, it might not be the most impactful model.

Video animations: Again video animations are hardly better in this situation than pictures on this topic. It is therefore advised to spare the effort of using video animations to explain morphology.

Sound: Sonified image over the surface of an astronomical object, where amplitude scales with (exaggerated) shape. In this situation we can use the sonified image to show the shape of the surface of the astronomical object in a way similar to the physical model. The amplitude of the sound would show the distance between the surface and the surface of the object. Pitch and time represent the 2D positions on the surface of the object.

Haptic: The surface of an astronomical object, where the feedback is the distance between the centre and surface at location. Even though this example for a haptic model is quite similar to the topographic counterpart it is not a fantastic model to use. Its use is quite similar to that of the physical model and since the haptic model is harder to create, it is likely better to use a physical model instead.

Scale

Physical model: Comparing the size of models of an astronomical object to a better known object on scale. Scale is an important part of astronomy, because this field of physics spans many orders of magnitude. To help explain the size of the many different scales of astronomy, physical models can be quite helpful. You might expect that blind or visually impaired students are worse at interpreting scale than not visually impaired students, however G. Jones, Taylor, and Broadwell 2009 show that impaired students understand scale on the same level, if not higher, as their not blind or visually impaired classmates. If a model of an object that is known to the student is compared to the model of a new object, sizes can be compared. This can help students learn the scale of the new object. Sometimes the difference in scale is too large to be able to be expressed using real models. In this case it might not be possible to use physical models, but you should always keep in mind that distances can also help to express scale. A much larger range of scales can be compared when you are comparing distances that are known to the students. An added benefit is that you do not need to create models to use this way of explaining scales.

Embellished tile: The faces of astronomical objects printed on the tile, so they can be compared in size. This model can be interpreted in two different ways, the faces of the astronomical objects can be printed on the same tile or the sizes of the tiles can be compared. Both cases can be fine, as long as the difference in scale between the objects is not very large. Again this is because the tiles can only be as large as the printer. Different planets can be compared for example, but not the size of galaxies compared to planets.

Embossed print: The faces of astronomical objects printed on the tile, so they can be compared in size. Since the objects are just differently sized dots, the embossed print model can work just as fine as the embellished tile model in this situation. The embossed print model can be used in a similar fashion to the embellished tile model.

Real examples: Objects on Earth can be compared in size, like telescopes, but no astronomical objects. Since real objects that can be found on Earth all appear in a similar scale, real examples can't address the very large and very small scales that astronomy covers.

Video animations: Moving through the universe with astronomical objects shown in their actual size. Not for blind or visual impaired students. Video animations might be the best

models to explain the many scales of astronomy, because they are dealing with effectively an infinite amount of space. An animation that zooms in and out of the different astronomical objects in the universe can address all of the scales that are important. Unfortunately video animations are not accessible for blind or visually impaired students.

Sound: Sonified image of the faces of astronomical objects, where high amplitude represents the object and low amplitude represents empty space. Sonified images can only represent the previously mentioned 3D models themselves, which makes them not very good at comparing scales. At best the sonified image can represent the embellished tile model where the astronomical objects are in the same tile. A high amplitude would represent the objects in that case and a low amplitude would represent empty space. An easier way to use sound to express scale could be achieved by not using sonified images at all. By just comparing the length or amplitude of a sound file, scale can also be compared. However this can be hard to interpret for the students.

Haptic: Not possible. It is hard to generate large structures using haptic models, which makes it also difficult for this type of model to help explain scale. It is most definitely not worth the effort to try to create a haptic model to explain scale.

Internal structure

Physical model: 3D intersection of an astronomical object with the different parts of its internal structure pointed out. This model looks quite similar to the physical model for composition/taxonomy. This because composition and internal structure both talk about the inside of an astronomical object. The difference is that subject of internal structure puts more emphasis on the shape and use of the different layers within an object, while the subject of composition deals more with what the different parts inside the objects are made of and is often more associated with solid objects. Going back to the physical model that can be used to describe internal structure, the different layers inside the object can be emphasised using a raised border between the different zones. You can differentiate the different layers by giving them different features like the ones that were discussed prior. Of course colour can not be interpreted by blind or visually impaired students, but the texture and height variation can be used for all students.

Embellished tile: Flat intersection of an astronomical object with the different parts of its internal structure pointed out. Again this model is quite similar to the embellished tile model used to explain composition. Using the methods described in the previous section, this model can help explain the internal structure of astronomical objects quite well. This model is most useful when describing spherically symmetric objects like stars. The advantage of using the embellished tile model over the physical model is just ease of creation.

Embossed print: Flat intersection of an astronomical object with the different parts of its internal structure pointed out. This model works very similar to the embellished tile with the difference being that not every feature can be used to explain the use of the different layers. Just like the composition/taxonomy topic, the embossed print model can only help to explain internal structure using colour. So if there are blind or visually impaired students involved it is preferable to use an embellished tile model instead.

Real examples: Not possible. It is impossible to show real astronomical objects that have significant internal structure on Earth.

Video animations: Moving through the intersection of an astronomical object with the different parts of its structure pointed out. An animation can be nice to show what the structure in an astronomical object looks like. By moving through the object, the animation can show how the different layers interact and where they are positioned with respect to each other.

Sound: Intersection of the astronomical object, where pitch represents layer type. The sonified image can be used to represent the embellished tile model, where the time and amplitude represent the 2D position over the tile and the pitch represents the type of layer that is at that position.

Haptic: An intersected object where the feedback is the layer type at that position. The haptic model can represent the 3D physical model of the intersection of an astronomical object, where the feedback is the layer that is present at the position inside the object.

Timescale

Physical model: Linear timeline where events (represented by 3D models) can be placed on. The timeline can also just be space. The timescale is a topic that can be expressed using 3D models in a similar way to the topic of scale. This is because, just like scale, astronomy deals with many different timescales both small and large. Showing timescales can be done in a similar way to showing physical scales as well. 3D objects that represent temporal events can be placed a certain distance away from eachother on a timeline or just with space between them. Comparing the different distances between events can allow you to explain timescales in astronomy better.

Embellished tile: Linear timeline where events (represented by 2D models) can be placed on. The timeline can also just be space. This model works very similar to the physical model above, where the timescale is defined by the distance between the models. The embellished tile model is usually preferable over the physical model, since it is easier to create.

Embossed print: Linear timeline where events (represented by 2D models) can be placed on. The timeline can also just be space. This model is almost the same as the embellished tile model and they can be used interchangeably. However in most cases, embossed prints are used on posters which are usually not big enough to represent a large range of timescales. This makes the embellished tile preferable over the embossed print model in most cases, but in certain cases the embossed print model can also be used.

Real examples: The timescales of events in a human life. The only possible feel for time that people truly have is for events that happen in their own life. These events though are rarely relevant in an astronomical context.

Video animations: Moving through time with events and their time shown. Similar to the video animation that can show scale, a similar video that shows timescale is also possible. Of course the challenge is again that the video needs to be found or made, but being able to show the different timescales of astronomy in a quick and easy to understand way might be worth the effort.

Sound: Sonified image of events, where high amplitude represents the event and low amplitude represents empty space. This sonified image can represent the embellished tile or embossed print model for timescale. The time of the sonified image between two events can be compared to the time between another set of events. This can help blind or visually

impaired students get a feel for different timescales in astronomy.

Haptic: Not possible. As previously discussed, it is hard to portray large structures using haptic devices. Therefore it is hard to compare meaningful differences in time between event pairs. It is therefore definitely not worth the effort to try to make a haptic device work for this topic.

Invisible fields

Physical model: Field lines of a certain field printed on top of a 3D surface. Since fields always have a configuration in all spatial dimensions it can be nice to show this by using a 3D model where the field lines are shown in their three dimensional configuration. This can help students who find it difficult to expand the two dimensional representation of fields which is used in books to our three dimensional world. A disadvantage is that this model can never show the real situation though, as a real field is present everywhere while this model only shows the field on a surface. This can give rise to more questions from the student as this improved model still does not show the true situation. However if the proper instructions are given, this physical model can help tactile learners a lot.

Embellished tile: Print of a field with the field lines exaggerated. This model basically represents a tactile counterpart of an often used flat representation of fields. This can be quite useful for blind or visually impaired students, as they will be able to observe this model now. However for tactile learners this type of model does not add a lot of value.

Embossed print: Print of a field with the field lines exaggerated. This model can be created exactly like the embellished tile above provided that the device that is used to create the embossments has a high enough resolution.

Real examples: Magnetic fields can be shown by using a magnet and metal dust. This model is one of the most widely used methods of explaining (magnetic) fields to students that encounter them for the first time. But this is of course for a good reason as the metal dust can clearly show the field lines which can show the tactile learners that these fields are actually real and that they can change depending on the magnets involved. Even blind or visually impaired students can learn from this experiment as they will be able to observe the magnets that cause the magnetic field configuration.

Video animations: Video animations are hardly better in this situation than pictures of fields. It is therefore advised to spare the effort of using video animations to explain them.

Sound: Sonified image of a field, where high amplitude represents the field lines. A sonified image can be created that represents the embellished tile model. Time and pitch can represent the 2D position and the amplitude can represent the presence of a field line at that position. For an optimal effect, the field lines should be a bit thicker and more separated. This way the often used flat picture can be represented as a sonified image as well.

Haptic: A 3D surface where the feedback is the presence of field lines at that position. The haptic model can represent the physical model in this situation. It can serve the exact same purpose, so in many cases it is just preferable to use a physical model instead, as this haptic model does not provide much more value to any kind of student.

Atom and molecule representations

Physical model: Atom and molecule kits that can be used to show the structure of atoms and

molecules. There are many ways that an atom can be represented using a physical model. These models often represent the atom as visualised by Bohr's model. In an educational setting with tactile learners, it can be very helpful to make use of interactable 3D models. Physical models are inherently interactable, however if the model can be created or changed by the students interacting with it, it is even more interactable. Atoms, protons, neutrons electrons are often represented by spheres and their bonds by sticks between them. Kits that contain these building blocks are readily available, especially for molecules. These kits can help tactile learners to understand the configuration of different molecules that can be found in space. In specific situations a 3D printed representation of a Bohr atom or molecule can also be used to explain the configurations.

Embellished tile: 2D representation of an atom or molecule with features like electrons and bonds exaggerated. There is no way that we can use a kit that the students can use to create or change atom and molecule models in an embellished tile model. The only way we can represent an atom or molecule in this way is using Bohr's model. And even then we can only show a flat representation where the spherical shape of the nuclear particles can be shown as a domes. This can help tactile learners and blind or visually impaired students to get a feel for the configuration of atoms and molecules, but if possible a physical model is preferable.

Embossed print: 2D representation of an atom or molecule with features like electrons and bonds exaggerated. The embossed print model is almost the same as the embellished tile model in this case. This is because nuclear particles and their bonds can be shown as the embossments on the tile/poster. It could be hard to show bonds using embossed print if the resolution of the printer is not high enough.

Real examples: Not possible. Atoms and molecules are too small to show as real examples.

Video animations: Not particularly useful. An animation featuring an atomic or molecular model can feature a 3D model of the object in question that can be seen from different angles. However it is easier to create such a model yourself than to create an entire video animation. I would therefore say that using a video animation to explain atoms and molecules is not particularly useful.

Sound: Sonified image of a face of an atom or molecule, where high amplitude represents the nuclear particles. A sonified image can be created to replicate the embellished tile model. However the embellished tile model can already be quite abstract, so without the proper instructions, the sonified image will be very hard to understand. Since it is easier to create the embellished tile model than a sonified image and the sonified image does not provide meaningful improvements, it is probably not worth to create this model.

Haptic: Not possible. It is very hard for a haptic device to create the physical model described above, so it is probably not worth it to use a haptic model, especially not when the physical model is quite good already.

Waves

Physical model: Not possible. Even though waves are emitted in three dimensions it is very hard and impractical to show a 3D wave propagation using a physical model. This is because wavefronts travel in shells, and it is very hard to show different layers of shells

nicely in a 3D model.

Embellished tile: Flat representation of a waveform with the peaks and troughs represented by height. This model consists of a plane wave or a spherical wave where the peaks and troughs are represented by height variation. This model is a 3D recreation of the usual flat representation of a continuous wave at a certain time. The tile represents a 2-dimensional plane and the height of the waves represent the amplitude of the wave. This model can help tactile learners and blind or visually impaired students to get a feel for how (invisible) waves work.

Embossed print: Flat representation of a waveform with the peaks represented by embossments. Like many topics before, the embossed print can help to explain this topic in the same way that the embellished tile model can. The difference here is just that resolution of the height of the waves is a lot lower for the embossed print model. The way that both models work though is exactly the same. This means that in most cases, the embellished tile model is preferable over the embossed print model however in the situation that it is easier to create embossed print models, you might want to use this model.

Real examples: Waves in water can be examined to show how other kinds of waves propagate as well. This example can work for tactile learners but blind or visually impaired students can have a hard time observing these waves unless they are submerged in water as well.

Video animations: Animation of the creation and propagation of a waveform. Video animations can show really well how waves are created and propagate. This is because an important part of waves is that they propagate in time. This is difficult to show using models, but can work perfectly fine in video animations. Since waves are a large topic in physics it is not that hard to find a suitable video animation for the topic at hand. Of course these animations can not help to teach the subject to blind or visually impaired students. But for tactile learners, these videos can be a huge help.

Sound: Sound of different (sound) waves. Of course a sonified image can be created that represents the embellished tile model. However something more appropriate can also be produced. Sounds are also waves, so the wavelength or amplitude dependence of a wave can be shown by listening to sounds with different wavelengths or amplitudes. Using some of the other models described above, the concept of waves can be effectively explained to all kinds of students but most of all blind or visually impaired students.

Haptic: Not particularly useful. Since it is very difficult to create a 3D physical model to help explain the topic of waves it is by extension also very difficult to produce an effective haptic model to explain this topic.

Now that the models in Figure 2 are explained I can move on to models that explain more general parts of astronomy education.

2.2.2 Diagram of general tools

The models in Figure 4 can be applied where necessary to any topic and subject in physics. They can help to explain several tools that are widely used to explain theory to students, namely graphs and tables. It should be noted that the tables are primarily discussed here
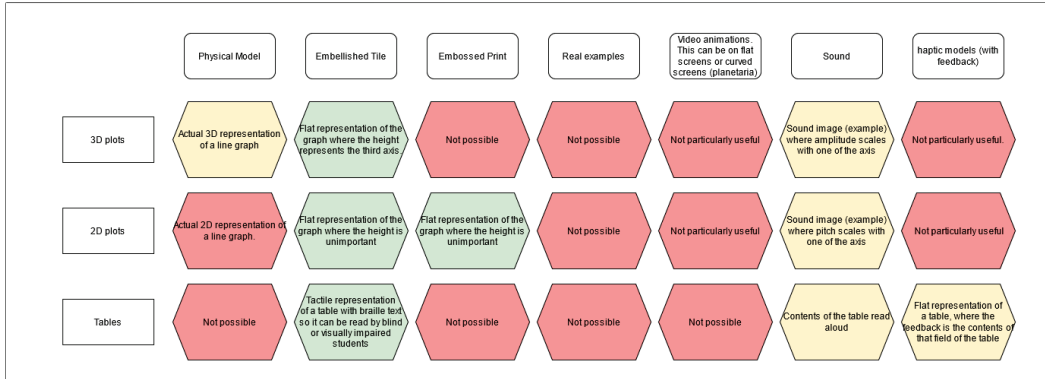
Figure 4: Diagram containing models to explain general tools that are used in astronomy and how well suited they are to explain the tool. DOI: 10.13140/RG.2.2.33175.65448

from the point of view of blind or visually impaired students. Like in the section before I will explain all the models in Figure 4.

3D plots

Physical model: Actual 3D representation of a line graph. The three axis of the graph are shown as perpendicular lines. The line of the graph is created as a real line in 3D space. This line might need some support because otherwise it can collapse, as it can be unstable. In that case the bottom of the model should be a solid tile onto which the supports can be fixed. This type of model can only show line plots and no dot plots. This model is also not very easy to create, but a great advantage is that it can be looked at from all angles.

Embellished tile: Flat representation of the graph where the height represents the third axis. The two dimensions of the tile can represent two of the three axis of the graph, while the height with respect to the tile represents the third axis. This type of model can show both line graphs and dot plots, while not being especially difficult to create. Unfortunately it is quite hard to show negative values using this model, but that can be sometimes worked around by shifting these values into the positive.

Embossed print: Not possible. The embossed print model can not show a third dimension and can therefore not be used to show 3D plots.

Real examples: Not possible. There are no plots that are actually real in this sense.

Video animations: Not particularly useful. It is possible to render a 3D plot and to create a video animation that can look at it from different angles, however the other models are easier to create in most situations.

Sound: Sonified image (example) where amplitude scales with one of the axis. This sonified image can recreate the embellished tile model, where time and pitch represent the tile axis while amplitude represents the third axis. This sonified image can create quite a fluent sound which helps the students to imagine the plots more naturally.

Haptic: Not particularly useful. It is possible to recreate the physical model (without the supports) as a haptic model, but it can be rather confusing to understand without good

21

explanation. It should be one of the upsides of the haptic model that it can be understood without much deep explanation. Another upside of haptic devices is that they generate feedback, which is also something that is not used in this model. Since these major upsides of the haptic device are not used, it is probably not a good idea to use this model.

2D plots
Physical model: Actual 2D representation of a line graph. It is possible to create a 2D graph using a 3D physical model. This can be done by showing the axis of the graph as two perpendicular lines. The line of the graph in that case can be shown as a physical line in the plane between the two axis. By doing this we basically create a flimsy physical representation of a graph that is similar to the embellished tile model described below, except for the fact that the physical model does not use a tile. Again, the physical model can not show be used to show dot plots.
Embellished tile: Flat representation of the graph where the height is unimportant. The tile of the model represents the two axis and the line or dots can be represented by heightened parts of the tile. The amount of height does not really matter and this model can show line graphs as well as dot plots.
Embossed print: Flat representation of the graph where the height is unimportant. Since the amount of height does not really matter for the embellished tile model, the embossed print model can show a 2D plot in exactly the same way as the embellished tile model. If you can create embossed prints easier than embellished tiles, it can be worth it to produced an embossed print model over the embellished tile model.
Real examples: Not possible. There are no plots that are actually real in this sense.
Video animations: Not particularly useful. It is not very useful for a video animation to show a 2D image, since it does not add any value from looking at it from different angles.
Sound: Sonified image (example) where pitch scales with one of the axis. The sonified image that can be created to show 2D plots is very similar to the one that can show 3D plots. The two dimensions can be represented by time and pitch. The main difference is that the missing dimension removes the need for a dependence on varying amplitude. So the line of the graph or the dots of the dot plots can be represented by a sound at a certain fixed amplitude at the time and pitch where it belongs.
Haptic: Not particularly useful. The haptic model can represent the physical model or the embellished tile model, but since it is much easier to print these models and the feedback of the haptic device would not be used, it is probably not worth it to create a haptic model to replace them instead.

Tables
Physical model: Not possible. The 3D representation of a table would have the same configuration as an embellished tile model, so I will explain it there instead of here.
Embellished tile: Tactile representation of a table with braille text so it can be read by blind or visually impaired students. This model basically recreates the printed table where the lines have a height and the text is replaced with braille. The blind or visually impaired students will most likely need some help to understand the model for the first time, but

after that similar models can be understood immediately.

Embossed print: Not possible. Since the embossed print model can not show braille, it can not be used to help blind or visually impaired students understand tables better.

Real examples: Not possible. There are no tables that are actually real in this sense.

Video animations: Not possible. Video animations can not be interpreted by blind or visually impaired students.

Sound: Contents of the table read aloud. Sonified images can usually be used to interpret the embellished tile model as sound. However in this case the structure of the table is not important, but the contents and they way they are arranged is important. So the sonified image can not just copy the embellished tile. Instead the sonified image can be used as a sound file that reads the contents of the table out in the way that they are arranged. This is most useful if the contents are not just numbers but text, since it is less abstract in that case, but it can work in both cases.

Haptic: Flat representation of a table, where the feedback is the contents of that field of the table. In this case, the haptic model can represent the embellished tile model. Here the feedback can be the contents of the table in that part of the table. This can either be in tangible braille on the surface or as voice coming from the device. What you choose depends on preference and the haptic device in question.

Now that the general tools are discussed, I can move on to the supporting devices that can help blind or visually impaired students to better learn the study material.

2.2.3   Diagram of supporting devices

The models and devices in Figure 5 come in three different categories. Models and devices that can help to interpret the study material, that can help to do measurements and that can improve the communication between students, both blind or visually impaired and not. There are two devices or models that help to interpret the study material, there is one device that can help to do measurements and there are three devices or models that can help to improve the communication between students. The devices and models shown in Figure 5 are described below.

Interpreting study material
Computers with speech (e.g. JAWS): Blind or visually impaired students often have difficulty in finding study materials that are easily interpretable by them. The books or online material is often not made with the needs of blind or visually impaired students in mind. In that case, these students can make use of computers with screen reading programs like the often used JAWS software installed (Harshman, Bretz, and Yezierski 2013). These will allow the student to access the online study material and, if they are supplied in a digital format, the books in away that is interpretable without the necessity of sight. These computers can read the information out loud for them even if a braille version of the study material is not available.
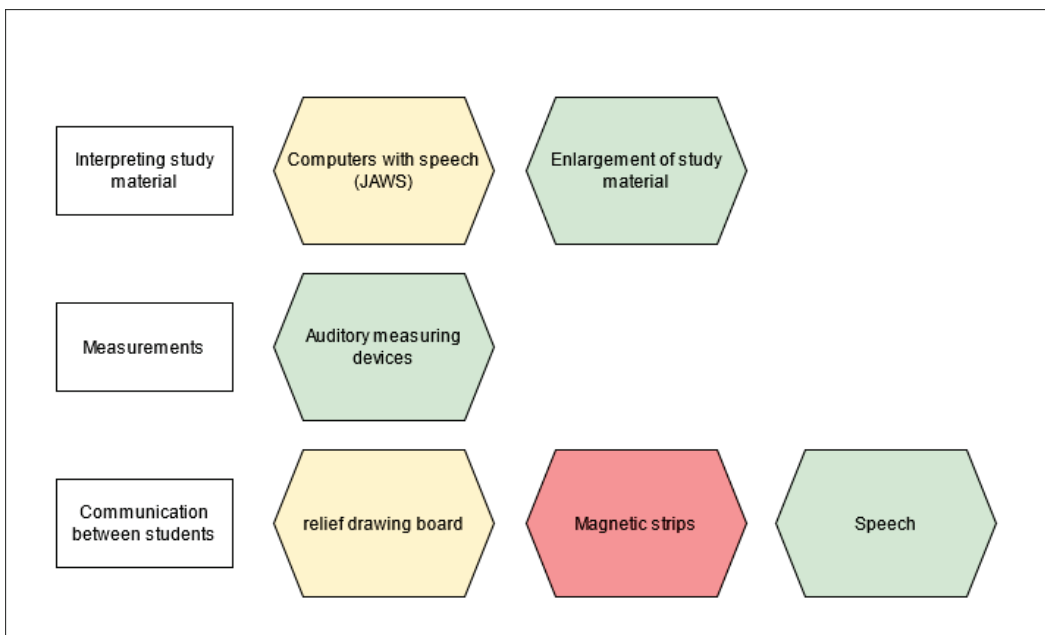
Figure 5: Diagram containing various types of supporting devices that can help blind or visually impaired students to participate in astronomy education and how well suited they are to do so. DOI: 10.13140/RG.2.2.20592.74241

Enlargement of study material: This method does not work for blind students, but visually impaired students can sometimes make use of enlarged study material. Whether or not they can make use of this depends on the student(s) in question, but when the vision of the student is not extremely impaired the existing study material can just simply be enlarged to allow the student(s) to interpret the material. Since this does not work for all students it is not the most reliable method to help impaired students to understand the material, but it is very easy to apply.

Measurements

Auditory measuring devices: Even in astronomy, measurements are sometimes done using handheld measuring devices like rulers or stopwatches. For instance when real distances in models are investigated or when the time between measurements is needed. There exist auditory versions of many handheld measuring devices. They return the result of the measurement as sound which can be understood by all students. This allows blind or visually impaired students to do measurements by themselves (Fraser and Maguvhe 2008).

Communication between students

Relief drawing board: When working together in groups, it can sometimes be hard for blind or visually impaired students to participate in the exchange of ideas. Showing notes or drawings with eachother is usually a large part of this, but blind or visually impaired students can obviously not take part in that. To allow them to do so anyway, a relief drawing board can be used. These devices allow students to draw with embossment, which enables blind or visually impaired students to feel what the other students have drawn. This can improve communication between students when working together (Toenders et al. 2017).

Magnetic strips: Magnetic strips largely work the same as the relief drawing board above, they can allow students to communicate ideas between them without relying on drawings or writing but on touch. The magnetic strips can be placed on a magnetic board where they can be used to create diagrams. An example of this model was investigated by Azevedo and Santos 2014. They used magnetic strips and ribbons to explain optics to blind students. On the whole, this method is more restricted than the above described relief drawing board, but they can be easier to create.

Speech: Finally, the most reliable method of communication between any set of students is speech. This section serves as a reminder that blind or visually impaired students should not be excluded from projects just because they can't see as well as others. Studies show that these students are just as smart and resourceful as other students if they get the chance to study the subject (Bülbül, Garip, and Özdemir 2015) and (Butler et al. 2017). Including the blind or visually impaired students in the conversation of the group helps just as much as including any other student.

2.3   Conclusion

In this section I described models that can be used to explain various topics in an astronomy bachelor education. These models can allow more students to effectively learn over the duration of the course. Some of the models allow blind or visually impaired students to be able to understand explanations that they would not be able to understand otherwise. tactile learners will also be able to take advantage of some of the models, because it fits better to the way that they learn. Many of the discussed models are able to be printed using a 3D printer, which makes them easy to create and use. Some of the discussed models are also rather exotic, such as the sonified images or the haptic devices. These are mostly discussed to improve the inclusion of blind or visually impaired students in astronomy education. It should be noted that by themselves, these models often do not provide a lot of value but together with explanations from the teacher they should help all students to better understand the course material.

3 3D model development

In this section I will discuss the development of the 3D models for observational astronomy. I will first explain how the models were designed and secondly how the models were created. This section can also serve as a guide to help the reader create 3D models of (astronomy) images for themselves.

3.1 Design of the models

According to the students' and teachers' experience of previous years it was determined by private conversation that the topics that the first years students struggled with the most were: the fitting of galaxies to models, the changing intensities of variable stars and point spread functions (PSFs). In order to get the most use out of the models made in this project I decided to focus on those topics.

3.1.1 Fitting of galaxies

From private conversation with first year teachers I learned that there were generally two parts of galaxy fitting that students had trouble understanding. First, students found it hard to imagine the shape of the fitted profile in relation to the galaxy it was fitted to. I.e. they had trouble to understand what they are exactly fitting to the galaxy in the image. Students may find this easier to understand if they can see the shape of the galaxy in the image and the fitted profile at the same time, which is what I am going to do with the printed model. The second problem is that the students found it difficult to imagine what the scaling factor, such as scaling radius, that appears in many galaxy models stands for. Usually this factor has a formal definition, for instance the radius for which the mass inside the model at that radius is a certain fraction of the total mass. However students may find it easier to understand if this radius is actually visualized in the image, which is what I am going to do with the printed model.

    To try and solve both problems together, a model is designed for each considered galaxy. The models should consist of two halves, one which represents the observed galaxy and one which represents the fitted profile. The horizontal plane of the model represents the x-y position in the image and the profile and the vertical height of the model represents the intensity of the galaxy image or the profile at that position. Since the profile is fitted to the galaxy the students should be able to see that the shape of the profile and the galaxy is very similar and that the main difference between the two sides of the model is that the galaxy side looks a bit more noisy. The second thing that the model should have is a feature that shows the position of the scaling radius in both the galaxy and profile side of the model. In practice the scaling radius is visualized by a cylinder that pokes out of the rest of the model at the position of the scaling radius. This way, the students should be able to see and feel the position of the scaling radius.

3.1.2 Variable stars

From private conversation with first year teachers I learned that the thing that students struggled to understand about variable stars was how they can be identified in an image. So the students have difficulty seeing the difference between normal stars and variable stars in an image. It is easy to understand why this might happen, normal images are often logarithmically scaled in colour shade which means that it can be hard to see by eye how the intensity of a variable star slightly changes. On top of that, a light curve might not mean a lot to a tactile student or a student who is unfamiliar with these kinds of graphs. To be able to capture the changing intensity of a variable star a series of models is designed. Each model consists of an image of the variable star with its surrounding stars at a certain time. The horizontal plane of the model represents the x-y position in the image and the vertical height of the model represents the intensity of the image at that position. This intensity is scaled such that the height difference between each image can both be sensed and such that the model is not extremely large. This way the students should be able to identify the variable star in the set of images themselves. Since it would be a waste of space to create a separate model for each individual image and to improve the ability to compare two images, every physical model consists of two images at different times with a border between them.

3.1.3 PSFs

From private conversation with first year teachers I also learned that there are two things that students struggled with in understanding PSFs. First, the shape of the PSF and how this depends on the telescope it is related to can be a source of confusion. Secondly, the way that different PSFs influence an image is also not always perfectly understood. To make the workings of PSFs clearer to students, a set of models is designed. These models consist of two halves separated by a border, on one of the halves a PSF is shown and on the other half two stars are shown as they would be observed using a telescope with the shown PSF. This is done for several different PSFs. This way the students should be able to observe the impact of the PSF, and therefore the telescope, on the shape of the star(s) in an image.

3.2 Creating the models

I will now describe in more detail how each of the above described model were created. I will discuss problems I ran into and the solutions I came up with as well as tips that the reader can use to create similar models themselves. How the models are created depends on the used 3D printer as well. The printer that was used during this project was a mini 3D printer (Labists 2021) and was personally owned by my supervisor Jake. The code referenced in this section was made by me (Postema and Noel-Storr 2021).

3.2.1 General starting point

Before a 3D model can be printed out, a digital 3D model has to be created. This 3D model can then be interpreted by the 3D printer software to generate instructions for the printer which makes the physical model in the end. There are many possible ways to create digital 3D models in many different file formats. Since I am primarily dealing with turning images into models, a computational way is the most appropriate way to generate the models. Since the computer language that I have the most experience with is Python I will use Jupyter notebooks (Kluyver et al. 2016) and Python packages to create the models. The most important Python package that I will use is "Numpy-stl" (Hattem 2021). This package allows for the creation of .stl files from python code using the well known "Numpy" package (Harris et al. 2020). The .stl file format belongs to certain digital 3D models and consists of a set of triangles in 3D space that represent the surface(s) of the model. These triangles are what you create when using Numpy-stl. All of the models in this thesis are created using functions that take an image and make triangles out of each set of 3 touching array components. The x and y value of the coordinates of each pixel is determined by the x and y position of the pixel in the image and its z value is determined by the intensity in that pixel. To turn these values into physical units I will scale them by the predetermined dimensions of the physical models. The printer that Jake and I used for instance could reliably print models that had a size of (x,y,z) = (80,80,40) mm which is why all of the models have this as an upper limit of the size. After each pixel is assigned coordinates in 3D space the triangles are drawn and the 3D model is created using Numpy-stl. Just this alone would basically create a sheet with the shape of the image. This can be printed if the image is rather smooth, but in any case this model is more difficult to handle and less rigid when printed. It is therefore always nice for any model to have a well defined layer underneath it that is connected to the edges of the rest of the model. You can do this using 3D editing software like Blender after creating the sheet but it can also be made with Numpy-stl using 2 big triangles for each of the sides and the bottom. In all of my models the layer had a width of 1.6, but if it turns out that the printed model is still too flimsy it might help to increase the width. These are all of the steps needed to create a digital 3D model out of a (properly normalized) 2D image. How the images are generated and altered depends greatly on the type of 3D model that is created and will therefore be discussed separately in the following sections.

3.2.2 Fitting of galaxies

In total, 7 models for galaxy fitting are created. Three spiral galaxy models, two elliptical galaxy models and two globular cluster models. This is done in order to show the small differences in the shape of these clusters to the students. It should be noted that globular clusters are not galaxies, however because these objects are discussed in the course and they have their own fitting profile Jake and I decided to include them as well. Multiple models for each cluster type are made, because it can show the slight differences between different individual galaxies. Three spiral galaxies were chosen, because one of the initially picked
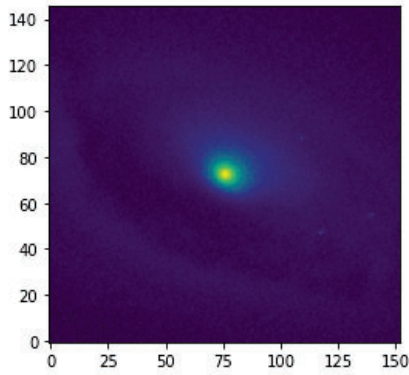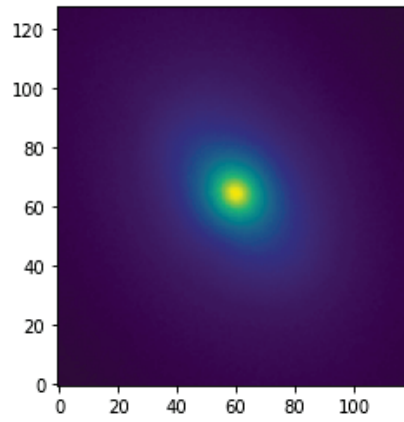
spiral galaxies was imaged edge on.
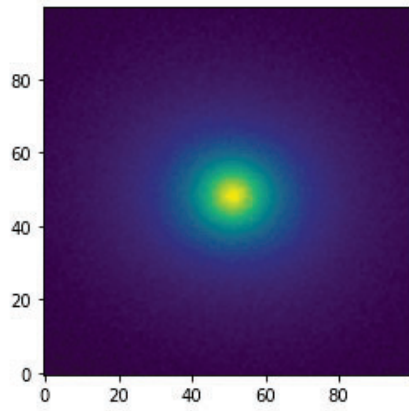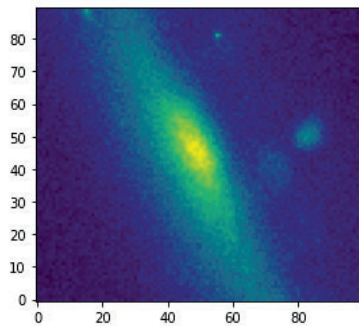

(a) Elliptical galaxy M60
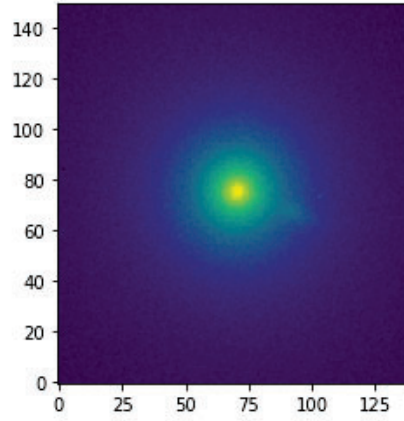
(b) Elliptical galaxy M87

(c) Spiral galaxy M64

(d) Spiral galaxy M81

(e) Spiral galaxy NGC5907

Figure 6: Reduced image of the modelled galaxies, yellow corresponds to high intensity and blue to low intensity. The x and y dimensions of the images are shown in pixels.

This makes for an interesting model, but it is hard to show the fitting properly in this model. To still be able to teach fitting well enough and to show what an edge on galaxy looks like when printed in 3D I decided to make one more spiral galaxy model. The actual images of the clusters that will be used to create the 3D models are made by last year's observational astronomy students. These images were made using the Blaauw observatory at the Zernike Campus, whose main use is to teach students how to do observations. I did this because I thought it would be fitting to the goal of this research to show that the results of last year's students can actually help this year's students. Furthermore this will also show that anyone can create nice 3D physical models using self made observations. The chosen spiral galaxies are: M 64, M 81 and NGC 5907 (the edge on one). The chosen elliptical galaxies are: M 60 and M 87. The chosen globular clusters are M 3 and M 53. The data of these galaxies are available at the Blaauw Observatory Knowledgebase (`https://sites.google.com/a/rug.nl/blaauw-observer/home`). The band that is used for each observation depends on which band was the most clearly observed, since those could create the best models. Before each of the images gets turned into a digital 3D model using a function like the one described in the previous section, some data altering is done. After the data was reduced, I zoomed in at the center of the galaxy such that I have a square image which encloses the galaxy. After this, the image is normalized by subtracting background noise. This background was found by taking the average pixel value in the corners of the images. The final reduced images of the galaxies are shown in figure 6 and the final reduced images of the globular clusters are shown in figure 7.

(a) Globular cluster M53
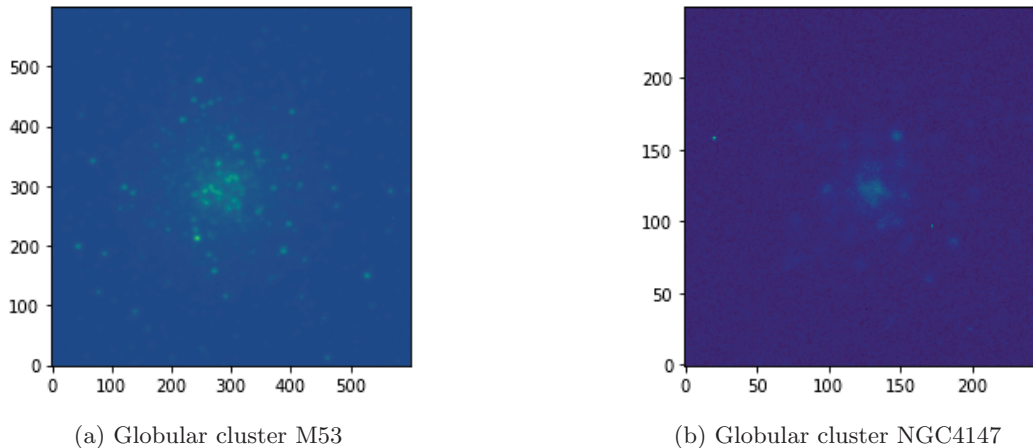
(b) Globular cluster NGC4147

Figure 7: Reduced image of the modelled globular clusters, yellow corresponds to high intensity and blue to low intensity. The x and y dimensions of the images are shown in pixels.

From figure 6, we can see that in the spiral galaxy M64 there might be some dust obscuring the light on the left side of the image and we can see that spiral galaxy NGC5907 is indeed edge on and zoomed in quite a lot to make its core visible. From figure 7, we can see that the globular clusters consist of individual point sources and that NGC4147 is not

easily differentiated from the background because of the low intensity of the stars. However we will still attempt to find a fit for all of these galaxies and clusters. The intensity as a function of radius for spherical and spiral galaxies very often follow a Sersic profile, which is shown in equation 1.

$$I(r) = I_e \exp\left\{-b_n\left[\left(\frac{r}{r_e}\right)^{1/n} - 1\right]\right\} \tag{1}$$

The fittable parameters in equation 1 are I_e, r_e and n. I_e is a scaling factor with units of intensity, r_e is the scaling radius with units of distance and n is the unitless Sersic index. b_n depends on n, because the scaling radius r_e is defined such that the intensity within that radius is half of the total luminosity of the galaxy. The luminosity of a galaxy with a Sersic profile inside a radius of r_e is given by:

$$L_{1/2} = \int_0^{r_e} 2\pi r I(r)\mathrm{d}r$$

$$L_{1/2} = 2\pi I_e e^{b_n} \int_0^{r_e} r e^{-b_n\left(\frac{r}{r_e}\right)^{1/n}}\mathrm{d}r$$

$$u = b_n^{2n}\left(\frac{r}{r_e}\right)^2 \;;\; \frac{\mathrm{d}u}{\mathrm{d}r} = \frac{2b_n^{2n}}{r_e^2}r$$

$$L_{1/2} = \frac{\pi I_e e^{b_n} r_e^2}{b_n^{2n}} \int_0^{u(r=r_e)} e^{-u^{1/(2n)}}\mathrm{d}u$$

$$t = u^{1/(2n)} \;;\; \frac{\mathrm{d}t}{\mathrm{d}u} = \frac{1}{2n}u^{1/(2n)-1} = \frac{1}{2n}t^{1-2n}$$

$$L_{1/2} = \frac{2\pi n I_e e^{b_n} r_e^2}{b_n^{2n}} \int_0^{t(r=r_e)} t^{2n-1}e^{-t}\mathrm{d}u$$

$$L_{1/2} = \frac{2\pi n I_e e^{b_n} r_e^2}{b_n^{2n}} \int_0^{b_n} t^{2n-1}e^{-t}\mathrm{d}u$$

$$L_{1/2} = \frac{2\pi n I_e e^{b_n} r_e^2}{b_n^{2n}}\gamma(2n, b_n)$$

Where $\gamma(2n, b_n)$ is the incomplete gamma function. The total luminosity of the galaxy has a very similar expression but the integral goes from 0 to infinity, so instead of the incomplete gamma function we have the full gamma function: $L_{tot} = \frac{2\pi n I_e e^{b_n} r_e^2}{b_n^{2n}}\Gamma(2n)$. Since we have $L_{tot} = 2L_{1/2}$, this means that b_n follows equation 2.

$$\Gamma(2n) = 2\gamma(2n, b_n) \tag{2}$$

Equation 2 can be solved numerically for a given n. Generally, elliptical galaxies are well described by a Sersic profile profile with $n \approx 4$ and spiral galaxies usually have $n \approx 1$. Equation 1 models the intensity as if the galaxy is circular, but in general this is definitely not true. Galaxies have an elliptical shape, I assumed that the shape of the galaxies does not change as a function of radius and determined their shape that way. Using this shape I created isochrones of each galaxy which I will then be able to fit to equation 1. The fitting was done with the help of the astropy Python package (Astropy Collaboration et al. 2018).

More specifically, the Levenberg-Marquardt algorithm was used with least squares statistics. When only this method was used to fit the galaxies, the result was not optimal, it could be seen from the digital 3D model that the shape of the model was not exactly the same as the shape of the data. Since spiral galaxies usually exist of multiple components (bulge, disk and halo) that each can be modelled with a Sersic profile with their own Sersic index I thought it was possible that the shape difference came about because I only took one component into account. By first fitting one Sersic profile to the center of the galaxy and after fitting a second Sersic profile to the entire galaxy with the first Sersic profile subtracted a profile that corresponds better with the real data was created. For each galaxy it was a challenge to find the radius of the inner Sersic profile.To make sure that the correct fit was made I compare the final inner Sersic fit to the measured isochrone of the data with the outer Sersic component subtracted. This comparison is shown in figure 8 for all of the elliptical and spiral galaxies. The optimal fits were found by changing the inner Sersic profile radius by hand and finding out where the best correspondence between the data and profile curves were. As can be seen in figure 8 most of the galaxies had a very nice correspondence between data and fit. Two notable outliers are the fit of the elliptical galaxy M60 and the fit of the spiral galaxy M81. In figure 8a we can see that the isochrones don't fit exactly to the inner Sersic profile because they are wobbling up and down a bit. This is likely due to the fact that the isochrones of a galaxy can be hard to determine near the center of the galaxy due to the lack of resolution for those small ellipses. In figure 8b we can see that the isochrones of M81 don't exactly fit for higher radii. However this is the best fit that could have been made for this galaxy and for the smaller radii this fit is very good. As we will see in section 4 the data for all of the galaxies does correspond quite well with the double Sersic profile, so I can conclude that the disagreements between the fit and the measured isochrones are not significant. At first it was thought that the inner Sersic profile belonged to the bulge and the outer Sersic profile belonged to the disk. However the fitting parameters did not correspond to previous research done on the same galaxies and there was also the fact that the double Sersic profile worked better for the elliptical galaxies while they generally consist of only one component. After conversation with Scott Trager, professor at the Kapteyn institute, it was found that it was found that not the bulge and the disk were fitted to the double Sersic profile, but the bulge and a single bright source in the middle of the galaxy. In order to print a model with sufficient detail I had to zoom in at the center of the galaxy. Because of this only the core of the galaxy is inside the image and the bright source in the middle has a significant size. The globular clusters were not fitted to a Sersic profile but a King profile, which is shown in equation 3

$$I(r) = Ar_c^2 \left(\frac{1}{\sqrt{r^2 + r_c^2}} - \frac{1}{\sqrt{r_t^2 + r_c^2}} \right)^2 \tag{3}$$

The fittable parameters in equation 3 are A, r_c and r_t. A is a scaling factor with units of intensity, r_c is the core radius with units of distance and r_t is the tidal radius with units of distance. Only one King profile fit well enough with the data which is as expected since globular clusters only have a single component.

(a) Elliptical galaxy M60

(b) Elliptical galaxy M87

(c) Spiral galaxy M64

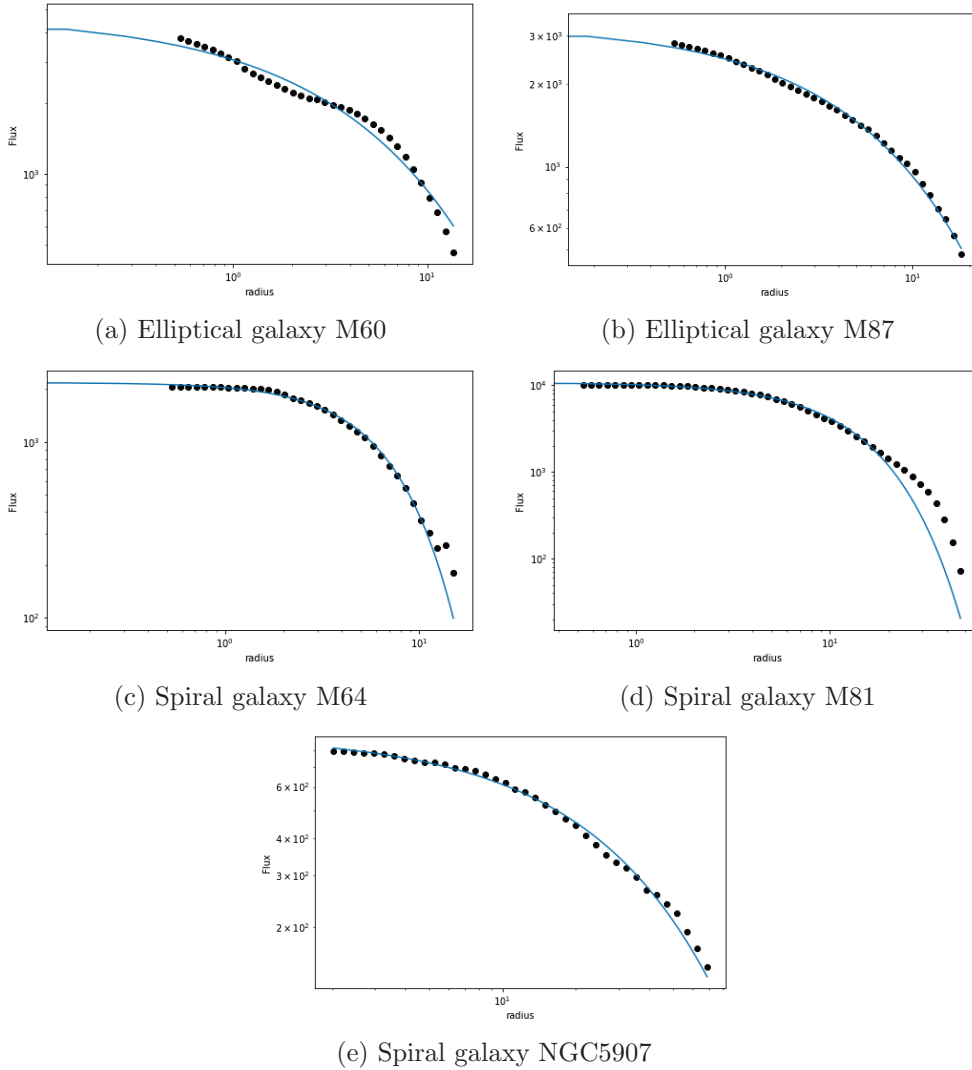(d) Spiral galaxy M81

(e) Spiral galaxy NGC5907

Figure 8: 1D fitted Sersic profiles (blue lines) compared to the measured isochrones of the data with the outer Sersic fit subtracted (dots) for each of the galaxy models. The radius has units of pixels.

To check how well the King fit corresponds to the data of the two globular clusters, the comparison between the isochrones and the King fit for both clusters is shown in figure 9. In figure 9a we can see a gap in the dots that represent the isochrones of the globular cluster data. This does not mean that there is no light coming from those positions but that the algorithm could not fit ellipses with that semi-major axis to the data. Besides that, we can see that the data of M53 fits quite well to the King profile fit. We can also see that the data of NGC4147 fits rather well to the fitted profile. The only place where the profile doesn't follow the isochrones is near the bend of the profile at a radius of 4 pixels. This is likely for

the same reason as to why there are isochrones missing for M53, the algorithm had difficulty fitting ellipses to the globular cluster. We can see that this is the case because the profile fits very well for the lower and higher radii.

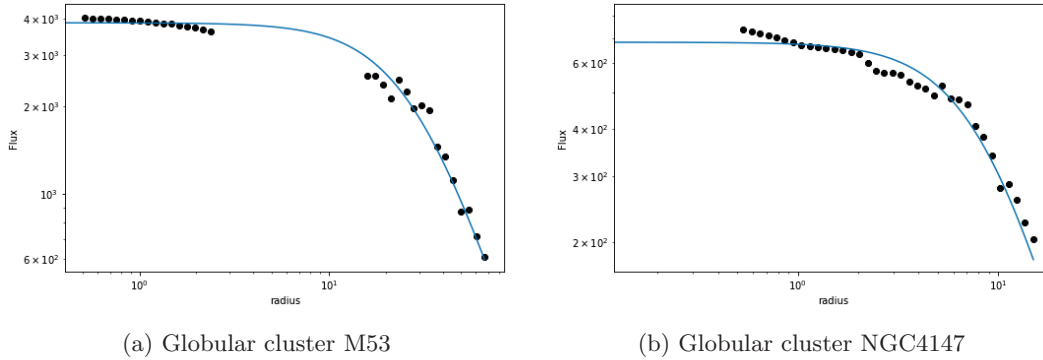(a) Globular cluster M53   (b) Globular cluster NGC4147

Figure 9: 1D fitted King profiles (blue lines) compared to the measured isochrones of the data (dots) for each of the globular cluster models.

Now that I know how to create the profile corresponding to each cluster and the (elliptical) shape of the cluster I can create a grid with the same size as the image that has intensity values in each pixel as calculated by the total profile. Next, the intensities are scaled such that the highest point has a height of 41.6 mm. The final image consists for one half out of that half of the data and for the other half out of that half of the generated grid. The x,y plane of this image is scaled such that its length is 80 by 80 mm at most. The final 3D models consist out of one additional component. This is a cylinder that comes out of the other component and shows the scaling radius (in case of the Sersic profile fitted models) or the core radius (for the King profile fitted models). This cylinder has the same (elliptical) shape as the galaxy or globular cluster, a height that is equal to the height of the other component at the scaling radius/core radius and a semi-major axis that is a little bit longer than the scaling radius. How much longer depends on what looks good for the model such that the cylinder does not overlap too much of the model but is also really easy to feel.

Combining both of these components together creates the digital 3D model which can then be printed. An example of what a digital 3D model looks like is shown in figure 10.

3.2.3 Variable stars

To explain the workings of variable stars, 6 models were created. Each of these models show the star YZ Boo and its surroundings at two different times. YZ Boo is a variable star, which means that its intensity changes over time with a certain frequency. If I show the intensity of YZ Boo with respect to its constant background at 12 different times its variable nature can be made clear. The observation of YZ Boo that I will use was done by Daan Vermaat, a (currently) second year astronomy student. These observations were done
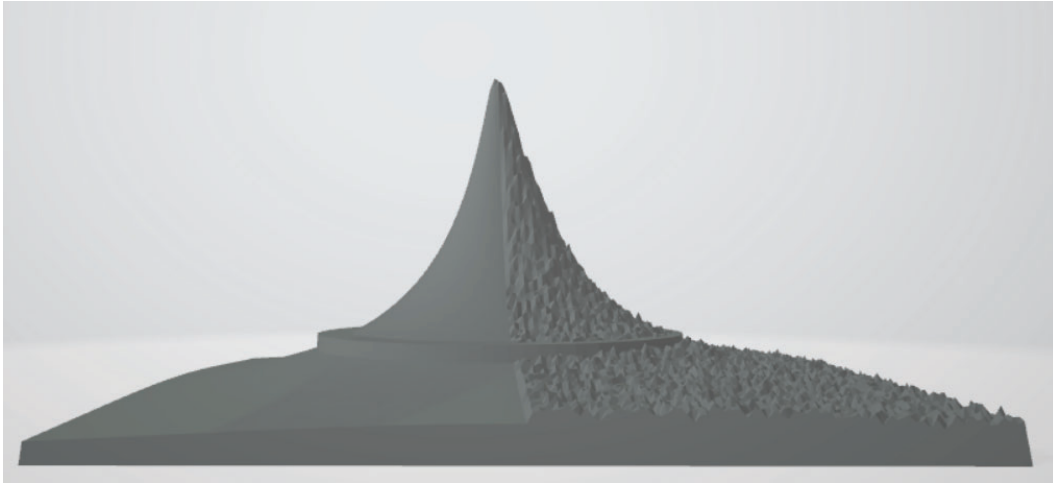
Figure 10: Side view of the digital 3D galaxy model of the elliptical M87. The right side shows the data and the left side shows the model. The cylinder that shows the scaling radius can also be seen on both sides.

during last year's observational astronomy course. I chose those observations, because they were incredibly well done and produced very nice results. This was in part due to the great data reduction that he performed, which is why I will use his reduced images to start off from. The R band observations were the most clear, so I used those to make the models. One of the advantages of using the data that Daan prepared is that each image has the stars in the same position. This makes it easier to just focus on the changing intensity instead of a possibly changing position of YZ Boo as well. One of Daan's observations is shown in figure 11. During last year's observational astronomy course, more then 12 images of YZ Boo were taken. However, to keep the amount of created models to a reasonable amount I decided to look for images that had a time difference of approximately 30 minutes, this can be seen in figure 13. To get an even number of images and a roughly consistent time difference between observations, the actual time difference between each images is around 28.4 minutes. This is shown in table 1. The six models together in a row should form a proper timeline of the intensity of YZ Boo, so each model consists of two images of YZ Boo with a time difference of almost 30 minutes and the time difference between each model is also almost 30 minutes. Since each image has the stars in the same position I can easily zoom in on YZ Boo and its neighbouring stars in every image at the same time. To improve the resolution of our model the image is zoomed in on YZ Boo and two major nearby (not variable) reference stars as well as some dimmer stars elsewhere in the image. Each individual zoomed in picture has dimensions of: 350 by 475 pixels. This means that the entire model will be 700 by 475 pixels. Since I wanted the longest axis in the x,y-plane to be 80 mm, the image will have a real size of 80 by 54 mm (rounded down). So in contrary to the galaxy fitting models, who are square, the variable star models will be rectangular. What an individual observation of YZ Boo and its neighbourhood looks like after being zoomed in is shown in figure 12. If I were to just create the physical 3D model from this without re-scaling the intensities, I

Figure 11: One of the observations done by Daan Vermaat. The star with the blue circle around it is YZ Boo, the stars with the red circles around them are the two major reference stars.
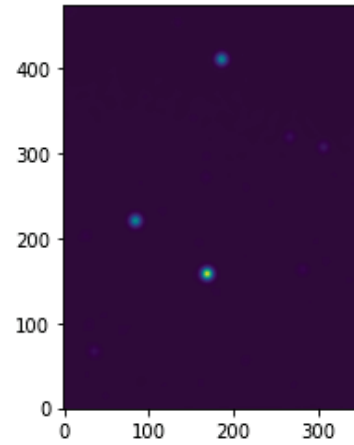

Figure 12: Zoomed in and rotated image of YZ Boo. YZ Boo is now the bottom major star and the reference stars are the other two major stars. This is the orientation that the images that are used to make the model have.
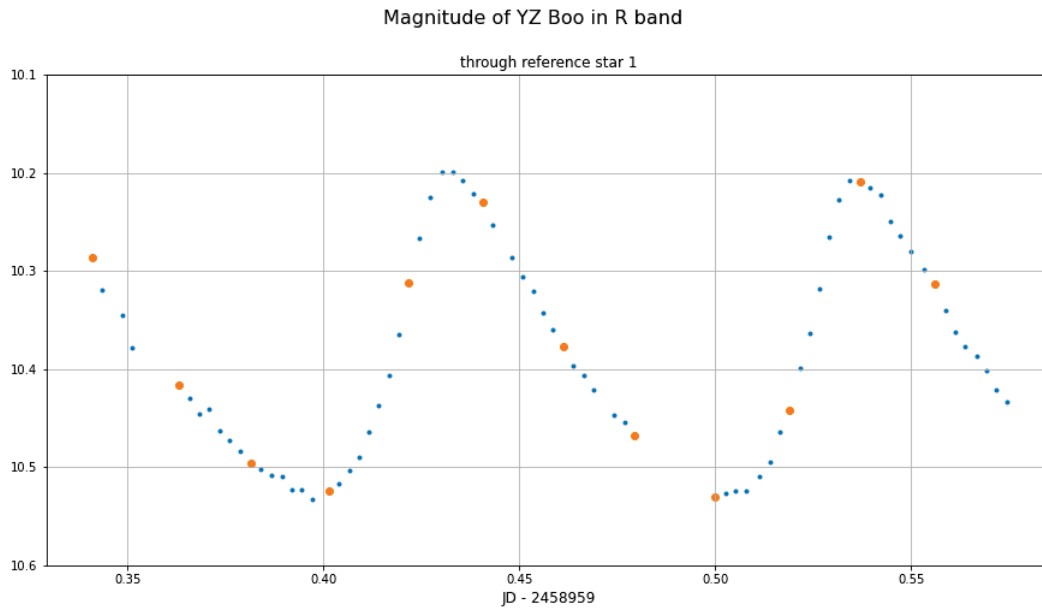

Figure 13: Light curve of YZ Boo created by Daan Vermaat. The observations used for the models are shown with orange dots. This figure shows that the observations in the models have an even separation in time.

would have two problems. First off all, the intensity peaks of the stars will appear too thin when printed, which in our case resulted in printing errors. Secondly, even if the model was printed correctly you wouldn't be able to tell the height of each peak apart. These problems were solved by altering the data in the images in a non-linear way. I can make the intensity peaks of the stars easier to print by making them fatter. This is done by convolving the entire image with a fatter PSF. Different Gaussian PSFs were tried until the image could be printed without errors. The second problem defeats the entire point of the models, so I had to do something about it as well. The reason why it was hard to feel a height difference was because the absolute difference in intensity between the images is very small compared to the total intensity of the peaks. I therefore have to rescale our intensity peaks such that the small difference is magnified. I also need to make sure that the shape of the peaks do not significantly change from the normal situations, otherwise I will give off the wrong idea. If I just decrease the scaling of intensity to height in millimeters as the intensity becomes higher, the peaks will become too flat at the bottom. To make the peaks still represent the shape of a real star I did the following. First, the intensities are linearly scaled such that the peak of the brightest reference star in the image always has a height of 6.6 mm. This was done so that the students will have a reference to investigate the variability of YZ Boo. The specific height was chosen because any higher than 5 mm (the extra 1.6 mm belongs to the layer below) would make rather pointy peaks, which are hard to print. This causes the height of YZ Boo's peak to be varying around 10 mm. However, due to the convolution with the fat PSF, the peaks do not look as peaky as they would be in reality. To fix this I will scale the intensity of YZ Boo's peak above a certain height logarithmically with physical height in mm. This will ensure that the peak will keep its peaky shape in the printed model while still being fat enough to print. Since I do not want to alter the shape of the reference stars the scaling will start above a height of 6.6 mm. The log base was chosen to be 2. This specific base was chosen because the height difference between peaks still needs to be observable. It is assumed that a height difference of 0.4 mm can still be felt by users of the models, so since this log base makes sure that the height differences between YZ Boo peaks within each model are higher than this value (as long as they are supposed to be different) it was chosen. This is shown in table 1. The logarithm base and height of the reference stars can be changed of course, but this setup worked well enough for our printer and demands for the model. The 3D model not only consists of two of these images, but also a border between them. This border was made very similarly to the layer underneath each model and was placed on the intersection between the two images.

3.2.4   PSFs

Three models were created to improve students' understanding of PSFs. Each model corresponds to a different kind of telescope. One big telescope, one medium telescope and one small telescope. These telescopes will have a thin, medium and fat PSF respectively. The 3D models show both the PSF of the telescope and what an observation of two point sources done by the telescope would look like. The considered shape of the PSF given by equation 4, where r is the distance in the image away from center of the PSF and Z is the height of

	Time difference between previous model (min)	Time difference within model (min)	Height difference between YZ Boo peaks with previous model (mm)	Height difference between YZ Boo peaks within model (mm)
Model 1	N.A.	28.6	N.A.	0.49
Model 2	30	28.4	1.49	0.31
Model 3	29.7	27	1.10	0.84
Model 4	27	27.5	0.71	0.78
Model 5	29.5	27.5	0.37	0.71
Model 6	29.6	27.6	1.33	0.62

Table 1: Time difference between the first observation of the model and the last observation of the previous model, time difference between the two observations in the model, height difference between the first observation of the model and the last observation of the previous model and height difference between the two observations in the model shown for each of the 6 created digital models.

the PSF at that position.

$$Z = \frac{\sin(r)}{r} \tag{4}$$

Since the PSF in equation 4 diverges when $r = 0$, I made sure that r will always be at least 0.01. The 3D model consists of two halves, one half only shows the PSF, the other half shows what two point sources would look like when observed with a telescope with that PSF. The first half, that only shows the PSF, was created by taking equation 4 and evaluating it in a grid with physical dimensions of 40 by 40 mm. The physical height of the PSF was scaled such that the highest peak will be 19.6 mm high in all of the models. The other half was created by making two PSFs like described above, one at a position (10,24) mm and the other at a position (30,8) in another grid with physical dimensions of 40 by 40 mm. Together, these grids will create an image that has dimensions of 40 by 80 mm. To create a clear distinction between the two sections, a border is created between them. This border was created in the same way as the border described in the section about the variable star model. The final digital 3D models are stored are publicly available (Postema and Noel-Storr 2021).

4 The models

In this section I will show pictures of the 3D printed physical models that were made using the previously described methods. I will also discuss how the first printed models helped to improve and create the final set of models. Any discrepancies between the 3D printed models and the digital model are also discussed if needed.

4.1 The first generation of models

Before I started the project me and my supervisor Jake had no experience with creating 3D models from observed data. The 3D printer that was used during this project was Jake's personal 3D printer. To get a grasp on what criteria we should take into account when creating the digital models, we started printing prototypes of what would later become the final models. Since I started designing the galaxy models first, they are the main early prototypes. The first printed model can be seen in figure 14.

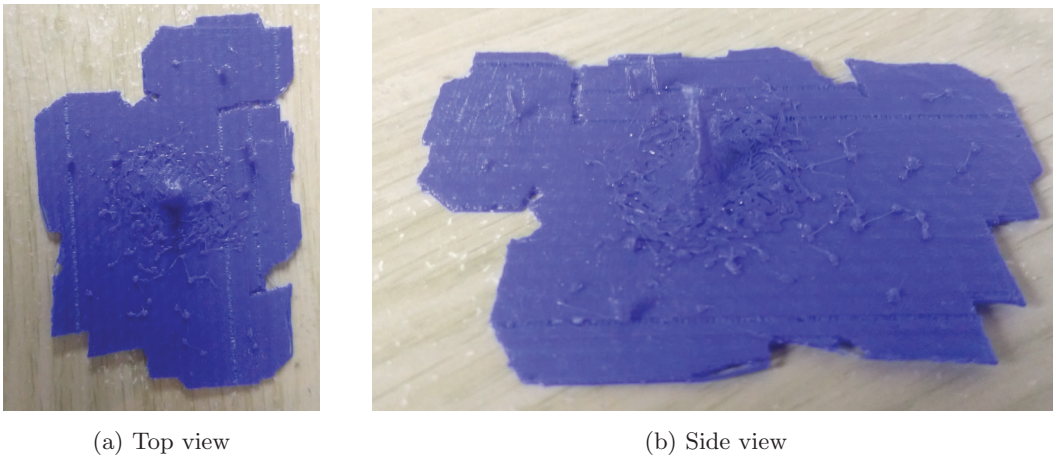

(a) Top view   (b) Side view

Figure 14: First printed prototype model as viewed from different angles.

This model just shows a galaxy, but clearly not in a very usable way. First off all, the peaks in the model are way too steep, secondly the model has a very poorly defined shape and thirdly the model is very thin which makes it flimsy. The main take-away that I took from this model is that I have to zoom in a lot more to show the galaxy in a reasonable resolution and to create a way more well defined shape. As for the Sersic fits of the models, they were printed by themselves at a certain point as well, this can be seen in figure 15.

40
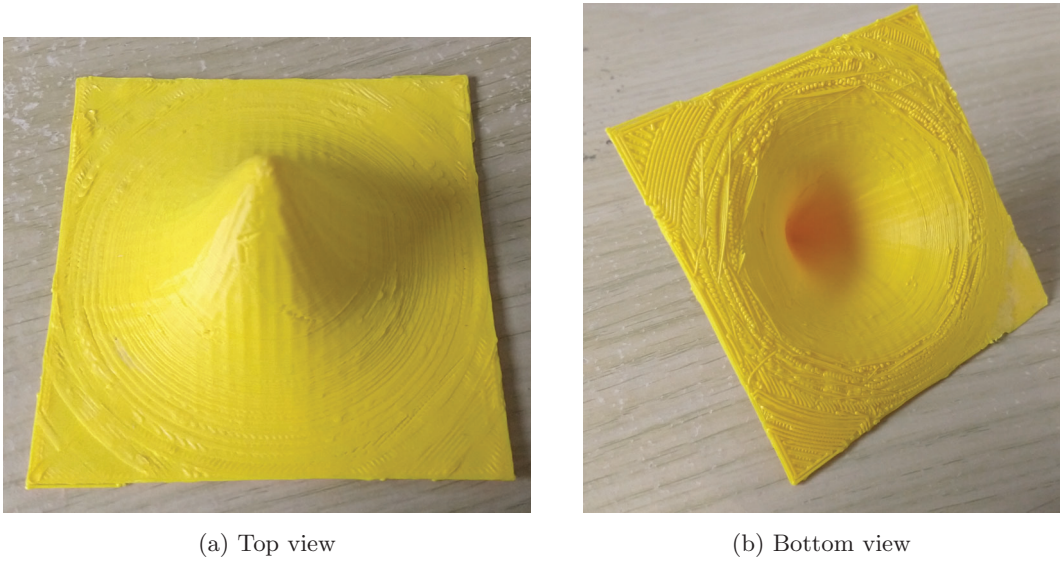
(a) Top view   (b) Bottom view

Figure 15: Printed Sersic profile prototype model as viewed from different angles. The model is quite flimsy and hollow which would be avoided in later models

We can already see that we have learned something from the previous prototype, the model's dimensions are well defined and its resolution is also a lot better as there are no steep peaks. However it is still a bit too flimsy as it was hollow from the inside. This was fixed in the later models by creating the 1.6 mm thick layer below them. Another problem that had to be solved for the galaxy models was how to create the indication for the scaling radius.
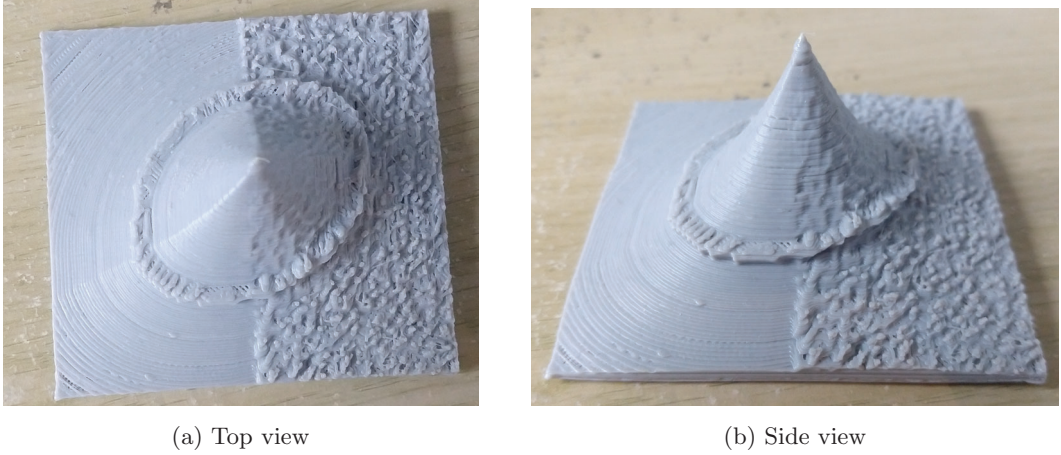
(a) Top view   (b) Side view

Figure 16: Printed prototype galaxy model with a poor scaling radius indicator as viewed from different angles. The scaling radius indicator seems like a part of the data rather than an artificial addition.

In an earlier prototype this was done by making the peaks at the position of the scaling radius go outward a bit more, as seen in figure 16. Unfortunately this made the indicator look like a part of the observed data, which is of course not meant to happen because it might confuse the students that use the model. To fix this I decided to implement the cylinder inside the model which comes out of the galaxy at the scaling radius. Some other prototypes for the galaxy models were also created before the final models were arrived at. They mainly differ from the final models by different scaling of the observed data or different fitted profiles. An example of this is shown in figure 17. In this figure we can see that the side corresponding to the fitted profile does not completely agree with the side corresponding to the observed data when looking at the outer edge of the model.

(a) Top view

(b) Side view
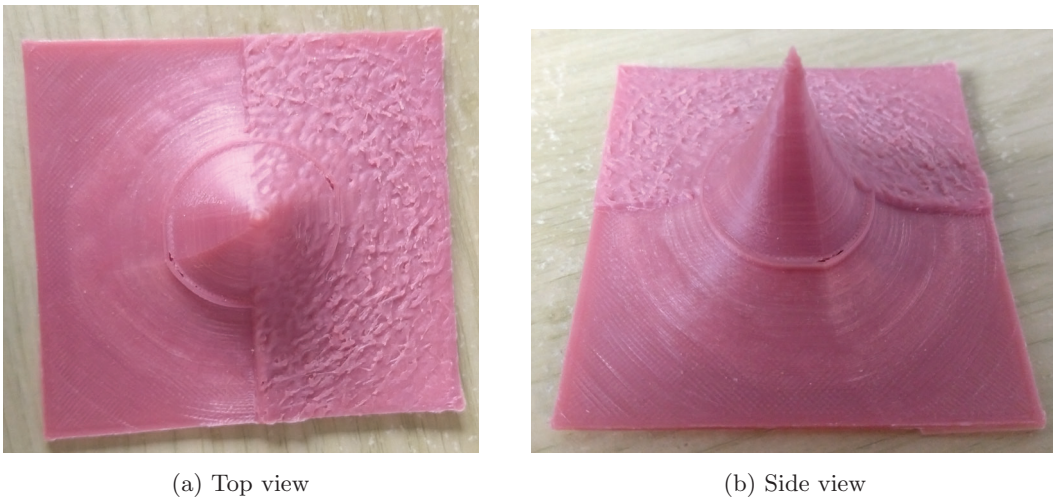
Figure 17: Printed prototype galaxy model as viewed from different angles. The difference in height between the data and model is too steep. The cylinder that represents the scaling radius is also too thin.
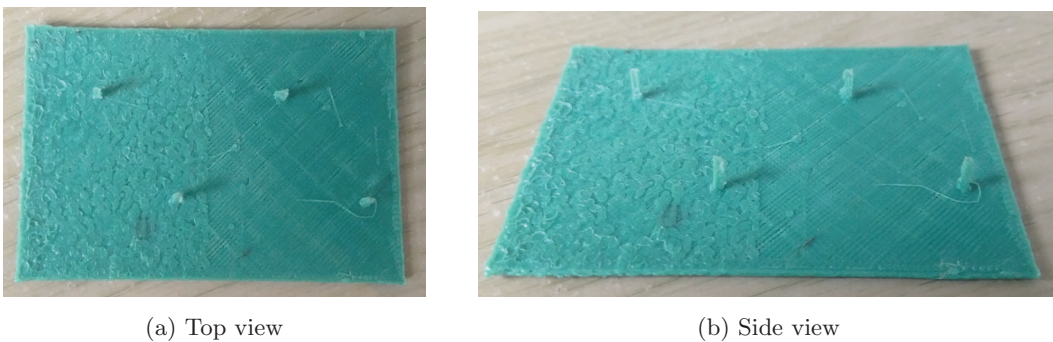

(a) Top view

(b) Side view

Figure 18: Printed prototype variable star model without border as viewed from different angles. The peaks seem indistinguishable and the two time records are hard to distinguish without a border between them.

The cylinder that indicates the scaling radius is also rather thin in this model which makes it hard to notice. Both of these shortcomings were improved in later models, one by creating a better fit with the observed data and the other by making the cylinder thicker. The variable star model also had a few prototypes before the final model was created. The first prototype did not have a border between the two images inside the model, as can be seen in figure 18. Though it was quickly decided that it was obvious that there should be one so that I can be sure that the students understand that there are two images inside each model. The main difficulty of creating the variable star models was making sure that the peaks of the stars got printed properly and so that they wouldn't break off easily. I decided that convolving the data with a fatter PSF would keep the data realistic while also improving our ability to print the model. To make the variable stars less peaky, it was also decided that the intensity would scale logarithmically above the peaks of the reference stars. This was done just for the variable stars because their peaks were the most prominent and therefore the most problematic. First a scaling of log 1.25 was tried, as shown in figure 19.
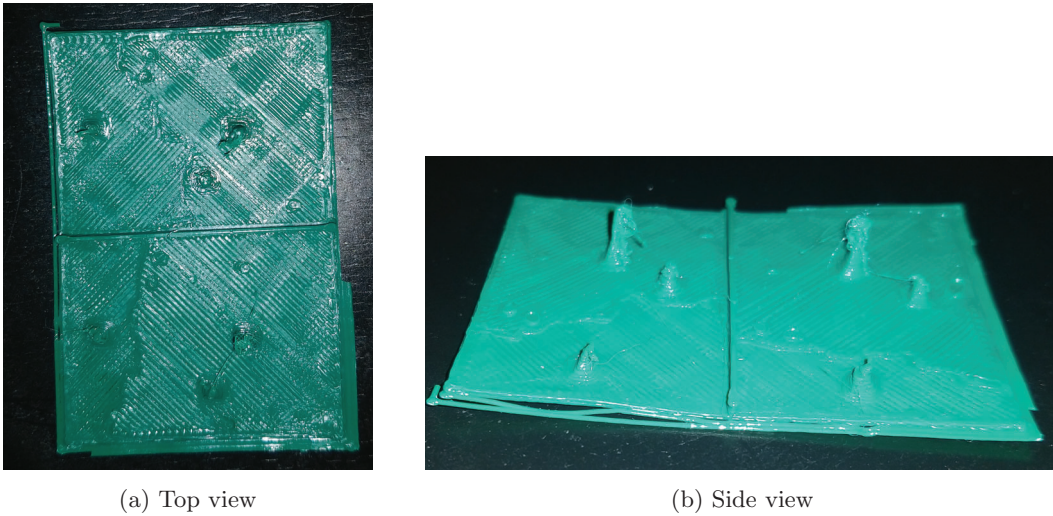

(a) Top view   (b) Side view

Figure 19: Printed prototype variable star model with a log 1.25 scaling above the reference star peaks. The log scaling in this model is still too small to make the difference in peak height noticeable.

However these peaks were still deemed to peaky and the model didn't look very nice, so the final model was created with a log 2 scaling, which looked a lot better.

Finally the creation of the PSF models was a lot easier compared to the other two models. This had two reasons. Firstly, the model used aspects that were already created for the previous models, like the border between the models and the use of PSFs. Secondly, the design of the PSF models is a lot simpler compared to the other two models, it had a lot less moving parts so there were less parts that might have trouble being printed. Despite this, there was still one problem with the first prototype. These models were printed just before the final testing of the models. Since there was very little time, only the models

with the narrowest and broadest PSF were printed. The PSF peaks of the model with the narrowest PSF unfortunately broke off as well. This problem only occurred in one of the models and it could clearly be seen where the peaks should be so it was not an extremely large problem, but if these models were to be redesigned this should be taken into account. The broadest prototype PSF model is shown in figure 20 and the narrowest prototype PSF model is shown in figure 21. All of the PSF models were later reprinted though.
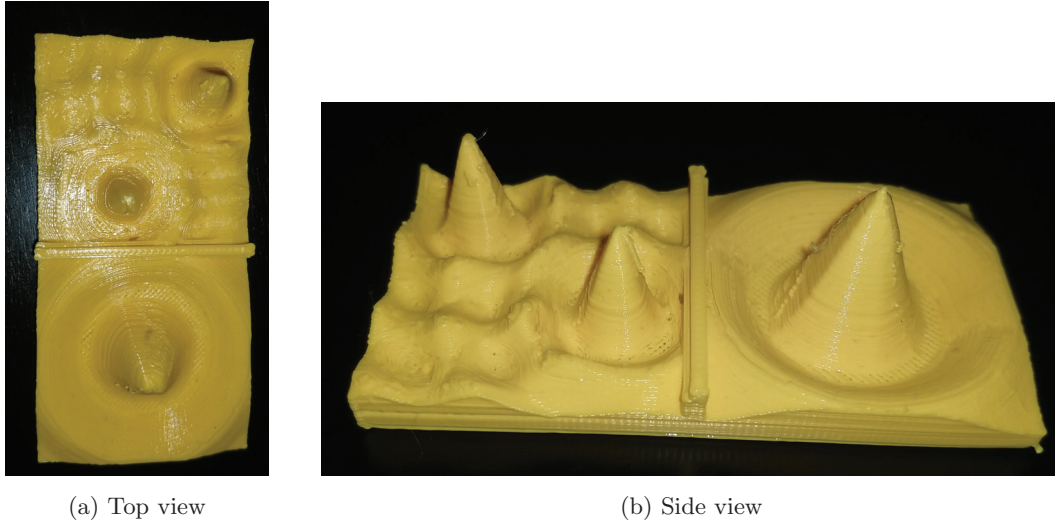

(a) Top view   (b) Side view

Figure 20: Printed prototype of the broadest PSF model.

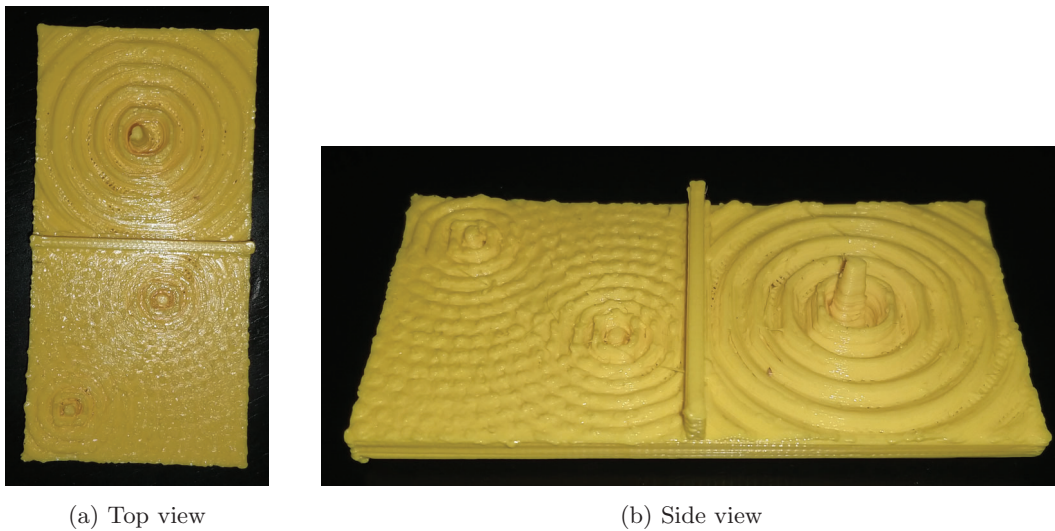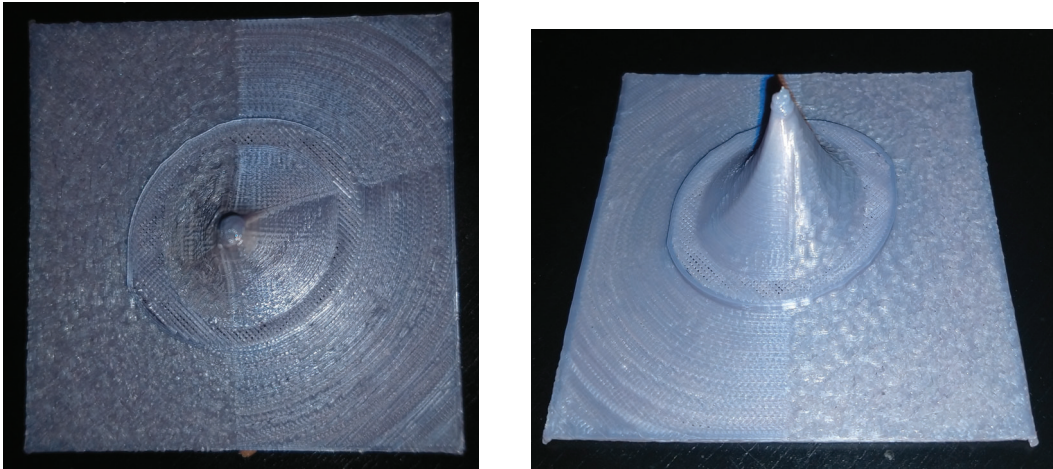(a) Top view   (b) Side view

Figure 21: Printed prototype of the narrowest PSF model.

44

At some point during the creation of the digital models, a swap to a higher resolution was made across all of the models. This was done because the printer could handle this higher resolution better than was earlier predicted, so it would only lead to better models in the end. This swap can for instance be seen when comparing the model in figure 16 with the models in the next section. This increase in resolution was achieved by making full use of the observed data cube instead of reducing its resolution to a predetermined pixel size, which was done previously. There was one disadvantage of the higher resolution though. The created .stl file for the different models became a bit too large for the printer software to turn into instructions for the printer. Because of this Jake and I had to use a method to make the model better interpretable. We did this by using the Netfabb software from Autodesk (Autodesk 2021). Netfabb has an option to "repair" digital 3D models, which was used on the digital 3D models. This allowed the printer program to create the directions for the printer itself and this way the higher resolution models were able to be printed.

4.2 The final models

After the criteria for the models were determined using the prototypes above, the final models were created with these criteria in mind. They were created exactly as described in section 3 and I will show them in this section.

4.2.1 Galaxy fitting models

(a) Top view   (b) Side view

Figure 22: The final printed elliptical galaxy model of M60.

The seven galaxy and globular cluster models are shown and discussed in this section. I created 2 elliptical galaxy models, M60 is shown in figure 22 and M87 is shown in figure 23. For the spiral galaxies I created 3 models, M64 is shown in figure 24, M81 is shown in figure

25 and NGC5907 is shown in figure 26. Lastly, for the globular clusters I created 2 models, M53 is shown in 27 and NGC4147 is shown in 28.

From all of these models, as a whole the spiral and elliptical galaxy models came out the nicest looking. You might wonder why the model of M87 in figure 23 looks a bit strange near the peak in the middle, but this was due to an unfortunate printing error. We know this is the case, because we can see in figure 10 the digital model of M87 is smooth near the top, so there is no mistake in the creation of the model. Another model that might appear imperfect is the model of M64 in figure 24. In this model the profile and the galaxy do not have the exact same shape. However this is likely due to absorption of light by an object between the galaxy and the telescope, for instance a gas cloud. I suspect this is the case because in the observed data the intensity dips greatly and then goes up again as a function of radius inside of a certain region.
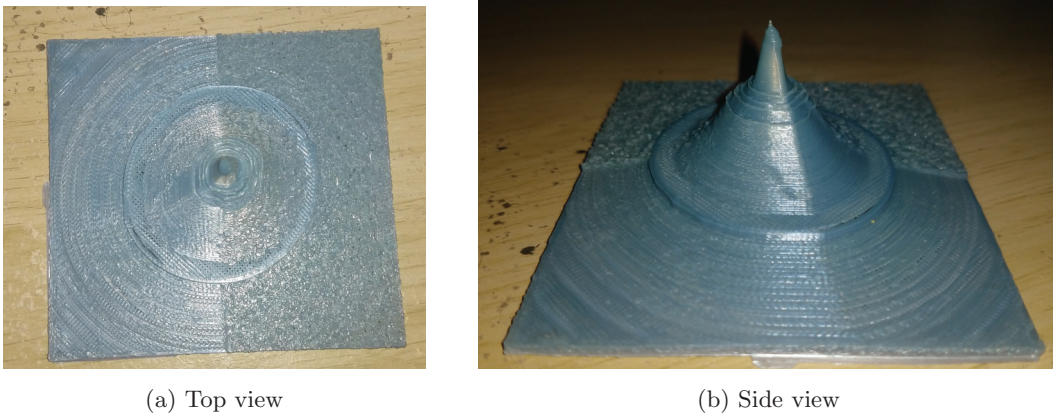

(a) Top view   (b) Side view

Figure 23: The final printed elliptical galaxy model of M87.

(a) Top view   (b) Side view
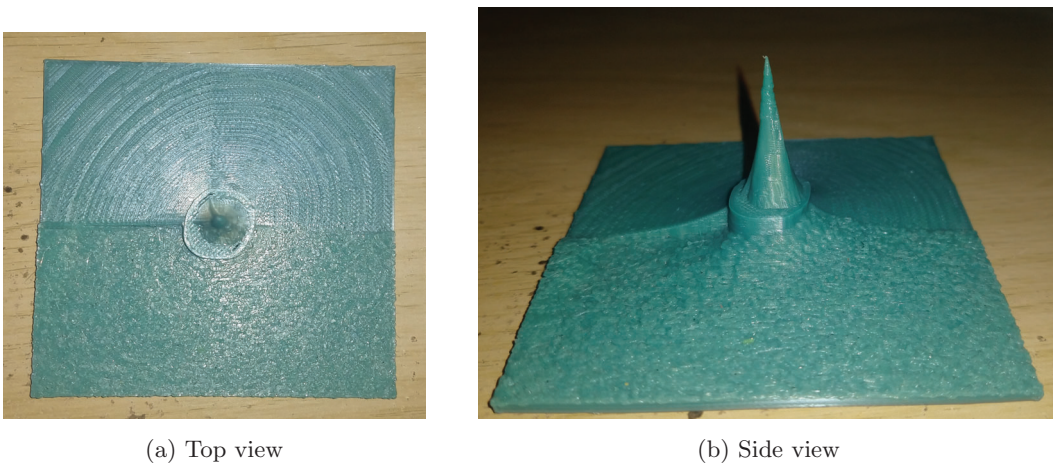
Figure 24: The final printed spiral galaxy model of M64.

Some of the the galaxy models are also quite small, specifically for M64 in figure 24 or M81 in figure 25. I could not zoom more in on these galaxies though because they were just so small inside the images already and that would decrease the resolution too much. On the other hand, the globular cluster models don't look very nice with their high peaks and asymmetric shape. However this is precisely what you would expect for an object that consists of a small collection of stars fitted to a smooth profile. Another thing that you can see in the globular cluster models are the lines of plastic connecting some of the peaks on the data side. This is a side effect from the printer which moves, sometimes too quickly, between the peaks. Using a better printer, this effect can be reduced but this was not possible for this project.

(a) Top view
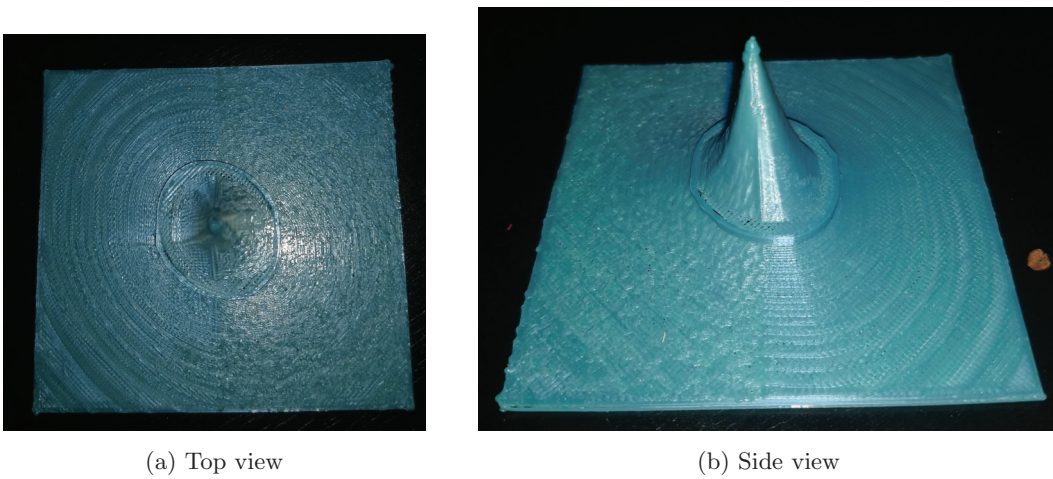
(b) Side view

Figure 25: The final printed spiral galaxy model of M81.

(a) Top view
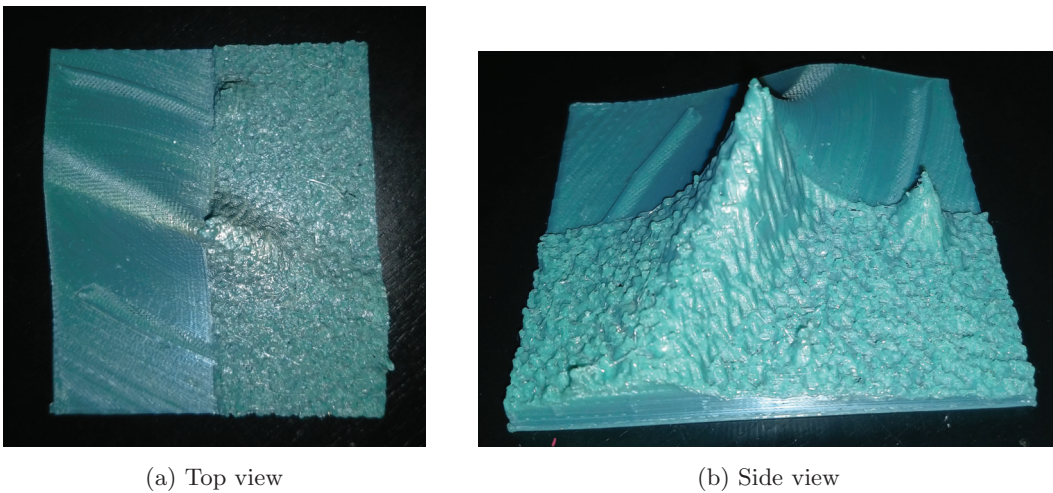
(b) Side view

Figure 26: The final printed spiral galaxy model of NGC5907.
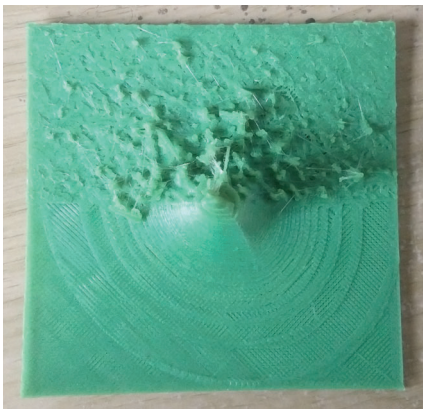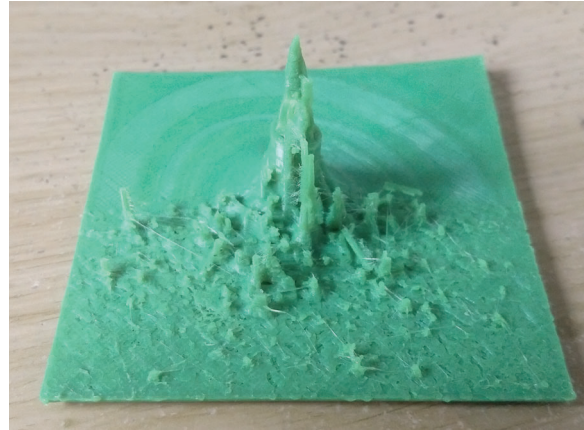
(a) Top view   (b) Side view

Figure 27: The final printed globular cluster model of M53.
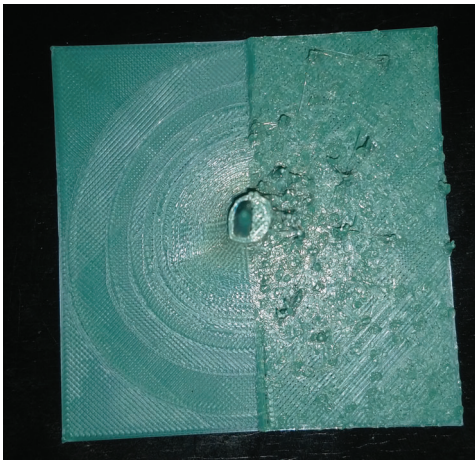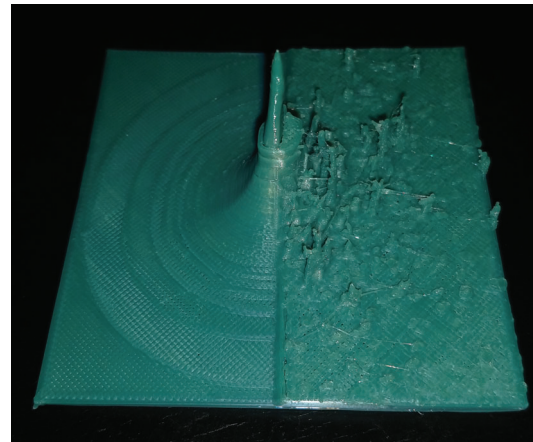
(a) Top view   (b) Side view

Figure 28: The final printed globular cluster model of NGC4147.

4.2.2 Variable star models

The six variable star models are shown and discussed in this section. These six models look quite similar and can be used to explain the workings of variable stars when displayed together. Because of this I will not show all of the separate models individually, but just one of them in figure 29. All of the models together in a row are shown in figure 30. By comparing figure 29 with figure 19 we can immediately see that the peaks in the final model are a lot better defined and better printed. The final model looks nicer and would feel nicer than the prototype model. This is the only difference though as the final and the prototype

model are used in the same way to explain variability. In figure 30 we can see what the models would look like when the students are using them. It is rather difficult to see from this picture how the height of YZ Boo differs between images, but the real height differences are shown in table 1 which is, as previously explained, observable. The models look exactly like Jake and I envisioned it to be, so I can conclude that the creation of the variable star models was a success.

(a) Top view

(b) Side view
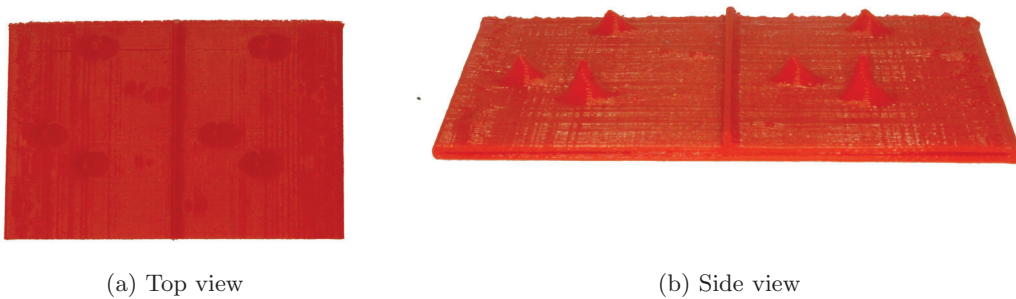
Figure 29: One of the final printed variable star models with a log 2 scaling above the reference star peaks.

(a) Top view

(b) Side view
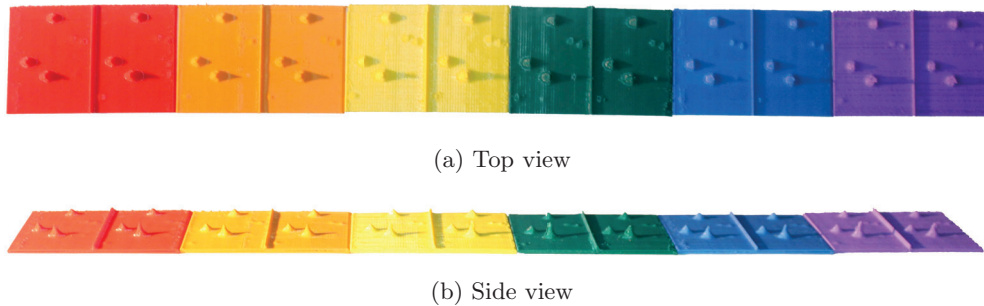
Figure 30: All of the final printed variable star models in a row.

4.2.3   PSF models

The three PSF models are shown and discussed in this section. As was mentioned before, there was a problem with the prototype PSF models, namely the peaks of the narrowest PSF broke off. This was fixed later on by printing them again. All of the three models are shown in figure 31. The models look exactly as I envisioned the PSF models to be like, so I can conclude that the PSF model design was a success without too much trouble.

(a) Top view

(b) Side view

Figure 31: Final printed PSF models. The broadest PSF is shown on the left, the medium PSF is shown in the middle and the narrowest PSF is shown on the right.

5 Feedback of the models

To assess how well the printed models are in helping the students understand their respective topic better I created a survey which the students can take to probe their opinions on the models. The student's opinions are of course important because they are the ones that should benefit from the models. Unfortunately the project was performed during the COVID pandemic so there was limited access to students and none of the students surveyed were blind or visually impaired.

5.1 Survey description

At the end of the observational astronomy course the students form groups to do different topics that were discussed during the course. These topics are: variable stars (2 groups), globular clusters (2 groups), spiral galaxies (1 group), elliptical galaxies (1 group) and PSFs (all groups). The questions related to the galaxies and globular clusters are denoted by "G", the questions related to the variable stars are denoted by "V" and the questions related to PSFs are denoted by "P". To test my models I wanted to show them to the groups and ask them about their opinions on the models. None of these groups have PSFs as their topic, but since PSFs are so generally used I showed these models to all of the groups. I showed the models during an informal meeting with each group separately and the survey was performed with a google form that the students could do during the meeting or later on. The goal of the survey is to find out if the 3D models are intuitive for the user, if the students' understanding of their subject grew after interacting with the model and if the level of understanding grew more for students with a tactile mindset. To achieve these goals, I first present the students with a set of 10 questions about their learning styles. After this, I ask four questions about the models specific to the group and four questions about the PSF models to the groups. The first two questions for each of these model types are asked to figure out if the model is intuitive to use and the other two questions serve to figure out if the students understand the topic better with the help of the model. The questions related to the intuitiveness of the models are denoted by 1 and 2 and the questions related to the understanding are denoted by 3 and 4. So the questions related to the intuitiveness of the galaxy models are G1 and G2 and the questions related to the understanding of the PSF models are P3 and P4. The final question of the survey gives the students the possibility to relay further remarks that they might have of the models. The questions on the survey (save from the final question) are all statements that can be answered on a scale of 5 possibilities from "Strongly disagree" to "Strongly agree". Additionally, to be able to remain in contact with individual students I also ask for their student number, so that questions could be asked about their answers if necessary. Because this is private information I also have to make sure that the students are okay with giving their private information away, which is done at the start of the survey. The entire survey is shown in appendix A. In total 13 students answered the survey.

5.2 Survey results

The answers that the students gave to the survey questions are shown in appendix B and the raw data of the survey is also available (Postema and Noel-Storr 2021). Some students showed more interest in the models in general after explanation of the models corresponding to their group, to these students I also showed the other models. After this, the students answered the survey, so they were also able to give feedback on the other models that were shown to them. Some students were not shown the PSF models so they were also unable to answer the questions related to the PSF models. However 10 out of the 13 students did answer the PSF questions so I can still draw conclusions about them. Finally, there was also one student that didn't answer exactly one question (student 7 in appendix B). This was likely done by accident since the explanation about the galaxy fitting models was given and the second question about the galaxy fitting models was answered. The learning type of each student is determined by calculating a score based on their answers on the ten learning type questions. Each question is answered with a score from 1 to 5 by the students, a 1 means that the student really disagrees with the statement and a 5 means that the student really agrees with the statement. For half of the learning type questions, a high score means that the student has abstract learning tendencies and for the other half, a high score means that the student has tactile learning tendencies. The total abstract or tactile learning tendency score of a student will equal the sum of the scores of their respective question type. If one score is significantly larger than the other, I can say that that student is an abstract or tactile learner. Significant in this case means a difference of 5 points. If the scores are about the same, I must say that it is inconclusive. As for the questions related to the models, I can give each model two scores as well, one for intuitiveness and one for increasing the understanding of the students. If the average score of a model is 4, one point above the "no opinion" score of 3, I can speak of a success. Otherwise, if the average score is 2, I can speak of a failure and everything between can be seen as inconclusive. The learning tendencies were calculated for each student as shown in table 2 and the average opinions on the models were also calculated as shown in table 3.

Student	1	2	3	4	5	6	7	8	9	10	11	12	13
Learning type	T	U	U	V	V	U	U	U	U	U	T	U	V

Table 2: The type of learning tendency for each of the students that answered the survey. T means tactile, V means Visual and U means unidentified. Instead of student numbers, each of the students is given a different ID instead to remain private.

From table 2, we can see that only two students were classified as tactile learners, while three students were classified as visual learners. For the other 8 students it was unclear what kind of learning style they prefer. From table 3, we can see that questions G2, V2, P2, G4, P3 and P4 were answered positively, while no questions were answered negatively on a whole. For each of the 12 questions in table A, 1 relates to the intuitiveness of the model before explanation, 2 relates to the intuitiveness of the model after explanation of what it represented and 3 and 4 relate to the improvement of the student's understanding of different

Question	G1	G2	V1	V2	P1	P2	G3	G4	V3	V4	P3	P4
Average score	3.7	5.0	3.1	4.4	3.2	4.8	3.8	4.0	3.6	3.8	4.2	4.2

Table 3: The average of the scores given by all of the 13 students on the 12 questions relating to the models. The galaxy questions are denoted by a G, the variable star questions are denoted by a V and the PSF questions are denoted by a P. The numbers 1 and 2 relate to the questions about the intuitive design of the models (questions 13 to 18 in appendix A) and the numbers 3 and 4 relate to the questions about the student's understanding of the model (questions 19 to 24 in appendix A).

aspects of each topic. With this and the information in table 3, I can draw the following conclusions: after explanation, the galaxy, variable stars and PSF models were a lot easier to interpret. Furthermore, the models helped the students understand galaxy fitting more and PSF models a lot more. They unfortunately didn't seem to have a conclusive effect on the variable star models though. The average answers on the 12 questions relating to the models of only the students with a tactile learning tendency are shown in figure 4.

Question	G1	G2	V1	V2	P1	P2	G3	G4	V3	V4	P3	P4
Average score	5.0	5.0	3.5	4.0	3.5	5.0	3.0	3.5	3.5	3.0	5.0	4.5

Table 4: The average of the scores given by the 2 students with a tactile learning tendency on the 12 questions relating to the models. The galaxy questions are denoted by a G, the variable star questions are denoted by a V and the PSF questions are denoted by a P. The numbers 1 and 2 relate to the questions about the intuitive design of the models (questions 13 to 18 in appendix A) and the numbers 3 and 4 relate to the questions about the student's understanding of the model (questions 19 to 24 in appendix A).

From table 4, we can see that the two students with a tactile learning tendency answered questions G1, G2, V2, P2, P3 and P4 positively. It turns out that to those students the galaxy fitting models were quite clear and that after explanation, the variable star and PSF models were also understandable. Furthermore, the PSF models really helped the students understand the topic better while the student understand questions for the other models were inconclusive. What is more important though is figuring out if the models had a more positive effect on the tactile learners than the group as a whole. This is the case for questions G1, G2, V1, V2, P1, P2, P3 and P4. From this we can see that the models were more intuitive for the tactile students than the group as a whole, but that they understood the subjects (except for PSF) a bit worse than the group as a whole. Finally, two students had remarks at the end of the survey. Student 6 remarked that the models were interesting especially after explanation. Student 13 remarked that their understanding of variable stars was already sufficient and that it wasn't immediately clear by eye which of the stars in the variable star models were variable. This leads me to believe that there are still some things I can improve about the created models. The general feeling that I got from the students while discussing the models was that they enjoyed playing around with

the models. They also thought that it was interesting to see a different way of showing the topics than they were used to in class. We can see this from the remark of student 6 as well. Some students even seemed to really understand the topics better due to the models, which is also reflected in the survey results. Although some other students seemed to have quite a strong grasp already of the subject they were doing their project on, so for them the models were less useful. This is also reflected in the survey results as one of the students made a final note that they already understood the variable stars theory. Over all, from speaking and interacting with the students and the models, I would say that it is always worth considering if you are able to use models in the classes you teach, because the interest of the students was definitely peaked.

6 Discussion and conclusion

In this section I will discuss the results of and what could have gone better during this research. I explored the possibility of using tactile models in astronomy education and recommendations were given for the design of these models for various different topics that could be encountered. These models can be especially helpful when teaching these topics to blind or visually impaired students or tactile learners. I created a helpful sheet to summarize my findings and used its content to develop my own 3D models to help teach the topics of galaxies, variable stars and PSFs to first year astronomy students. The creation process of these models took a few iterations before the final design was arrived at. After I was happy with the design of the 3D models, they were shown to some of the first year students of "Observational astronomy" in order to survey them for their opinion on the models. I planned to use the model during the lectures so that it could help all of the students which would also make sure that we would have the most amount of students to get feedback from at the end. However, because this research was done during the COVID pandemic this was not possible. If this research were to be done again it would most certainly be preferable to shown the model to the students during class. Not all of the problems were caused by the quarantine though. The results from the survey were unfortunately not always conclusive which is of course not desirable. This is in part due to the fact that the number of students that answered the survey was not as large as hoped from the start. It is also possible that more questions could have helped to get a more conclusive survey, although I did not want to make the survey too long as the students answered it in their own free time. One more thing to consider is that asking for the student number of the participants at the start of the survey might have influenced the answers that they would give. Knowing that the survey was not completely anonymous might have caused that the students gave higher scores to the models but we can not be sure about this. One final thing that could have influenced the results of the survey is the models that the students were presented with. This is of course what you would want and expect as the models are the objects that the students should give their opinions. However as was mentioned earlier, some of the models that were shown to the students were not printed perfectly. This means that the students did not give their opinion on the real final models, but since those models look a lot like the models shown to the students and the students were explained what the printing mistakes were I would argue that the survey result should still hold up. The feedback from the students made it clear that the models were not all perfect, especially the variable star models were not as informative as I would have hoped. However I do not think that an overhaul of the design is necessary. What I do think though is that if this model were to be created once more, the variability of the variable star must be a lot clearer. Only by looking really closely or by laying a ruler on top of the row of models could the students see that the height of one of the stars was changing. It was one of the main challenges for the variable star models to scale the height of YZ Boo in the model. However it seems that the model that the students used still did not have a good enough scaling such that it was helpful for the students. So if a newer version of these models were to be created I would focus on making a better intensity scaling such that the differences in height between the intensity peaks would be

more noticeable. This could be done by changing our log scaling even more or by creating an entirely different way of scaling. In either case it would also be helpful to make use of a printer that can print steeper peaks. Finally, making multiple sets of variable star models can also be useful. Specifically making a set of models for a case where the variable star generally has a lower intensity than the neighbouring stars. This might make the scaling even more difficult, but as one of the students that answered the survey noted it would represent their own projects better. I think that the other models succeeded though, so for the time being there are no design changes I would recommend for those. With the help of the survey we can also see that the tactile learners had a worse understanding of the subjects in general than the group as a whole, however it is hard to say if this is due to the models or due to the lectures they had before. I would argue that the models did fulfill their purpose though, as the topic of PSFs was not specifically treated during class and this was the only topic that the tactile learners did understand better than the group as a whole. This shows that the models do have an especially positive impact on the understanding of the tactile learners. With the help of the algorithms written during this project the students could possibly create their own 3D models of their own data. Even though some of the results of this research are inconclusive, not a lot of research has been done into the use of 3D models in astronomy education. Because of this qualitative results are always welcome to advance this field.

Appendices

A   The survey

The first 10 questions of this survey are used to check your learning preferences. The next six questions relate to your ability to intuitively understand the properties of and information shown by the model. The final six questions relate to the impact that the models have on your understanding of the subject it is related to. Only answer the questions related to the model(s) you used. Try to answer as little: "Neither agree nor disagree" as possible. Additionally two questions concerning personal information are asked at the start of the survey.

1. My S-number is:

    S ....

2. Data usage: O I am okay with having my response being anonymously included into research into astronomy education.

3. I prefer to see information written on a chalkboard and supplemented by visual aids and assigned readings.
    O Strongly disagree O Disagree O Neither agree nor disagree O Agree O Strongly agree

4. I like to write things down or to take notes for visual review.
    O Strongly disagree O Disagree O Neither agree nor disagree O Agree O Strongly agree

5. I prefer to use posters, models, or actual practice and other activities in class
    O Strongly disagree O Disagree O Neither agree nor disagree O Agree O Strongly agree

6. I enjoy working with my hands or making things. O Strongly disagree O Disagree O Neither agree nor disagree O Agree O Strongly agree

7. I am skillful with and enjoy developing and making graphs and charts.
    O Strongly disagree O Disagree O Neither agree nor disagree O Agree O Strongly agree

8. I can remember best by writing things down.
    O Strongly disagree O Disagree O Neither agree nor disagree O Agree O Strongly agree

9. I can easily understand and follow directions on a map.
    O Strongly disagree O Disagree O Neither agree nor disagree O Agree O Strongly agree

10. I play with coins or keys in my pocket.
    O Strongly disagree O Disagree O Neither agree nor disagree O Agree O Strongly agree

11. I can understand a news article better by reading about it in a newspaper than by listening to a report about it on the radio.
    O Strongly disagree O Disagree O Neither agree nor disagree O Agree O Strongly agree

12. I think the best way to remember something is to picture it in your head.
    O Strongly disagree O Disagree O Neither agree nor disagree O Agree O Strongly agree

13. When I observed the galaxy fitting model it was immediately clear what it represented.
    O Strongly disagree O Disagree O Neither agree nor disagree O Agree O Strongly agree

14. After explanation of the galaxy fitting model it was clear how to interpret the model.
    O Strongly disagree O Disagree O Neither agree nor disagree O Agree O Strongly agree

15. When I observed the variable star model it was immediately clear what it represented.
    O Strongly disagree O Disagree O Neither agree nor disagree O Agree O Strongly agree

16. After explanation of the variable star model it was clear how to interpret the model.
    O Strongly disagree O Disagree O Neither agree nor disagree O Agree O Strongly agree

17. When I observed the PSF model it was immediately clear what it represented.
    O Strongly disagree O Disagree O Neither agree nor disagree O Agree O Strongly agree

18. After explanation of the PSF model it was clear how to interpret the model.
    O Strongly disagree O Disagree O Neither agree nor disagree O Agree O Strongly agree

19. After explanation of the galaxy fitting model I have a feeling that I better understand how galactic fits are created.
    O Strongly disagree O Disagree O Neither agree nor disagree O Agree O Strongly agree

20. After explanation of the galaxy fitting model I have a feeling that I better understand what galactic fits look like.
    O Strongly disagree O Disagree O Neither agree nor disagree O Agree O Strongly agree

21. After explanation of the variable star model I have a feeling that I better understand how variable stars behave.

O Strongly disagree O Disagree O Neither agree nor disagree O Agree O Strongly agree

22. After explanation of the variable star model I have a feeling that I better understand how light curves are created.
O Strongly disagree O Disagree O Neither agree nor disagree O Agree O Strongly agree

23. After explanation of the PSF model I have a feeling that I better understand what a PSF looks like.
O Strongly disagree O Disagree O Neither agree nor disagree O Agree O Strongly agree

24. After explanation of the PSF model I have a feeling that I better understand how PSFs influence observations.
O Strongly disagree O Disagree O Neither agree nor disagree O Agree O Strongly agree

25. Are there any remarks you would like to make about any of the models?

B   Survey results

Student	1	2	3	4	5	6	7	8	9	10	11	12	13
Learning type Q1	2	3	4	4	5	5	4	2	4	4	4	4	5
Learning type Q2	2	4	4	4	5	5	3	5	3	3	2	3	1
Learning type Q3	5	2	5	2	3	4	5	4	3	3	4	5	2
Learning type Q4	4	2	2	2	2	5	5	3	3	4	3	3	1
Learning type Q5	2	2	3	4	3	5	5	4	3	2	1	4	4
Learning type Q6	2	5	4	4	5	3	2	4	3	4	5	3	1
Learning type Q7	5	4	4	3	5	5	5	4	4	4	1	4	4
Learning type Q8	2	1	3	1	4	4	5	4	2	2	3	4	1
Learning type Q9	2	5	1	4	5	1	3	2	5	3	5	2	5
Learning type Q10	5	4	4	3	4	5	5	4	5	4	5	3	5
Galaxy fitting Q1	5					2	4	3	4		5	3	
Galaxy fitting Q2	5					5	5	5	5		5	5	
Variable star Q1	3		4	5	2	1	3	2	5		4	2	3
Variable star Q2	3		4	5	4	5	3	4	5		5	5	5
PSF Q1	4	3				1	3	4	5	3	3	2	4
PSF Q2	5	5				5	5	4	5	5	5	5	4
Galaxy fitting Q3	3					5		4	4		3	4	
Galaxy fitting Q4	3					5	5	4	4		4	3	
Variable star Q3	3		3	4	4	5	3	4	4		4	4	2
Variable star Q4	3		3	4	5	5	3	5	5		3	4	2
PSF Q3	5	3				5	3	4	4	4	5	5	4
PSF Q4	4	3				5	4	5	3	4	5	5	4

Table 5: All of the answers (values from 1 to 5) to the survey by the 13 students that answered it. The student numbers are omitted for the privacy of the students. The full questions are shown in appendix A. The learning type questions relate to questions 3 to 12 in appendix A. For the other questions, the numbers 1 and 2 relate to the questions about the intuitive design of the models (questions 13 to 18 in appendix A) and the numbers 3 and 4 relate to the questions about the student's understanding of the model (questions 19 to 24 in appendix A).

Student 6 had the remark: "They were very interesting, especially once they were explained" and student 13 had the remark: "For the variable star models, I already understood very well how they behaved from my own code and images, which is why I didn't really learn anything new from them. Also because of the size of the variable star models the difference in brightness between images wasn't too clear nor was it clear which star in that model was the variable star on first sight (our star is definitely not the brightest in our images)."

References

Yerlikaya, Asli and Mahir Yerlikaya (Nov. 2016). "Models Usage in Teaching Astronomy and Visual Literacy". In: *Participatory Educational Research* Special, pp. 77–94.

Cole, Merryn et al. (June 2018). "Spatial thinking in astronomy education research". In: *Phys. Rev. Phys. Educ. Res.* 14 (1), p. 010139. DOI: 10.1103/PhysRevPhysEducRes.14.010139. URL: https://link.aps.org/doi/10.1103/PhysRevPhysEducRes.14.010139.

Aldajani, Neda F (Nov. 2016). "Exploration of the Effectiveness of Tactile Methods". Not published.

Hasper, Eric et al. (2015). "Research and Teaching: Methods for Creating and Evaluating 3D Tactile Images to Teach STEM Courses to the Visually Impaired." In: *The journal of college science teaching* 44, pp. 82–89.

DigitalEngineering247 (July 2021). *Sculpteo Aids Rosetta Mission with 3D Printed Comet.* URL: https://www.digitalengineering247.com/article/sculpteo-aids-rosetta-mission-with-3d-printed-comet/feed.

News, Softpedia (July 2021). *NASA Releases 3D Printing Models of the Moon, Asteroids and Spacecraft.* URL: https://news.softpedia.com/news/NASA-Releases-3D-Printing-Models-for-the-Moon-Asteroid-and-Spacecraft-451906.shtml.

group, China printing (June 2022). *3D Embossed PVC Posters Printing.* URL: https://www.chinaprintinggroup.com/product/3D-Embossed-PVC-Posters-Printing.html.

Vogel, Tracy (Dec. 2020). *Explore - From Space to Sound.* URL: https://www.nasa.gov/content/explore-from-space-to-sound.

Jones, M. Gail et al. (Dec. 2006). "Visualizing Without Vision at the Microscale: Students With Visual Impairments Explore Cells With Touch". In: *Journal of Science Education and Technology* 15.5-6, pp. 345–351. DOI: 10.1007/s10956-006-9022-6.

Jones, Gail, Amy Taylor, and Bethany Broadwell (May 2009). "Concepts of Scale Held by Students With Visual Impairment". In: *Journal of Research in Science Teaching* 46, pp. 506–519. DOI: 10.1002/tea.20277.

Harshman, Jordan, Stacey Lowery Bretz, and Ellen Yezierski (2013). "Seeing Chemistry through the Eyes of the Blind: A Case Study Examining Multiple Gas Law Representations". In: *Journal of Chemical Education* 90.6, pp. 710–716. DOI: 10.1021/ed3005903. eprint: https://doi.org/10.1021/ed3005903. URL: https://doi.org/10.1021/ed3005903.

Fraser, William and Mbulaheni Maguvhe (Mar. 2008). "Teaching life sciences to blind and visually impaired learners". In: *Journal of Biological Education - J BIOL EDUC* 42, pp. 84–89. DOI: 10.1080/00219266.2008.9656116.

Toenders, F.G.C. et al. (June 2017). "Analysing the physics learning environment of visually impaired students in high schools". English. In: *Physics Education* 52.4. ISSN: 1361-6552. DOI: 10.1088/1361-6552/aa737c.

Azevedo, A and A. Santos (July 2014). "Teaching optics to blind pupils". In: *Physics Education* 49, p. 383. DOI: 10.1088/0031-9120/49/4/383.

Bülbül, M. Şahin, Belkıs Garip, and Ömer Özdemir (Nov. 2015). "Using a Force Concept Inventory Test with Visually Impaired and Blind Students". In: *European Journal Of Physics Education* 6. DOI: 10.20308/ejpe.09583.

Butler, Matthew et al. (2017). "Understanding the graphical challenges faced by vision-impaired students in Australian universities". In: *Higher Education Research & Development* 36.1, pp. 59–72. DOI: 10.1080/07294360.2016.1177001. eprint: https://doi.org/10.1080/07294360.2016.1177001. URL: https://doi.org/10.1080/07294360.2016.1177001.

Labists (June 2021). *High Precision Mini 3D Printer, X1 Entry-Level 3D Printer DIY Kit.* URL: https://labists.com/products/mini-3d-printer-labists-x1.

Postema, Jasper and Jake Noel-Storr (July 2021). *PracticalAstronomyCrew/3dmodel-observation-interpreting: 2021 MSc Thesis Jasper Postema.* Version v1.0. DOI: 10.5281/zenodo.5068689. URL: https://doi.org/10.5281/zenodo.5068689.

Kluyver, Thomas et al. (2016). "Jupyter Notebooks ? a publishing format for reproducible computational workflows". In: *Positioning and Power in Academic Publishing: Players, Agents and Agendas.* Ed. by Fernando Loizides and Birgit Scmidt. IOS Press, pp. 87–90. URL: https://eprints.soton.ac.uk/403913/.

Hattem, Rick van (May 2021). *Numpy-Stl package.* URL: https://pypi.org/project/numpy-stl/.

Harris, Charles R. et al. (Sept. 2020). "Array programming with NumPy". In: *Nature* 585.7825, pp. 357–362. DOI: 10.1038/s41586-020-2649-2. URL: https://doi.org/10.1038/s41586-020-2649-2.

Astropy Collaboration et al. (Sept. 2018). "The Astropy Project: Building an Open-science Project and Status of the v2.0 Core Package". In: *Astronomical Journal* 156.3, 123, p. 123. DOI: 10.3847/1538-3881/aabc4f. arXiv: 1801.02634 [astro-ph.IM].

Autodesk (June 2021). *Netfabb Connected software for additive manufacturing, design, and simulation.* URL: https://www.autodesk.eu/products/netfabb/overview.